Institut für Theoretische Physik I
Universität Stuttgart
Pfaffenwaldring 57
70550 Stuttgart

Local Aspects of Modular Quantumsystems in Nonequilibrium

Von der Fakultät Mathematik und Physik
der Universität Stuttgart zur Erlangung der Würde eines Doktors der Naturwissenschaften (Dr. rer. nat.) genehmigte Abhandlung

Vorgelegt von

Markus Joachim Henrich

aus Eberbach

Hauptberichter:	Prof. Dr. Günter Mahler
Mitberichter:	Prof. Dr. Ulrich Weiß
Tag der mündlichen Prüfung:	14. August 2007

Institut für Theoretische Physik der Universität Stuttgart

2007

(Dissertation Universität Stuttgart)

Contents

1. Introduction

> Thermodynamics is quite different. It neither claims a unique domain of systems over which it asserts primacy, nor does it introduce a new fundamental law analogous to Newton's or Maxwell's equations. In contrast to the specificity of mechanics and electromagnetism, the hallmark of thermodynamics is generality.
>
> H. B. Callen [14]

The development of thermodynamics is connected with the study of thermodynamical machines which started in the pioneering work of S. Carnot on the maximum efficiency a heat engine [16]. Thermodynamics at that time has been based on phenomenological concepts of pressure, temperature, etc. , but it was realized that heat is a form of energy transfer. The development of this important fact is associated with the names of R. Mayer, J. Joule, R. Clausius. It was the latter who introduced the concept of entropy to thermodynamics and thus gave work and heat a mathematical concept [19] which, in principle, is still valid today. In addition, the maximum entropy principle would explain how thermodynamical processes behave.

A conceptual problem of entropy within this phenomenological approach could be traced back to the absence of a deeper meaning what entropy is and why it should always increase (as the 2nd law states). L. Boltzmann explained the second law and thus entropy by his molecular chaos hypothesis with his famous H-theorem [6]. Despite a lot of criticism and hostilities his statistical interpretation of thermodynamics was extended by W. Gibbs in his celebrated work [37]. There, the ensemble theory was developed and the statistical aspect of thermodynamics was given a mathematical structure. It was A. Einstein in [23] who, as one of the first, made use of the statistical aspect to explain Brownian motion. Then, statistical mechanics began to take over the leadership in the further development of thermodynamics. Nevertheless, a main problem remained unsolved: How could macroscopic irreversible phenomena be explained out of reversible microscopic dynamics without further

assumptions?

At the beginning of the 20th century the very successful theory of quantum mechanics was developed. Soon the statistical aspects of quantum mechanics was discovered by M. Born [8] and J. von Neumann [95] who also linked quantum mechanics to thermodynamics. Nevertheless, the old problem of the emergence of irreversible phenomena was not convincingly solved in the opinion of a considerable fraction of physicists. Recently, J. Gemmer, et. al. developed in [33] an approach which was able to explain the emergence of irreversible phenomena within the reversible Schrödinger dynamics. In this so-called *Quantum Thermodynamics* the dominating principle is entanglement which implies for the small part of bipartite systems an irreversible dynamics. The reached stationary state follows the maximum entropy principle. The picture of molecular chaos is dispensable within this approach and no additional assumption like, e.g., the ergodic hypothesis are any longer necessary.

Quantum thermodynamics thus is able to explain how an even small quantum system can reach a thermal stationary state. This equilibrium theory paves the way to nonequilibrium phenomena as studied in quantum transport scenarios like heat conduction in low dimensional systems. This topic is still under controversial discussion because of the different results which alternate approaches achieve (cf. the short note in [12]). The mainstream strategies are the Peierls-Boltzmann equation [74] or the Kubo-formula [53]. There, quasi-particles are responsible for the heat transport, also in insulators. Quantum thermodynamics and also the nonequilibrium aspects of this approach tries to explain transport phenomena without involving this quasi-particle picture as developed in [63].

Besides dealing with nonequilibrium phenomena in quantum systems it is quite interesting and important to understand the emergence of stationary states and their local properties. By local we mean the properties of the subunits a system is made of. If, for example, such states exist it will be interesting to see to what extent the thermodynamic concepts of temperature, pressure, heat and work, etc. are still valid. Recently it has been found, that the existence of temperature on the nanoscale is depending on the size of the system [40]. For nonequilibrium situations these concepts are still unclear.

In this thesis we want to make use of the thermodynamic concepts and to investigate under what conditions they are still applicable for small quantum systems in nonequilibrium situation. The main focus lies on stationary nonequilibrium states. The way how to reach this states is interwoven with the question how a system decays. The local properties of small quantum system will be studied as well as the transport behavior. In addition we investigate driven quantum systems in nonequilibrium situations.

The outline of this thesis is as follows: The first part deals with time inde-

pendent or not externally driven systems. In Chap. 2 we give a summary of the main thermodynamic quantities and concepts used. A short introduction into irreversible processes is given. In Chap. 3 we introduce the typical models under investigation. We characterize their main properties and show their evolution in time. Sect. 4 gives an overview of how a quantum system could relax to a thermal state and derives the quantum master equation (QME) with the help of projection operator technique.

In Chap. 5 we define local properties of a quantum system embedded in a larger quantum system. Here we will present a new approach to the quantities heat and work for quantum systems. The heart of this definition will be the so called LEMBAS (**L**ocal **E**ffective **M**easurement **Bas**is). This basis allows for an effective description and thus to an effective local dynamics of the considered system. This effective description is the cornerstone for the local properties.

In Chap. 6 we study nonequilibrium phenomena within a QME approach for quantum systems. The transport behavior of 1-dim Heisenberg chains based on LEMBAS will be investigated for homogeneous as well as for inhomogeneous chains. Chap. 7 shows an numerical experiment about a local temperature measurement.

The second part of the thesis deals with externally driven nonequilibrium stationary states. First, we introduce thermodynamical processes known from classical thermodynamics for single quantum systems especially for TLS (two level systems) in Chap. 8. In Chap. 9 these processes will be combined to thermodynamical cycles like the Carnot-cycle, etc.. As will be seen, it is not possible to realize all kind of cycles in an easy way. In the last chapter, Chap. 10, we study a heat engine consisting of a spin chain. The described cycles will be comparable to an Otto-cycle. Although the heat engine is working in finite time, it nearly behaves as the theoretical model predicts.

Part I.

Nonequilibrium Steady States

2. Basic Principles of Quantum Thermodynamics

> Im allgemeinen Fall gibt es keine einfache Beziehung zwischen $đW$ und $đQ$ einerseits und den beiden Termen des statistischen Ausdruckes für $\mathrm{d}E$ andererseits.
>
> B. Diu et. al. in [21]

In this first chapter we want to give a short overview of the thermodynamic and statical concepts used throughout the thesis. Most can be found in textbooks on thermodynamics and statical mechanics. We adapt the concepts to quantum systems and highlight the usefulness of the celebrated Gibbs fundamental form. We give a commonly used definition for heat and work. In the last part a short introduction to nonequilibrium thermodynamics is given with a derivation of Fourier's law of heat conduction for classical systems.

2.1. Entropy

Entropy is the fundamental concept of thermodynamics and statistical physics. For quantum systems the basic entropy is given by the von Neumann-entropy

$$S = -\mathrm{Tr}\left\{\hat{\rho}\ln\left(\hat{\rho}\right)\right\} = -\sum_n p_n \ln\left(p_n\right), \tag{2.1}$$

where $\hat{\rho}$ is the density matrix of the considered system and the p_n's are the corresponding occupation probabilities. If $\hat{\rho}(t)$ is diagonal in the energy eigenbasis of the considered system one can take (2.1) as the thermodynamic entropy.

2.2. Temperature

In classical thermodynamics the temperature T of a system is given by

$$T = \frac{\partial S}{\partial U}, \tag{2.2}$$

with the internal energy $U(S, V, N)$. From statistical physics we known that a system coupled to a heat bath will possess a temperature induced by the bath which results in a canonical state of the form

$$\hat{\rho} = \frac{1}{Z} \exp\left(-\frac{\hat{H}}{k_{\mathrm{B}} T}\right). \tag{2.3}$$

Z denotes the partition sum and k_{B} the Boltzmann constant[1]. Putting (2.3) into (2.1) and taking the derivative with respect to E, the energy eigenvalues of $\hat{H}$, will be equivalent to (2.2). For a two-level system (TLS) this yields

$$T = \frac{E_1 - E_0}{\log(p_1) - \log(p_0)}, \tag{2.4}$$

where E_n are the eigenvalues and p_n the occupation propabilities of level n.

That even small quantum systems like a single spin, e.g., can have a temperature can only be justified if the quantum system stays in contact with a heat bath [33]. The hypothesis is that a quantum system possesses a measurable temperature T if

- the system is in a canonical state of the form (2.3), and
- when disturbed, e.g., by a measurement the state will relax again into the thermal state.

This definition will be used throughout the present work.

2.3. Gibbs Fundamental Relation

Thermodynamics is built upon two different kinds of parameters: extensive and intensive. The extensive parameters are energy U, entropy S, Volume V (plus other extensive "mechanical" variables) and particle number N_i. They are additive when two or more systems are brought in contact. The conjugate variables are the intensive parameters, namely the temperature T, pressure p and chemical potential μ given by

$$T \equiv \left(\frac{\partial U}{\partial S}\right)_{V,N_i}, \tag{2.5}$$

$$p \equiv -\left(\frac{\partial U}{\partial V}\right)_{S,N_i} \quad \text{and} \tag{2.6}$$

$$\mu_i \equiv \left(\frac{\partial U}{\partial N_i}\right)_{S,V}. \tag{2.7}$$

[1] In the following we will set $k_B = 1$ as well as $\hbar = 1$ until otherwise stated.

For two systems coupled with each other these variables are constant (in equilibrium), and identical (contact variables).

The fundamental relation for the internal energy $U(S, V, N_i)$ is given by

$$\mathrm{d}U = T\mathrm{d}S - p\mathrm{d}V + \sum_i \mu_i \mathrm{d}N_i = đQ + đW, \tag{2.8}$$

where we have introduced heat $đQ$ and work $đW$. In general, we may write

$$đW = \sum_\nu x_\nu \mathrm{d}X_\nu, \tag{2.9}$$

where the x_ν denotes the intensive conjugate variables to the extensive variables X_ν. The fundamental relation (2.8) contains all thermodynamic information about the considered system. In quantum mechanics the energy is given by the energy expectation value

$$U = \langle \hat{H} \rangle = \mathrm{Tr}\left\{\hat{H}\hat{\rho}\right\} = \sum_n E_n p_n. \tag{2.10}$$

Here, $\hat{H}$ denotes the Hamilton operator, E_n the corresponding eigenvalues of the considered system and $\hat{\rho}$ the density operator with p_n the respective occupation probabilities. It is assumed that the spectrum of $\hat{H}$ is discrete.

Considering a change of $\langle \hat{H} \rangle$ in time

$$\frac{\mathrm{d}}{\mathrm{d}t}\langle \hat{H} \rangle = \underbrace{\mathrm{Tr}\left\{\frac{\mathrm{d}}{\mathrm{d}t}\hat{H}\hat{\rho}\right\}}_{\mathrm{I}} + \underbrace{\mathrm{Tr}\left\{\hat{H}\frac{\mathrm{d}}{\mathrm{d}t}\hat{\rho}\right\}}_{\mathrm{II}}, \tag{2.11}$$

as in statistical physics (e. g., [21]) the change of the energy spectrum $\dot{\hat{H}}$ [part I in (2.11)] is taken as work. Fig. 2.1 shows as illustration a potential well for a particle in a box. By changing the volume of the box the energy splitting changes. Part II in (2.11) reflects only the change of occupation propabilities which will be associated with heat. Eq. (2.11) can be rewritten with the help of (2.10) in the form

$$\mathrm{d}U = \sum_n \mathrm{d}E_n p_n + \sum_n E_n \mathrm{d}p_n, \tag{2.12}$$

so that

$$đW = \sum_n \mathrm{d}E_n p_n \tag{2.13}$$

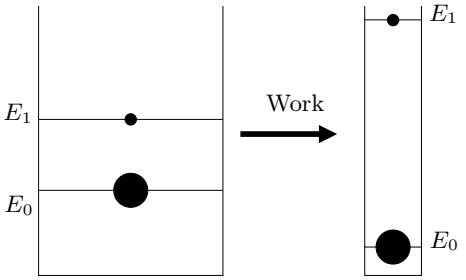

Figure 2.1.: Example where work is included by changing the volume and thus the spectrum for a particle in the box. The dots indicate the occupation propabilities.

and

$$đQ = \sum_n E_n \mathrm{d}p_n. \tag{2.14}$$

When dealing with thermal states the density operator $\hat{\rho}$ of the considered system will be canonical given by

$$\hat{\rho}(T, \hat{H}) = \frac{\exp(-\hat{H}/T)}{\mathrm{Tr}\left\{\exp(-\hat{H}/T)\right\}}. \tag{2.15}$$

The density operator $\hat{\rho}$ (and thus p_n) is therefore a function of the temperature T as well as of $\hat{H}$. That (2.14) is equivalent to $T\mathrm{d}S$ can be seen from

$$\begin{aligned}
\mathrm{d}S &= -\sum_n \mathrm{d}p_n \log(p_n) + p_n \mathrm{d}\log(p_n) \\
&= -\sum_n \mathrm{d}p_n \left[\log(p_n) + 1\right] \\
&= -\sum_n \mathrm{d}p_n \log(p_n)
\end{aligned} \tag{2.16}$$

where we used the condition $\sum_n \mathrm{d}p_n = 0$. The derivation is only valid if $\hat{\rho}$ is diagonal in the energy eigenbasis, otherwise $\hat{\rho}$ does not commutate with $1/(\dot{\hat{\rho}})$. We continue with the property that we have a canonical state

$$\begin{aligned}
\mathrm{d}S &= -\sum_n \mathrm{d}p_n \left[-\frac{E_n}{T} - \log(Z)\right] \\
&= \frac{1}{T}\sum_n E_n \mathrm{d}p_n.
\end{aligned} \tag{2.17}$$

In the last step we used again $\sum_n \mathrm{d}p_n = 0$. By comparing (2.17) with (2.14), the definition of $đQ$, it can be seen that (2.17) is equivalent to $T\mathrm{d}S$.

2.4. Irreversible Processes: Currents and Onsager Reciprocity

So far we have given a short overview about equilibrium properties. If the system has been thermalized, in principle the Gibbs fundamental relation is fulfilled and all thermodynamic properties are known.

Thermodynamic processes can be studied within the thermostatic approach with two different methods:

- by comparing the initial and the final state of a system at the beginning and the end of a thermal process
- by introducing an ideal physical or quasistatic process requiring that the thermal processes are very slow.

Using either of these methods one cannot observe what the considered system is actually doing. In reality a vast variety of processes and states are nonequilibrium states, and therefore a much better concept to treat these problems would be a description involving real irreversible processes. A way to irreversible thermodynamics is paved by using the equilibrium properties and adding the postulate of time reversal symmetry of physical laws [14].

Of interest is, e.g., the heat transport through a continuous system like a wire. For simplicity and treating discrete quantum systems later on, one divides such a system into small cells. It is assumed that for each cell the equilibrium thermodynamics is still valid.

Let, for example a system of two subunits posses i extensive parameters X_1^i and X_2^i, so that for the complete system $X_{\mathrm{tot}}^i = X_1^i + X_2^i = \mathrm{const}$. Now, if both subunits are brought into contact the following equalities hold

$$\mathcal{F}^i = \left(\frac{\partial S_1 + \partial S_2}{\partial X^i}\right)_{X_{\mathrm{tot}}^i} = \frac{\partial S_1}{\partial X_1^i} - \frac{\partial S_2}{\partial X_2^i} = F_1^i - F_2^i. \tag{2.18}$$

F_1^i and F_2^i are the generalized thermodynamic forces. In equilibrium both forces have the same value and thus the so called affinities $\mathcal{F}^i$ are zero. In nonequilibrium these forces drive the system to a stationary state if one exists.

Considering only energy exchange between the subunits, (2.18) reads, in the entropic representation,

$$\mathcal{F}^i = \frac{1}{T_1} - \frac{1}{T_2}. \tag{2.19}$$

As can be seen a temperature gradient drives the system by causing a heat flow between both subunits. The response to this force are the $\frac{\mathrm{d}X^i}{\mathrm{d}t}$ which are the currents J^i defined by

$$J^i := \frac{\mathrm{d}X^i}{\mathrm{d}t}. \tag{2.20}$$

Finally, the rate of entropy production is given by

$$\frac{\mathrm{d}S}{\mathrm{d}t} = \sum_i \frac{\partial S}{\partial X_1^i}\frac{\mathrm{d}X_1^i}{\mathrm{d}t} = \sum_i \mathcal{F}^i J^i, \tag{2.21}$$

the sum of the products of each affinity with its associated current.

This procedure can be extended to continuous systems where the extensive quantities are substituted by densities [$X^i \to x(q,t)$, with the position vector q] and intensive parameters will become fields [e. g., $T \to T(q,t)$]. The rate of the local entropy production σ is then given by

$$\sigma = \frac{\partial s}{\partial t} + \nabla \cdot J^s. \tag{2.22}$$

Note that, as a result of the 2nd law, σ can never become negative. If the extensive parameters are constants the rate of change of the respective densities is connected to the currents J^i via

$$\frac{\partial x^i}{\partial t} + \nabla \cdot J^i = 0, \tag{2.23}$$

which is a continuity equation. Specifically, the energy current per volume takes the form

$$\frac{\partial u}{\partial t} + \nabla \cdot J_u = 0 \tag{2.24}$$

A simplification can be obtained by considering only linear systems. These are systems without memory and they behave purely resistive.[2] In this case the currents only depend on the affinities at the same instant. E.g., Ohm's law of electrical and Fourier's law of heat conduction belong to this kind of class. To understand the procedure one can expand the currents in the power of the affinities

$$J_i = \sum_i L_{ji}\mathcal{F}_J + \frac{1}{2!}\sum_{k,j} L_{kji}\mathcal{F}_k\mathcal{F}_j + \cdots . \tag{2.25}$$

[2] E.g., an inductance in a circuit is not purely resistive.

L_{ji} is the matrix of transport coefficients

$$L_{ji} = \frac{\partial J_i}{\partial \mathcal{F}_j} \tag{2.26}$$

and the L_{kji} are the second-order transport coefficients given by

$$L_{kji} = \frac{\partial^2 J_i}{\partial \mathcal{F}_k \partial \mathcal{F}_j} \tag{2.27}$$

Eq. (2.27) and higher orders, which are similarly defined, can be neglected in the linear regime. Using the Onsager reciprocity (cf. [69, 70]) the matrix L_{ji} has to be symmetric $L_{ji} = L_{ij}$. These are the basics of the linear response theory leading to the Kubo-formula (cf. [53]).

2.5. Heat Conduction: Fourier's Law

Heat conduction can be observed if two bodies or systems at different temperatures are brought into contact with each other in such a way, that they can exchange energy and thus heat. The heat flows according to the 2nd law, from the hot to the cold system. It was J. B. J. Fourier (1822) (see, e.g., [31]) who found a phenomenological equation for the thermal conduction, namely

$$J = -\kappa \nabla T. \tag{2.28}$$

Here, J is the heat current given by the change of heat Q of a system, ∇T the temperature gradient and κ the thermal conductivity. The quantity κ is a property of the investigated material. In general, there exists no theoretical method to estimate κ.

To derive (2.28) one considers a volume of some material with the density ρ per volume and a heat capacity c per mass at temperature $T(x, y, z)$. In general, $T(x, y, z)$ is a scalar field depending on all three coordinates. In an infinitesimal volume $\mathrm{d}V$ one can find the infinitesimal heat

$$\mathrm{d}Q = \int_V c\rho T(x, y, z)\mathrm{d}V. \tag{2.29}$$

The change of heat (which is nothing else than the change of energy) is equivalent to the change of temperature

$$-\frac{\partial Q}{\partial t} = -\frac{\partial}{\partial t} \int \rho c T \mathrm{d}\tau. \tag{2.30}$$

On the other side the heat flowing out of the volume is given by the current through the surface of this volume

$$-\frac{\partial Q}{\partial t} = -\kappa \oint \nabla T \mathrm{d}\boldsymbol{f}. \tag{2.31}$$

By combining (2.30) with (2.31) we get the following balance equation

$$\begin{aligned} \frac{\partial}{\partial t} \int \rho c T \mathrm{d}\tau &= \kappa \oint \nabla T \mathrm{d}\boldsymbol{f} \\ &= \kappa \int \nabla \cdot \nabla T \mathrm{d}V \end{aligned} \tag{2.32}$$

with the help of Gauß integral.

3. Modular Quantum Systems

> One aspect of statistical mechanics is the study of models. It should be appreciated that almost all Hamiltonians, even those regarded as "fundamental" are really models, even if they cannot be solved exactly.
>
> E. H. Lieb in [55]

Almost everything we find in nature is composed of millions and millions of atoms which by themselves are constructed out of subatomic particles sometimes called the particle zoo. This is more or less well established within the framework of quantum mechanics. In the present work the modular character of nature is mimicked by using quantum systems constructed out of (mainly) weakly interacting subsystems. Due to the fact that many particle physics is a puzzling and mostly not exactly solvable problem, we restrict ourselves to two-level systems (TLS), especially, spin systems. We do so due to the simplicity in representation and calculation. But it would lead in the wrong direction to say that the results obtained within this work are only restricted to spins.

The modular character is also important for the study of thermal transport and processes. E.g., for one-dimensional chains it is necessary to know the structure of the subunits and their couplings. If the interaction between the subunits would not exchange energy, no thermal process was possible. Also for the interaction between a heat bath and a system, and especially which part of the system does interact with the bath, the modularity is important. Otherwise it would not be so easy to get nonequilibrium situations (which are definitely observable in nature).

3.1. Model System

To simulate a scenario as presented in the introduction to this chapter the Hamiltonian of a system will have the form

$$\hat{H} = \sum_{\mu} \hat{H}_{\mu}^{\mathrm{loc}} + \lambda \hat{V}_{\mu,\mu+1}. \tag{3.1}$$

$\hat{H}_{\mu}^{\mathrm{loc}}$ is the local Hamiltonian of subunit μ with next nearest-neighbor interaction $\hat{V}_{\mu,\mu+1}$ of the strength λ. If one want to stay in the weak coupling limit the following relation must be fulfilled, $\lambda \lll \langle \hat{H}_{\mu} \rangle$.

The Heisenberg coupled spin-chain with a next nearest-neighbor interaction is a well known and widely studied system in solid state physics (see e.g. [38, 91]). The Hamiltonian is given by

$$\hat{H} = \sum_{\mu} \left[\frac{\delta_{\mu}}{2} \hat{\sigma}^z + \lambda \left(\sum_{i=x,y} \sigma_{\mu}^i \otimes \sigma_{\mu+1}^i + \Delta \hat{\sigma}^z \otimes \hat{\sigma}^z \right) \right], \tag{3.2}$$

with the Pauli-operators σ^i of the μth spin and a so called anisotropy factor Δ. Eq. (3.2) is also known as the XXX or isotropic model if $\delta_{\mu} = \lambda$. By introducing different parameters for the different parts for the spatial components in the second part of (3.2) of the form λ_x, λ_y and λ_z the model becomes anisotropic and one distinguishes different kind of models (e.g. XXZ, XYZ, etc.). The XXX model can further be distinguished through the sign of λ. In the present form for $\lambda > 0$ one speaks of an antiferromagnetic chain whereas if λ is negative it is a ferromagnetic chain. Excluding the $\hat{\sigma}^z$ part of the interaction part in (3.2) leads to the Förster coupling [60]. Furthermore the chain will be called inhomogeneous if the δ_{μ}'s are different.

3.2. Evolution of a system

The evolution of the state of a quantum system is given by the time dependent Schrödinger-equation

$$\frac{\mathrm{d}}{\mathrm{d}t} |\psi(t)\rangle = -\frac{i}{\hbar} \hat{H}(t) |\psi(t)\rangle. \tag{3.3}$$

The state $|\psi(t)\rangle$ evolves under a unitary time-evolution from an initial state $|\psi(t_0)\rangle$

$$|\psi(t)\rangle = \hat{U}(t, t_0) |\psi(t_0)\rangle. \tag{3.4}$$

$U(t, t_0)$ is the so called time-evolution operator. The time derivative of (3.4) reads

$$\frac{\partial}{\partial t}\hat{U}(t) = -\mathrm{i}\hat{H}(t)\hat{U}(t, t_0) \tag{3.5}$$

For a time independent Hamiltonian (3.5) can be integrated to

$$\hat{U}(t, t_0) = \mathrm{e}^{-\mathrm{i}\hat{H}(t-t_0)}, \tag{3.6}$$

which is valid for conservative systems. By introducing the density operator of a system,

$$\hat{\rho}(t_0) = \sum_i p_i |\psi_i(t_0)\rangle\langle\psi_i(t_0)|, \tag{3.7}$$

the evolution of (3.7) is given by the Liouville-von Neumann-equation [95]

$$\frac{\mathrm{d}}{\mathrm{d}t}\hat{\rho}(t) = -\mathrm{i}\left[\hat{H}, \hat{\rho}(t)\right]. \tag{3.8}$$

This can be cast in a form analogous to the Schrödinger-equation

$$\frac{\mathrm{d}}{\mathrm{d}t}\hat{\rho}(t) = \hat{\mathcal{L}}(t)\hat{\rho}(t). \tag{3.9}$$

where we have introduced the super- or Liouville operator $\hat{\mathcal{L}}$. $\hat{\rho}(t)$ are now states in the Liouville-space [29]. As for the dynamics of $|\psi(t)\rangle$ a formal solution can be obtained by

$$\hat{\rho}(t) = \mathrm{e}^{\hat{\mathcal{L}}(t-t_0)}\hat{\rho}(t_0). \tag{3.10}$$

3.3. Environment

To study thermodynamic properties of small systems, they have to be embedded into a much larger environment, which is able to impart thermodynamical behavior onto the small system. Otherwise the validity of the concepts presented in Chap. 2 cannot be guaranteed anymore. Different kind of properties has to be satisfied by an environment (especially the interaction between the system and the environment has to be small) to enable an environment to act as thermal bath. E.g., a heat bath should be able to induce a stationary state onto the system which could be represented by one parameter, the temperature T.

As developed in [33] it is even possible that the Schrödinger dynamics can show thermal behavior if one splits the complete system into a small part, the system under investigation, and a much larger part acting as environment for the system. The global von Neumann entropy does not change due to the fact that the Schrödinger dynamics is unitary. But for the reduced system of interest the local von Neumann entropy will be maximized as stated by the 2nd law of thermodynamic [34, 71]. Thus thermodynamics emerges from Schrödinger dynamics under proper constraints.

That this could happen even for relatively small environments is a result of the structure of the tensor-Hilbert space, where the dimension is multiplicative, in contrast to classical phase-space, which is additive. One could say that the thermodynamic limit is thus taken over the dimensions of the Hilbert space. It is this fact, the larger embedding, which enables us to give even a single spin thermodynamic properties like temperature.

On the other side the fast growing of the Hilbert space dimensions prevents us to solve large systems. Therefore one is searching for different kind of techniques enabling the computation of such systems. One possible way to solve this problem is the open system approach leading to rate equations or to the so called quantum master equation (QME) described in Chap. 4.

4. Thermal Environment

> It (completely positive maps) is very powerful magic: the interaction sits apart from the system and the reservoir and does nothing; by doing so, it forces the motion of the system to be completely positive, with dramatically physical consequences.
>
> P. Pechukas in [73]

The relaxation of a quantum system to a stationary thermal state has been under debate for quite a long time. To observe this relaxation different kind of approaches can be found. E.g., thermalizing a quantum systems can be achieved by pure Schrödinger dynamics (cf. [33]), the path integral approach introduced by Feynman and Vernon [28, 98], or with the quantum master equation (QME) (cf. [10]). The present work relies on the QME, although many problems with the derivation and especially with the used approximations are known (see e.g., [11]). On the other side the QME has servered as tool over more then four decades. The advantage of the QME lies in its great flexibility and a wide range of applications on different topics like, e.g., quantum optics [96], molecular dynamics [62], etc.

4.1. Open System Approach

A well known and often studied approach to thermal relaxation for quantum systems is the quantum master equation (QME) approach. The considered system is coupled to an environment or heat bath, which is, in general, much larger as the considered system. The complete dynamics of this closed system is often not exactly solvable, because the Hilbert space of the total system is vast.

The problem could be avoided by concentrating on the dynamics of the quantum system which shall be thermalized. Instead of studying the dynamics of the total closed system, one studies only the small system, which is thus considered as an open system. The influence of the environment is then only acting as a dissipative part on the small system dynamics.

4.2. Projection Operator Technique

A way to describe the dynamics of open systems exactly is given by the projection operator technique based on Nakajima [67] and Zwanzig [102, 103]. The idea behind this is that by studying a system one is not interested in the complete dynamics. Instead, only a relevant part of the system is considered, whereas the rest or irrelevant part (the environment) will be contracted. The total Hamiltonian of a large system

$$\hat{H} = \hat{H}_\mathrm{s} + \hat{H}_\mathrm{env} + \alpha \hat{H}_\mathrm{int} \tag{4.1}$$

is composed of the Hamiltonian of the relevant system $\hat{H}_\mathrm{s}$, a Hamiltonian of the environment $\hat{H}_\mathrm{env}$ and the interaction between system and environment $\hat{H}_\mathrm{int}$ scaled with the interaction strength α. The Liouville-von Neumann equation for the density matrix $\hat{\rho}(t)$ of the whole system reads

$$\frac{\mathrm{d}}{\mathrm{d}t}\hat{\rho}(t) = -\mathrm{i}[\hat{H}, \hat{\rho}] = \mathrm{i}\hat{\mathcal{L}}\rho(t). \tag{4.2}$$

$\hat{\mathcal{L}}$ is a super-operator in Liouville-space (see Sect. 3.2). Then, a super-operator $\hat{\mathcal{P}}$ is introduced which projects onto the relevant part of the system,

$$\hat{\mathcal{P}}\hat{\rho}(t) = \mathrm{Tr}_\mathrm{env}\left\{\hat{\rho}(t)\right\} \otimes \hat{\rho}_\mathrm{env} := \hat{\rho}_\mathrm{s}(t) \otimes \hat{\rho}_\mathrm{env} \tag{4.3}$$

with an arbitrary fixed state $\hat{\rho}_\mathrm{env}$ of the environment. It can be checked that $\hat{\mathcal{P}}$ fulfills the projection operator properties (see e.g. [10]). As mentioned above, it is also possible to introduce a projection $\hat{\mathcal{Q}}$ which only takes the information of the irrelevant part into account

$$\hat{\mathcal{Q}}\hat{\rho}(t) = (\hat{1} - \hat{\mathcal{P}})\hat{\rho}(t), \tag{4.4}$$

the Liouville-von Neumann equation (4.1) can thus be divided into two parts

$$\frac{\mathrm{d}}{\mathrm{d}t}\hat{\mathcal{P}}\hat{\rho}(t) = \hat{\mathcal{P}}\hat{\mathcal{L}}\hat{\mathcal{P}}\hat{\rho}(t) + \hat{\mathcal{P}}\hat{\mathcal{L}}\hat{\mathcal{Q}}\hat{\rho}(t) \tag{4.5}$$

$$\frac{\mathrm{d}}{\mathrm{d}t}\hat{\mathcal{Q}}\hat{\rho}(t) = \hat{\mathcal{Q}}\hat{\mathcal{L}}\hat{\mathcal{Q}}\hat{\rho}(t) + \hat{\mathcal{Q}}\hat{\mathcal{L}}\hat{\mathcal{P}}\hat{\rho}(t) \tag{4.6}$$

with the help of

$$\hat{\rho} = (\hat{\mathcal{P}} + \hat{\mathcal{Q}})\hat{\rho}. \tag{4.7}$$

The solution of (4.6) can be inserted into (4.4) and integrated startin with an initial state $\hat{\rho}(t_0)$

$$\frac{\mathrm{d}}{\mathrm{d}t}\hat{\mathcal{P}}\hat{\rho}(t) = \hat{\mathcal{P}}\hat{\mathcal{L}}\hat{\mathcal{P}}\rho(t) + \hat{\mathcal{P}}\hat{\mathcal{L}}\int_{t_0}^{t}\mathrm{d}s\exp\left[(t-s)\hat{\mathcal{Q}}\hat{\mathcal{L}}\right]\hat{\mathcal{Q}}\hat{\mathcal{L}}\hat{\mathcal{P}}\hat{\rho}(t) + \\ + \hat{\mathcal{P}}\hat{\mathcal{L}}\exp\left[(t-t_0)\hat{\mathcal{Q}}\hat{\mathcal{L}}\right]\hat{\mathcal{Q}}\hat{\rho}(t_0). \tag{4.8}$$

This integro-differential equation contains the complete information about the evolution of the system without approximations. The second term is a memory term including all information from the initial time t_0 to t and is referred to non-Markovian behavior. Thus (4.8) is mostly not easier to solve than the complete Liouville-von Neumann equation (4.2).

Eq. (4.8) can be simplified for proper initial conditions like a factorisable state $\hat{\rho}(t_0) = \hat{\rho}_s(t_0) \otimes \hat{\rho}_{\mathrm{env}}$ for which

$$\hat{\mathcal{Q}}\hat{\rho}(t_0) = 0, \tag{4.9}$$

is satisfied and the last term in (4.8) vanishes.

In order to solve (4.8) it is, on the one hand, possible to make an expansion in the coupling constant α up to second order. On the other hand, to regain a markovian behavior one continues with a coarse grained description in time. This coarse graining is satisfied, if the relaxation time of the memory effects is much shorter than the time-scale, on which the state of the system is changing. The obtained markovian quantum master equation with the so called *Born-Approximation* finally reads

$$\frac{\mathrm{d}}{\mathrm{d}t}\hat{\mathcal{P}}\hat{\rho}(t) = \hat{\mathcal{P}}\hat{\mathcal{L}}\hat{\mathcal{P}}\hat{\rho}(t) + \hat{\mathcal{P}}\hat{\mathcal{L}}\int_{t_0}^{t}\mathrm{d}s\exp\left[(t-s)\hat{\mathcal{Q}}\hat{\mathcal{L}}\right]\hat{\mathcal{Q}}\hat{\mathcal{L}}\hat{\mathcal{P}}\hat{\rho}(t) \tag{4.10}$$

Going to the description for the reduced density matrix $\hat{\rho}_{\mathrm{s}}$ of the relevant system in the interaction picture (4.10) is given by

$$\frac{\mathrm{d}}{\mathrm{d}t}\hat{\rho}_{\mathrm{s}}(t) = -\alpha^2\int_{t_0}^{t}\mathrm{d}s\,\mathrm{Tr}_{\mathrm{env}}\left\{[\hat{H}_{\mathrm{int}},[\hat{H}_{\mathrm{int}}(t-s),\hat{\rho}_{\mathrm{s}}(t)\otimes\hat{\rho}_{\mathrm{env}}]]\right\}. \tag{4.11}$$

This is the so called Redfield equation [77] which is still in Markovian form because of the coarse graining in time. Note that (4.11) is local in time because of the Born-Approximation.

In general, the interaction between the system and environment is given by

$$\hat{H}_{\mathrm{int}} = \sum_k \hat{X}_k \otimes \hat{Y}_k, \tag{4.12}$$

where the hermitian operators $\hat{X}_k$ belong to the system and the $\hat{Y}_k$ to the environment. In the interaction picture they take the form

$$\hat{X}_k(t) = \mathrm{e}^{\mathrm{i}\hat{H}_\mathrm{s}t}\hat{X}_k\mathrm{e}^{-\mathrm{i}\hat{H}_\mathrm{s}t} \tag{4.13}$$

$$\hat{Y}_k(t) = \mathrm{e}^{\mathrm{i}\hat{H}_\mathrm{env}t}\hat{Y}_k\mathrm{e}^{-\mathrm{i}\hat{H}_\mathrm{env}t} \tag{4.14}$$

Inserting (4.12) with the interaction representation (4.13) and (4.14) into (4.11) yields

$$\frac{\mathrm{d}\hat{\rho}_\mathrm{s}(t)}{\mathrm{d}t} = -\alpha^2\int_{t_0}^{t}\mathrm{d}s\,\mathrm{Tr}_\mathrm{env}\left\{\left[\sum_k \hat{X}_k(t)\hat{Y}_k(t),\left[\sum_l \hat{X}_l(s)\hat{Y}_l(s),\rho_\mathrm{s}(t)\hat{\rho}_\mathrm{env}\right]\right]\right\}, \tag{4.15}$$

where we used the abbreviation $\hat{X}_k(t)\hat{Y}_k(t) = \hat{X}_k(t)\otimes\hat{Y}_k(t)$. To proceed, further assumptions about the environment have to be taken. Typical for thermodynamic purposes is that the environment is in a thermal equilibrium state fulfilling the condition

$$[\hat{H}_\mathrm{env},\hat{\rho}_\mathrm{env}] = 0. \tag{4.16}$$

Introducing the bath correlation functions

$$\Gamma_{lk}(t,s) = \mathrm{Tr}_\mathrm{env}\left\{\hat{Y}_l(t)\hat{Y}_k(s)\hat{\rho}_\mathrm{env}\right\} \tag{4.17}$$

and making use of (4.14) and (4.16) and the permutation relation under the trace operation, the following relations hold

$$\Gamma_{lk}(t,s) = \mathrm{Tr}_\mathrm{env}\left\{\hat{Y}_l(t-s)\hat{Y}_k(0)\hat{\rho}_\mathrm{env}\right\} = \Gamma_{lk}(t-s) \tag{4.18}$$

$$\Gamma^*_{lk}(t,s) = \mathrm{Tr}_\mathrm{env}\left\{\hat{\rho}_\mathrm{env}\hat{Y}_k(0)\hat{Y}_l(s-t)\right\} = \Gamma_{kl}(s-t). \tag{4.19}$$

By unraveling the double commutator in (4.15) with the help of the bath correlation functions, this leads to

$$\frac{\mathrm{d}\hat{\rho}_\mathrm{s}(t)}{\mathrm{d}t} = \alpha^2\sum_{k,l}\int_{t_0}^{t}\mathrm{d}s\Gamma_{lk}(t,s)\left[\hat{X}_k(s)\hat{\rho}_\mathrm{s}(t),\hat{X}_l(t)\right] + \mathrm{H.\ c.}. \tag{4.20}$$

Transforming (4.20) back to the Schrödinger picture and using the substitution $t-s=\tau$, the QME reads

$$\frac{\mathrm{d}\hat{\rho}_\mathrm{s}(t)}{\mathrm{d}t} = -\mathrm{i}[\hat{H}_\mathrm{s},\hat{\rho}_\mathrm{s}(t)] + \alpha^2\sum_{k,l}\int_{t_0}^{t}\mathrm{d}s\Gamma_{lk}(\tau)\left[\hat{X}_k(-\tau)\hat{\rho}_\mathrm{s}(t),\hat{X}_l(0)\right] + \mathrm{H.\ c.}.$$

(4.21)

The second term in (4.21) is the so called dissipator, abbreviated by

$$\hat{\mathcal{D}}(\hat{\rho}_{\mathrm{s}}(t)) := \alpha^2 \sum_{k,l} \int_{t_0}^{t} \mathrm{d}s \Gamma_{lk}(\tau) \left[\hat{X}_k(-\tau)\hat{\rho}_{\mathrm{s}}(t), \hat{X}_l(0) \right] + \text{H. c.}. \tag{4.22}$$

4.3. Secular Approximation and Lindblad-form

It was shown in [22] that (4.11) is not the generator of a dynamical semi-group. In short, a dynamical semi-group would map density operators onto density operators. All properties like the trace and positivity of a density operator are conserved by a generator of the proper form. In order to obtain a QME which fulfills these properties one has to perform an additional approximation, the so called *secular approximation* (SA).

In order to do this approximation one has to take a closer look at the system-bath coupling operators of (4.12). The operators $\hat{X}_k$ belonging to the system are now decomposed into operators of the system Hamiltonian $\hat{H}_{\mathrm{s}}$

$$\hat{X}_k(\omega) = \sum_{\epsilon' - \epsilon = \omega} \hat{\Pi}(\epsilon) \hat{X}_k \hat{\Pi}(\epsilon'). \tag{4.23}$$

Here, ϵ are the eigenvalues of $\hat{H}_{\mathrm{s}}$ and $\hat{\Pi}(\epsilon)$ are the respective projection operators onto the eigenspaces. Summing up over all possible frequencies one gets again

$$\hat{X}_k = \sum_{\omega} \hat{X}_k(\omega) \tag{4.24}$$

The operators (4.24) obey the relations

$$\hat{X}_k^\dagger(\omega) = \hat{X}_k(\omega), \tag{4.25}$$

$$[\hat{H}_{\mathrm{s}}, \hat{X}_k(\omega)] = -\omega \hat{X}_k(\omega) \quad \text{and} \tag{4.26}$$

$$[\hat{H}_{\mathrm{s}}, \hat{X}_k^\dagger(\omega)] = +\omega \hat{X}_k^\dagger(\omega). \tag{4.27}$$

With the help of this, the interaction picture operators are now easily obtained

$$\mathrm{e}^{\left(\mathrm{i}\hat{H}_{\mathrm{s}}t\right)} \hat{X}_k(\omega) \mathrm{e}^{\left(-\mathrm{i}\hat{H}_{\mathrm{s}}t\right)} = \mathrm{e}^{\left(-\mathrm{i}\hat{H}_{\mathrm{s}}t\right)} \hat{X}_k(\omega), \tag{4.28}$$

$$\mathrm{e}^{\left(\mathrm{i}\hat{H}_{\mathrm{s}}t\right)} \hat{X}_k^\dagger(\omega) \mathrm{e}^{\left(-\mathrm{i}\hat{H}_{\mathrm{s}}t\right)} = \mathrm{e}^{\left(\mathrm{i}\hat{H}_{\mathrm{s}}t\right)} \hat{X}_k^\dagger(\omega), . \tag{4.29}$$

The decomposition (4.24) thus enables transitions between the different discrete energy levels. The complete interaction Hamiltonian (4.12) in the interaction picture reads now

$$\hat{H}_{\mathrm{int}} = \sum_k \sum_\omega \mathrm{e}^{-\mathrm{i}\omega t} \hat{X}_k(\omega) \otimes \hat{Y}_k(t) = \sum_k \sum_\omega \mathrm{e}^{\mathrm{i}\omega t} \hat{X}_k(\omega)^\dagger \otimes \hat{Y}_k^\dagger(t). \quad (4.30)$$

Here $\hat{Y}_k(t) = \mathrm{e}^{-\mathrm{i}\omega t}\hat{Y}_k\mathrm{e}^{\mathrm{i}\omega t}$ are the interaction picture operators of the environment. Putting (4.30) into the QME (4.11) yields

$$\frac{\mathrm{d}\hat{\rho}_{\mathrm{s}}(t)}{\mathrm{d}t} = \sum_{\omega,\omega'} \sum_{k,l} \mathrm{e}^{\mathrm{i}(\omega'-\omega)t} \Gamma_{kl}(\omega)[\hat{X}_l(\omega)\hat{\rho}_{\mathrm{s}}(t), \hat{X}_k^\dagger(\omega')] + \mathrm{H.c.}, \quad (4.31)$$

where the Fourier transform of $\Gamma_{lk}(t)$

$$\Gamma_{lk}(\omega) = \int_{-\infty}^{\infty} \mathrm{d}t \mathrm{e}^{\mathrm{i}\omega t} \Gamma_{lk}(t) \quad (4.32)$$

is used.

By performing the secular approximation, terms of the form, where $\omega' \neq \omega$ in (4.31), are being neglected. This is motivated by the fact that these so called non-secular terms oscillate much faster than the system relaxes. Eq. (4.31) thus simplifies to

$$\frac{\mathrm{d}\hat{\rho}_{\mathrm{s}}(t)}{\mathrm{d}t} = \sum_\omega \sum_{k,l} \Gamma_{kl}(\omega)[\hat{X}_l(\omega)\hat{\rho}_{\mathrm{s}}(t), \hat{X}_k^\dagger(\omega)] + \mathrm{H.c.} \quad (4.33)$$

By rearranging the correlation functions into a real and imaginary part the imaginary part will be cast into the so called Lamb-shift ($\hat{H}_{\mathrm{L}}$) and one arrives finally at

$$\frac{\mathrm{d}\hat{\rho}_{\mathrm{s}}(t)}{\mathrm{d}t} = -\mathrm{i}[\hat{H}_{\mathrm{L}}, \hat{\rho}_{\mathrm{s}}] + \sum_\omega \sum_{k,l} \gamma_{kl}(\omega)[\hat{X}_l(\omega)\hat{\rho}_{\mathrm{s}}(t), \hat{X}_k^\dagger(\omega)] + \mathrm{H.c.}. \quad (4.34)$$

In order to proof if we now have a generator of a dynamical semi-group the correlation functions $\gamma_{kl}(\omega)$ can be transformed in a basis where they are diagonal. If the $\gamma_{kl}(\omega)$ are positive, (4.34) possess the desired property and is then the celebrated Lindblad-equation.

The advantage of the Lindblad-form (4.34) is its structure and its generality. Finding some environment operators $\hat{X}$, the system will always be damped in a manner, such that all basic properties of $\hat{\rho}_{\mathrm{s}}$ are conserved. On the other side, this bears the risk to write down environment operators, which are not

realizable within a concrete physical scenario. An important application of the Lindblad-equation is the stochastic unravelling [15, 75]. This method is a powerful tool for numerical simulations which can be much more efficient as a QME in non-Lindblad-form .

4.4. Example: TLS in Contact with a Heat Bath

To give an intuitive example for the derived QME, the decay of a TLS is treated with focus on the difference between the Redfield-equation (4.11) and the Lindblad-equation (4.34). The example is orientated on the optical QME which can be found in many textbooks on Quantum Optics (cf. [10, 60, 96]). The Hamiltonian of the TLS is given by

$$\hat{H}_\mathrm{s} = \frac{\delta}{2}\hat{\sigma}^z, \tag{4.35}$$

with the an energy splitting δ. A system of uncoupled harmonic oscillators with the Hamiltonian

$$\hat{H}_\mathrm{env} = \sum_{k=1}^{\infty} \omega_k \left(\hat{b}_k^\dagger \hat{b}_k + \frac{1}{2}\right) \tag{4.36}$$

is used as a bath. $\hat{b}_k$ and $\hat{b}_k^\dagger$ are the bosonic creation and annihilation operators. The interaction between the bath (or the electro-magnetic field) takes the form

$$\hat{H}_\mathrm{int} = \hat{X} \otimes \left(g_j \hat{b}_j \mathrm{e}^{-\mathrm{i}\omega_j t} + g_j^* \hat{b}_j^\dagger \mathrm{e}^{\mathrm{i}\omega_j t}\right) \tag{4.37}$$

$\hat{X}$ can be decomposed in the transition operators of the form (e.g. [10])

$$\hat{X} = \hat{\sigma}^x = \hat{\sigma}^+ + \hat{\sigma}^-. \tag{4.38}$$

The correlation function is solved with the method as given in App. B. Therefore the QME in Redfield-form reads

$$\begin{aligned}
\frac{\mathrm{d}\hat{\rho}_s(t)}{\mathrm{d}t} &= -\mathrm{i}\left[\hat{H}_s, \hat{\rho}_s(t)\right] + N(1+\omega)\left(\hat{\sigma}^-\hat{\rho}_s(t)\hat{\sigma}^+ - \frac{1}{2}\left[\hat{\sigma}^+\hat{\sigma}^-, \hat{\rho}_s(t)\right]_+\right) + \\
&\quad + N(\omega)\left(\hat{\sigma}^+\hat{\rho}_s(t)\hat{\sigma}^- - \frac{1}{2}\left[\hat{\sigma}^-\hat{\sigma}^+, \hat{\rho}_s(t)\right]_x\right) + \\
&\quad + N(\omega)\left(\hat{\sigma}^+\hat{\rho}_s(t)\hat{\sigma}^+ - \hat{\sigma}^-\hat{\rho}_s(t)\hat{\sigma}^-\right) - \\
&\quad - N(1+\omega)\left(\hat{\sigma}^+\hat{\rho}_s(t)\hat{\sigma}^+ - \hat{\sigma}^-\hat{\rho}_s(t)\hat{\sigma}^-\right).
\end{aligned} \tag{4.39}$$

The last two terms in (4.39) are "sandwich-terms" which would be neglected within the secular approximation. Without them, (4.39) is the well known Lindblad-form for TLS (cf. [10]). The additional sandwich-terms cause a different damping of the off-diagonal elements of $\hat{\rho}_s$.

4.5. Heat Current

The dynamics induced by the QME introduced in the previous sections is irreversible. The incoherent dynamical part (the dissipator) is responsible for the change of the entropy of the considered system. It is possible to calculate the entropy production rate σ for the relaxation process, which is always larger than zero [10].

Of interest for the following chapters is the energy current, which can be obtained with the help of the dissipator. The change of the energy is given by the derivative of $\langle \hat{H}_s \rangle$

$$\frac{\mathrm{d}}{\mathrm{d}t}\langle \hat{H}_s \rangle = \mathrm{Tr}\left\{ \dot{\hat{H}}_s \hat{\rho} \right\} + \mathrm{Tr}\left\{ \hat{H}_s \dot{\hat{\rho}} \right\} \tag{4.40}$$

According to (2.11) only the last term of (4.40) is associated with the heat or energy current. Putting (4.21) into (4.40) yields

$$J = \mathrm{Tr}\left\{ \hat{H}_s \dot{\hat{\rho}}_s \right\} = \mathrm{Tr}\left\{ \hat{H}_s \hat{\mathcal{D}}(\hat{\rho}_s) \right\}. \tag{4.41}$$

J is the energy or heat current induced by a heat bath.

5. Local Thermodynamic Properties of a Quantum System

> No quantum system is completely isolated from its environment. This basic yet fundamental observation has been one of the key insights allowing an appropriate understanding of the dynamical emergence of classical properties in quantum systems.
>
> J. Eisert and M. B. Plenio in [24]

Thermodynamics typically deals with weakly interacting systems in such a way that the energy and entropy still remain extensive variables. As a result, the presented quantities of Chap. 2 are only valid in the so called weak coupling limit. On the other side, in a composite quantum system, even a very weak interaction does influence the local properties of the individual subunits. Therefore it is questionable if all effects of the coupling could and should be negelected when one is interested in local properties of a subunit.

Additionally the definition of the quantities heat and work, although expressed in the language of quantum mechanics, is still borrowed from classical statistical physics. The definitions of heat and work given in (2.14) and (2.13) are problematic for quantum systems. E.g., a time dependent Hamilton operator which induces a driving force to the system may cause inversion in the system. This process cannot be explained with the given definitions of heat and work. Especially a microscopic derivation of heat and work for such kind of processes is quite unclear.

In this chapter we want to derive a concept, which makes it possible to treat interacting quantum systems also from the local point of view. The approach introduces an effective dynamics which sheds new light on the concept of heat and work. After having established the basic concept we will address the local energy current between adjacent systems, in contrast to the boundary energy current between the system and the bath, which have been defined in Sect. 4.5.

5.1. Local Effective Measurement Basis (LEMBAS)

The approach presented in the following will be based on the **LEMBAS**, **L**ocal **E**ffective **M**easurement **Bas**is [97]. The main idea behind it is the fact that a measurement of the energy of some system is performed in a basis chosen by the experimentalist. Take for example a TLS with a local energy splitting. Typically, measuring the spectrum will be performed in the energy eigenbasis of the considered TLS. But if the system under investigation is interacting with the surroundings, they might influence the local energy spectrum. The parts of the interaction which can be expanded in the local measurement basis will contribute to the local spectrum and will thus be measured.

To illustrate the principle take, e.g., a laser which measures the spectrum of a TLS coupled to another TLS. By choosing a specific polarization (e.g., x-direction) the measurement basis is chosen (z-direction). Measuring the spectrum of, say, system A would show an absorption line when the TLS and the laser are in resonance. If the interaction between both TLS possesses a part, which could be detected with a laser in x-polarization this would contribute to the absorption frequency and is thus different from the unperturbed system. As a result a local effective basis is found.

The dynamical behavior of system A in this effective basis can be described with an effective Hamiltonian and the energy change is given by the change of the expectation value of this new effective Hamiltonian. By defining now quantities like heat and work as in Sect. 2.2 it turns out that they are framework or basis dependent.

5.1.1. Effective Dynamics

Consider a bipartite quantum system with the Hamiltonian

$$\hat{H} = \hat{H}_A + \hat{H}_B + \hat{H}_{\text{int}}, \tag{5.1}$$

where $\hat{H}_\mu$ is the local Hamiltonian of subsystem μ and $\hat{H}_{\text{int}}$ the interaction between both systems. Until now, it is still unclear how the effective dynamics induced by the rest of the system onto the considered system looks like. Beginning with the Liouville-von Neumann-equation for the total system

$$\frac{\mathrm{d}\hat{\rho}(t)}{\mathrm{d}t} = -\mathrm{i}\left[\hat{H}, \hat{\rho}(t)\right], \tag{5.2}$$

the reduced dynamics for subsystem A can be obtained by tracing out system B

$$\frac{\mathrm{d}\hat{\rho}_A(t)}{\mathrm{d}t} = -\mathrm{i}\,\mathrm{Tr}_B\left\{\left[\hat{H}_A + \hat{H}_B + \hat{H}_{\mathrm{int}}, \hat{\rho}(t)\right]\right\}. \tag{5.3}$$

Taking into account that $\hat{H}_B$ is traced out, the dynamics of (5.3) and therefore only $\hat{H}_A$ and the interaction $\hat{H}_{\mathrm{int}}$ are responsible for the reduced dynamics of system A. Especially to cope with $\hat{H}_{\mathrm{int}}$ the following factorization of the state is assumed

$$\hat{\rho} = \hat{\rho}_A \otimes \hat{\rho}_B + \hat{C}_{AB}. \tag{5.4}$$

$\hat{C}_{AB}$ includes all possible correlations between system A and B. It is emphasized that still no approximation is made by (5.4). By virtue of (5.4) fulfills the requirements for the factorization approximation (FA, cf. [32]) and putting (5.4) into the right side of (5.3) yields

$$\mathrm{Tr}_B\left\{-\mathrm{i}\left[\hat{H}_{\mathrm{int}}, \hat{\rho}_A \otimes \hat{\rho}_B\right]\right\} = -\mathrm{i}\left[\hat{H}^{\mathrm{eff}}, \hat{\rho}_A\right], \tag{5.5}$$

where effective Hamiltonian $\hat{H}^{\mathrm{eff}}$ has been identified with

$$\hat{H}^{\mathrm{eff}} = \mathrm{Tr}_B\left\{\hat{H}_{\mathrm{int}}(\hat{1}_A \otimes \hat{\rho}_B)\right\}. \tag{5.6}$$

The remaining part of the dynamics will be written as

$$-\mathrm{i}\left[\hat{H}_{\mathrm{int}}, \hat{C}_{AB}\right] \equiv \hat{\mathcal{L}}_{\mathrm{inc}}(\hat{\rho}). \tag{5.7}$$

To understand the motivation behind this identification, we study the time derivative of the local von Neumann-entropy (2.1) of system A:

$$\begin{aligned}
\frac{\mathrm{d}S_A}{\mathrm{d}t} &= -\,\mathrm{Tr}\left\{\frac{\mathrm{d}\hat{\rho}_A}{\mathrm{d}t}\log\hat{\rho}_A + \hat{\rho}_A\frac{\mathrm{d}\log\hat{\rho}_A}{\mathrm{d}t}\right\} \\
&= -\,\mathrm{Tr}\left\{-\mathrm{i}\left(\left[\hat{H}_A + \hat{H}^{\mathrm{eff}}, \hat{\rho}_A(t)\right] + \left[\hat{H}_{\mathrm{int}}, \hat{C}_{AB}\right]\right)\log\hat{\rho}_A\right\} \\
&= -\,\mathrm{Tr}\left\{-\mathrm{i}\left[\hat{H}_{\mathrm{int}}, \hat{C}_{AB}\right]\log\hat{\rho}_A\right\} \\
&= -\,\mathrm{Tr}\left\{\hat{\mathcal{L}}_{\mathrm{inc}}(\hat{\rho})\log\hat{\rho}_A\right\}.
\end{aligned} \tag{5.8}$$

In the second step, it has been observed that the dynamics of $\hat{H}_A$ and $\hat{H}^{\mathrm{eff}}$ are unitary and therefore do not contribute to the change of entropy. In addition the derivation given in App. A was used. We thus note that, only $\left[\hat{H}_{\mathrm{int}}, \hat{C}_{AB}\right]$ contributes to a change of S_A and thus is identified as the incoherent part $\hat{\mathcal{L}}_{\mathrm{inc}}(\hat{\rho})$. If an additional environment, as in the open system approach (cf. Chap. 4) was present, additional incoherent terms would appear as well.

5.1.2. A new Look on Heat and Work

The local dynamics of the reduced density operator, e.g., for system A, $\hat{\rho}_A$, is given by the Liouville-von Neumann-equation

$$\frac{\mathrm{d}\hat{\rho}_A}{\mathrm{d}t} = -\mathrm{i}\left[\hat{H}_A + \hat{H}^{\mathrm{eff}}, \hat{\rho}_A(t)\right] + \hat{\mathcal{L}}_{\mathrm{inc}}(\hat{\rho}). \tag{5.9}$$

Here, $\hat{\rho}$ denotes the density operator of the total system, $\hat{H}^{\mathrm{eff}}$ an effective Hamiltonian induced by the interaction with the subsystem B and $\hat{\mathcal{L}}_{\mathrm{inc}}(\hat{\rho})$ is a superoperator acting on the Liouville-space (a so called incoherent part) of the total system state. Because of $\hat{\mathcal{L}}_{\mathrm{inc}}(\hat{\rho})$, the dynamics given in (5.9) do not lead to closed differential equations anymore.

$\hat{H}^{\mathrm{eff}}$ is now split up into two parts (see Sect. 5.1.1)

$$\hat{H}^{\mathrm{eff}} = \hat{H}_1^{\mathrm{eff}} + \hat{H}_2^{\mathrm{eff}}, \tag{5.10}$$

under the condition that

$$\left[\hat{H}_1^{\mathrm{eff}}, \hat{H}_A\right] = 0 \quad \text{and} \quad \left[\hat{H}_2^{\mathrm{eff}}, \hat{H}_A\right] \neq 0. \tag{5.11}$$

The motivation of this splitting is given by the LEMBAS principle. Because of the interaction between A and B, a local energy measurement would also include a part which is expandable in this local measurement basis[1], if present. The part of (5.11) commuting with the *local* Hamiltonian $\hat{H}_A$ is always included and thus one would get as a new local description an *effective* Hamiltonian

$$\hat{H}_A^{\mathrm{L}} = \hat{H}_A + \hat{H}_1^{\mathrm{eff}}. \tag{5.12}$$

We will use the following notation:

- The Hamiltonian without any interaction will be called *local* without any special index.
- The Hamiltonian obtained with LEMBAS will be called *effective*. We use the index L to indicate the effective description.

This terminology will be used for all following quantities derived with the local or effective Hamiltonian (e.g., temperature, etc.).

The change of the effective energy is now given by

$$\mathrm{d}U = \frac{\mathrm{d}}{\mathrm{d}t}\,\mathrm{Tr}\left\{\hat{H}_A^{\mathrm{L}}\hat{\rho}_A\right\}\mathrm{d}t = \mathrm{Tr}\left\{\frac{\mathrm{d}\hat{H}_A^{\mathrm{L}}}{\mathrm{d}t}\hat{\rho}_A\right\}\mathrm{d}t + \mathrm{Tr}\left\{\hat{H}_A^{\mathrm{L}}\frac{\mathrm{d}\hat{\rho}_A}{\mathrm{d}t}\right\}\mathrm{d}t \tag{5.13}$$

[1] It is possible to proof that this expansion is unique [83].

In contrast to Sect. 2.3, before we define heat and work, we first put (5.9) and (5.12) into (5.13) which results in

$$\mathrm{d}U = \mathrm{Tr}\left\{(\dot{\hat{H}}_A + \dot{\hat{H}}_1^{\mathrm{eff}})\hat{\rho}_A - \mathrm{i}\left[\hat{H}_A^{\mathrm{L}}, \hat{H}_2^{\mathrm{eff}}\right]\hat{\rho}_A\right\}\mathrm{d}t + \mathrm{Tr}\left\{\hat{H}_A^{\mathrm{L}}\hat{\mathcal{L}}_{\mathrm{inc}}(\hat{\rho})\right\}\mathrm{d}t. \quad (5.14)$$

In order to obtain (5.14) the cyclic property of the trace operation was used. Work and heat can now be identified with

$$đW = \mathrm{Tr}\left\{(\dot{\hat{H}}_A + \dot{\hat{H}}_1^{\mathrm{eff}})\hat{\rho}_A - \mathrm{i}\left[\hat{H}_A^{\mathrm{L}}, \hat{H}_2^{\mathrm{eff}}\right]\hat{\rho}_A\right\}\mathrm{d}t \quad \text{and} \quad (5.15)$$

$$đQ = \mathrm{Tr}\left\{\hat{H}_A^{\mathrm{L}}\hat{\mathcal{L}}_{\mathrm{inc}}(\hat{\rho})\right\}\mathrm{d}t. \quad (5.16)$$

The justification of this definition is based on the idea that heat and especially heat flow is linked to entropy and entropy change. Within this definition all kind of processes are describable.

5.2. Effective Dynamics for Interacting Spins

To illustrate the consequences of these definitions, the effective dynamics of two interacting spins is given. It is mentioned that the terminology of work and heat in the case of only a few spins without a thermal environment might be questionable. On the other side it gives an intuitive picture of the principle at work.

The dynamics of two interacting spins is studied with the local Hamiltonian

$$\hat{H}_\mu = \frac{\delta_\mu}{2}\hat{\sigma}^z, \quad (5.17)$$

with $\mu = A, B$. As interaction a Heisenberg type of coupling is chosen of the form [cf. (3.2) with anisotropy $\Delta = 1$]

$$\hat{H}_{\mathrm{int}} = \lambda(\hat{\sigma}^x \otimes \hat{\sigma}^x + \hat{\sigma}^y \otimes \hat{\sigma}^y + \hat{\sigma}^z \otimes \hat{\sigma}^z) \quad (5.18)$$

and with λ being the coupling constant. The effective dynamics $\hat{H}^{\mathrm{eff}}$ of spin A [cf. (5.6)] reads

$$\hat{H}^{\mathrm{eff}} = \mathrm{Tr}_B\left\{\lambda(\hat{\sigma}^x \otimes \hat{\sigma}^x + \hat{\sigma}^y \otimes \hat{\sigma}^y + \hat{\sigma}^z \otimes \hat{\sigma}^z)(\hat{1}_A \otimes \hat{\rho}_B)\right\}. \quad (5.19)$$

The first two terms vanish (see App. C) and only the $\hat{\sigma}^z$ part of the interaction

does contribute to $\hat{H}^{\text{eff}}$ in the form

$$\begin{aligned}\hat{H}^{\text{eff}} &= \text{Tr}_B \left\{ \lambda \begin{pmatrix} 1 & 0 & 0 & 0 \\ 0 & -1 & 0 & 0 \\ 0 & 0 & -1 & 0 \\ 0 & 0 & 0 & 1 \end{pmatrix} \begin{pmatrix} b_{11}(t) & b_{12}(t) & 0 & 0 \\ b_{21}(t) & b_{22}(t) & 0 & 0 \\ 0 & 0 & b_{11}(t) & b_{12}(t) \\ 0 & 0 & b_{21}(t) & b_{22}(t) \end{pmatrix} \right\} \\ &= \lambda \begin{pmatrix} b_{11}(t) - b_{22}(t) & 0 \\ 0 & b_{22}(t) - b_{11}(t) \end{pmatrix} \\ &= -\delta_b(t)\, \hat{\sigma}^z, \end{aligned} \tag{5.20}$$

where $\delta_b(t) = \lambda(b_{11}(t) - b_{22}(t))$ and the b_{ij} are the matrix elements of $\hat{\rho}_B$. $\delta_b(t)$ only influences the local energy splitting as a kind of additional or effective magnetic field. Therefore $\hat{H}_2^{\text{eff}} = 0$ [see (5.10) and (5.11)] and the local effective Hamiltonian (5.12) is given by

$$\hat{H}_A^{\text{L}} = \frac{\delta_A}{2} \hat{\sigma}^z - \delta_b(t)\, \hat{\sigma}^z. \tag{5.21}$$

If a thermal environment was present, both spins would be in a thermal state. Because $\hat{H}_A$ and $\hat{H}_B$ are time-independent and $\hat{\rho}_A$ is diagonal, (5.15) would be zero. Only an effective potential induced by (5.20) is present. For two spins with a Förster interaction [with the anisotropy $\Delta = 0$ and without a $\hat{\sigma}^z$ contribution in (5.18)] $\hat{H}^{\text{eff}} = 0$ and no effective dynamics at all would arise.

The given example for the effective Hamiltonian for two coupled spins could easily be expanded to systems consisting of more spins. The diagonal elements of all the other systems would then contribute to (5.21).

5.3. Probability Flux Through Modular Quantum Systems

For closed quantum systems it can be shown that the Schrödinger dynamics conserves the sum of all occupation probabilities of the system. Analogously as in classical continuum mechanics a probability flux can be derived which satisfies a continuity equation (see, e.g., [20]). Here, we want to derive a continuity equation for quantum systems with an energy exchanging interaction but without particle transport. This is equivalent to the typical thermodynamic situation if one is only interested in heat transport induced by contact equilibrium.

Treating modular quantum systems like spin chains makes it necessary to derive a discrete version of the continuity equation. First, with the help of the

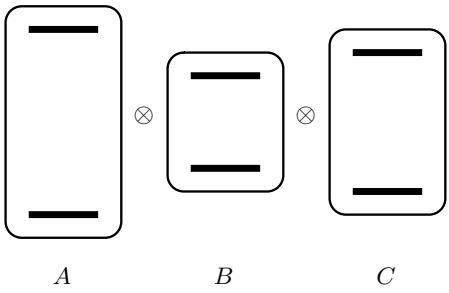

Figure 5.1.: System consisting of three quantum systems, e.g., three TLS with arbitrary local energy splittings.

effective dynamics introduced in Sect. 5.1, the parts responsible for probability exchange are identified. In the next step the probability current could be defined. The presented approach, although derived for spins, is in principle also extendable to n-level systems with a respective coupling.

For simplicity a system with only three subunits is considered as depicted in Fig. 5.1. The system consists of three TLS with an arbitrarily chosen energy splitting. The interaction between two adjacent spins is a Heisenberg coupling and the Hamiltonian reads

$$\hat{H}_s = \hat{H}_A + \hat{H}_B + \hat{H}_C + \hat{V}_{AB} + \hat{V}_{BC}, \tag{5.22}$$

with the local Hamiltonian $\hat{H}_\mu$ and the interaction parts $\hat{V}_{\mu,\mu+1}$. The state of the total system is given by

$$\hat{\rho}_s(t) = \hat{\rho}_A(t) \otimes \hat{\rho}_B(t) \otimes \hat{\rho}_C(t) + \hat{C}_{ABC}. \tag{5.23}$$

The local Liouville-von Neumann-equation (5.9) with the effective Hamiltonian according to (5.20) reads then

$$\begin{aligned} \frac{\mathrm{d}\hat{\rho}_B(t)}{\mathrm{d}t} &= -\mathrm{i}\left[\hat{H}_B^{\mathrm{L}}, \hat{\rho}_B(t)\right] + \hat{\mathcal{L}}_{\mathrm{inc}}(\hat{\rho}(t)) \\ &= -\mathrm{i}\mathrm{Tr}_{AC}\left\{\left[\hat{H}_A + \hat{H}_B + \hat{H}_C + \hat{V}_{AB} + \hat{V}_{BC}, \hat{\rho}(t)\right]\right\}, \end{aligned} \tag{5.24}$$

if no additional dissipator from a thermal environment is present. We are interested in the change of the occupation probabilities of the diagonal elements of $\hat{\rho}_B$ to derive a continuity equation for the probability flux. The probability to find system B in the ground state could be obtained by a projection onto the respective subspace. The coherent part of (5.24) is unitary and conserves

thus probability per definition. Therefore only the flux induced by $\hat{\mathcal{L}}_{\rm inc}(\hat{\rho}(t)$ has to be considered (see 5.8)

$$\frac{\mathrm{d}\hat{\rho}_B(t)}{\mathrm{d}t} = -\mathrm{i}\mathrm{Tr}_{AC}\left\{\left[\hat{V}_{AB}+\hat{V}_{BC},\hat{C}_{AB}(t)\right]\right\}. \tag{5.25}$$

If the projection operators $\hat{P}_{ii}$ $(i=1,2)$ act on (5.24) and a Heisenberg interaction is assumed for an arbitrary state $\hat{\rho}(t)$ the change of p_B induced by the incoherent dynamics is given by

$$\dot{p}_B^{11} = 2\lambda\left[\underbrace{(c_{35}+c_{46}-c_{53}-c_{64})}_{J^1_{BA}}+\underbrace{(-c_{23}+c_{32}-c_{67}+c_{76})}_{J^1_{BC}}\right] \tag{5.26}$$

and

$$\dot{p}_B^{22} = 2\lambda\left[\underbrace{(-c_{35}-c_{46}+c_{53}+c_{64})}_{J^2_{BA}}+\underbrace{(c_{23}-c_{32}+c_{67}-c_{76})}_{J^2_{BC}}\right]. \tag{5.27}$$

The c_{ij} are the matrix elements of $\hat{\rho}(t)$ which could be time dependent, which is excluded here.

Making use of a discrete continuity equation, the first part of (5.26) is the probability flux between system A and B indicated by J^1_{BA} whereas the second part can be identified with the flux between B and C and is therefore called J^1_{BC}. The same is done in (5.27). By summing up (5.26) and (5.27) one can see that all currents J sum up to zero. As a result the total probability of system B is conserved.

The probability fluxes for system A and C can be derived in an analogous way as for system B. One finds the following relations

$$J^1_{BA} = -J^1_{AB},\ J^2_{BA} = -J^2_{AB},\ J^1_{BC} = -J^1_{CB} \quad \text{and} \quad J^2_{BC} = -J^2_{CB} \tag{5.28}$$

which confirms the total conservation of probability. It is emphasized that the derived probability flux is independent of the effective Hamiltonian, $\hat{H}^{\rm eff}$.

5.4. Local Energy Current in Quantum Systems

As already discussed in Sect. 2.4, when dealing with nonequilibrium states it is interesting to study the currents flowing through the system under investigation. However, especially for the study of energy transport in quantum

systems it is necessary to derive a proper definition for the energy current. For a system in a stationary state the current flowing into a system should be equal the current flowing out of the system if no sources and sinks of energy are present. This is the law of energy conservation which leads to a continuity equation for the energy.

The purpose of this section is twofold. First, it is discussed under what conditions an energy or heat current through a modular quantum system can be defined. Second, we want to check whether the derived energy currents satisfy the extensivity condition. In the following this is done for a spin-chain with a Hamiltonian as given in the previous section and in Sect. 2.4.

In (5.14) the total change of the local energy was given, which separates into a part called $đW$ (5.15) and a part $đQ$ (5.16). In order to derive an energy current we first need to know the form of $\hat{\mathcal{L}}_{\rm inc}$. As in the preceding section one gets for subsystem μ of a system with n subsystems

$$\hat{\mathcal{L}}^{\mu}_{\rm inc} = \sum_{\mu}^{n} \left(-\mathrm{i}\mathrm{Tr}_{\rm rest} \left\{ \left[\hat{H}_{\mu} + \hat{H}_{\rm int}, \hat{\rho}(t) \right] \right\} \right) + \mathrm{i} \left[\hat{H}_{\mu} + \hat{H}^{\rm eff}(\mu), \hat{\rho}_{\mu}(t) \right], \quad (5.29)$$

by taking the trace over the rest of the system. Substituting this into the definition of $đQ$ in (5.15) yields

$$\begin{aligned} đQ = \mathrm{Tr}_{\mu} \left\{ -\mathrm{i}\mathrm{Tr}_{\rm rest} \left\{ \left[\hat{H}^{\rm L}_{\mu}, \sum_{\mu}^{n} \hat{H}_{\mu} + \hat{H}_{\rm int} \right] \hat{\rho}(t) \right\} \right\} + \\ + \mathrm{Tr}_{\mu} \left\{ \mathrm{i} \left[\hat{H}^{\rm L}_{\mu}, \hat{H}_{\mu} + \hat{H}^{\rm eff} \right] \hat{\rho}_{\mu}(t) \right\} \end{aligned} \quad (5.30)$$

where we made use of some trace relations. We already know from (5.21) that

$$\left[\hat{H}^{\rm L}_{\mu}, \hat{H}_{\mu} \right] = 0, \ \left[\hat{H}^{\rm L}_{\mu}, \hat{H}^{\rm eff}(\mu) \right] = 0 \quad \text{and} \quad \left[\hat{H}^{\rm L}_{\mu}, \hat{H}_{\mu+1} \right] = 0. \quad (5.31)$$

Therefore one is left with

$$đQ = \sum_{\mu}^{n} \mathrm{Tr}_{\mu} \left\{ -\mathrm{i}\mathrm{Tr}_{\rm rest} \left\{ \left[\hat{H}^{\rm L}_{\mu}, \hat{H}_{\rm int} \right] \hat{\rho}(t) \right\} \right\} \quad (5.32)$$

or, using $\hat{H}_{\rm int} = \lambda \sum_{\mu}^{n} (\hat{\sigma}^x_{\mu} \otimes \hat{\sigma}^x_{\mu+1} + \hat{\sigma}^y_{\mu} \otimes \hat{\sigma}^y_{\mu+1} + \hat{\sigma}^z_{\mu} \otimes \hat{\sigma}^z_{\mu+1})$ (λ being the interaction strength),

$$đQ = \sum_{\mu}^{n} \mathrm{Tr}_{\mu} \left\{ -\mathrm{i}\mathrm{Tr}_{\rm rest} \left\{ \left[\delta^{\rm L}_{\mu} \hat{\sigma}^z_{\mu}, \lambda (\hat{\sigma}^x_{\mu} \otimes \hat{\sigma}^x_{\mu+1} + \hat{\sigma}^y_{\mu} \otimes \hat{\sigma}^y_{\mu+1}) \right] \hat{\rho}(t) \right\} \right\} \quad (5.33)$$

omitting the $\hat{\sigma}^z$-part of $\hat{H}_{\mathrm{int}}$ because of the commutation-relation and $\delta_\mu^{\mathrm{L}} = \delta_\mu + \delta_\mu(t)$. The commutator can be separated into two parts

$$\begin{aligned}\hat{J}_{\mu-1,\mu} &= \mathrm{i}2\delta_\mu\lambda(\hat{\sigma}_{\mu-1}^+ \otimes \hat{\sigma}_\mu^- - \hat{\sigma}_{\mu-1}^- \otimes \hat{\sigma}_\mu^+) \quad \text{and} \\ \hat{J}_{\mu,\mu+1} &= \mathrm{i}2\delta_\mu\lambda(\hat{\sigma}_\mu^+ \otimes \hat{\sigma}_{\mu+1}^- - \hat{\sigma}_\mu^- \otimes \hat{\sigma}_{\mu+1}^+),\end{aligned} \tag{5.34}$$

which has been derived as energy current operator in [63, 66] by considering the change of the Hamiltonian $\frac{\mathrm{d}}{\mathrm{d}t}\hat{H}_\mu$. The continuity equation for the energy, which was used to get from (5.33) to (5.34), is only satisfied for homogeneous system, where $\delta_\mu = \delta_{\mu+1}$ holds.

This is a result of the derived continuity equation for the probability flux, which is a conserved quantity. The derivation of the heat current is analogous to the derivation of the probability flux. The only difference is that for the heat current the local energy expectation value is taken. For inhomogeneous systems, where δ_μ varies from subsystem to subsystem, the continuity equation for the probability flux is still satisfied. At the same time the heat current (5.34) can no longer satisfy a continuity equation.

5.5. Global and Local Energy Conservation

After having seen that an energy current in the presented local approach cannot be uniquely defined, one could also ask, if the effective and local energies sum up to the global energy, which, for a closed system, should be a conserved quantity. Especially for inhomogeneous systems we saw that the energy current could differ from subsystem to subsystem. On the other side, due to global energy conservation this missing energy must emerge somewhere.

5.5.1. Homogeneous Systems

First, let us check, whether the energy defined with the effective basis $\hat{H}_\mu^{\mathrm{L}}$ of all subunits μ sum up to the global energy. The principle can again easily be studied for two interacting spins with the Hamiltonian given in (3.2). It is assumed that the initial state of both spins is diagonal of the form [2]

$$\hat{\rho}_\mu(0) = \begin{pmatrix} p_\mu & 0 \\ 0 & 1-p_\mu \end{pmatrix}, \tag{5.35}$$

with $\mu = A, B$.

[2] We restrict ourself here due to a clear representation of the basic principle. This is motivated for the study of stationary states, too. There the local state for a TLS is a diagonal one.

Solving the Liouville-von Neumann-equation for the complete system and calculating the energy expectation value for $\hat{H}_s$ leads to

$$\langle \hat{H}_s \rangle = \frac{\delta_A - \delta_B}{2} - \lambda\Delta, \tag{5.36}$$

with the local energy splittings δ_A, δ_B, the coupling strength λ and the anisotropy factor Δ [cf.(3.2)]. In addition, we set $p_A = 0$ and $p_B = 1$ in the following until otherwise stated. This result will be compared with the energy expectation values of the effective Hamiltonian $\hat{H}_\mu^{\mathrm{L}}$. The reduced density operators for system A and B can be obtained by tracing out the respective system. The analytical results can be found in App. D. Here only the results for the homogeneous case $\delta_A = \delta_B = \delta$ is given,

$$\langle \hat{H}_A^{\mathrm{L}} \rangle = \frac{1}{2}\cos(4t\lambda)\left[\delta - 2\Delta\lambda\cos(4t\lambda)\right] \quad \text{and} \tag{5.37}$$

$$\langle \hat{H}_B^{\mathrm{L}} \rangle = -\frac{1}{2}\cos(4t\lambda)\left[\delta + 2\Delta\lambda\cos(4t\lambda)\right], \tag{5.38}$$

Adding (5.38) to (5.37) results in

$$\langle \hat{H}_A^{\mathrm{L}} \rangle + \langle \hat{H}_B^{\mathrm{L}} \rangle = 2\Delta\lambda\cos(4t\lambda)^2. \tag{5.39}$$

This is about the positive factor $2\cos(4t\lambda)^2$ larger than the total energy given in (5.36) by taking into account that the first term of (5.36) vanishes due to $\delta_A = \delta_B$. The somewhat larger energy obtained from $\langle \hat{H}_\mu^{\mathrm{L}} \rangle$ is a result of the interaction, which is included in (5.37) and (5.38) in equal parts. This will become clear by investigating the differential quantities later on. Before, we want to calculate the energy given by the local Hamiltonian $\hat{H}_\mu$, reading

$$\langle \hat{H}_A \rangle = \frac{1}{2}\delta\cos(4t\lambda) \quad \text{and} \tag{5.40}$$

$$\langle \hat{H}_B \rangle = -\frac{1}{2}\delta\cos(4t\lambda). \tag{5.41}$$

The sum of (5.41) and (5.42) is zero because all the energy is "hidden" in the interaction. Finally, the following relation for the different energies holds

$$\sum_\mu \langle \hat{H}_\mu^{\mathrm{L}} \rangle > \langle H_s \rangle > \sum_\mu \langle \hat{H}_\mu \rangle. \tag{5.42}$$

The somewhat larger energy obtained within the effective description can be traced back to the complementarity of each single local energy measurement. Each single measurement includes the complete interaction with the rest of the system.

To see how the energy in the system is moving the different parts of the energy are studied. Because the system is closed, the total energy is conserved. The change of $\langle \hat{H}_\mu^{\mathrm{L}} \rangle$ is given in (5.14), (5.15) and (5.16). For $\delta_a = \delta_b = \delta$ (5.15) reads

$$đW_A = 2\Delta\lambda^2 \sin(8t\lambda) \quad \text{and} \tag{5.43}$$
$$đW_B = 2\Delta\lambda^2 \sin(8t\lambda), \tag{5.44}$$

whereas (5.16) takes the form

$$đQ_A = 2\lambda \left[-\delta \sin(4t\lambda) + \Delta\lambda \sin(8t\lambda)\right] \quad \text{and} \tag{5.45}$$
$$đQ_B = 2\lambda \left[\delta \sin(4t\lambda) + \Delta\lambda \sin(8t\lambda)\right]. \tag{5.46}$$

The sum of all $đW_\mu$ and $đQ_\mu$ does not vanish and is given by

$$D = 8\Delta\lambda^2 \sin(8t\lambda), \tag{5.47}$$

a term quadratic in the order of the coupling strength and thus for very weak coupling neglectable. To understand this deviation, the derivative of the total energy expection value is considered

$$\begin{aligned}\frac{\mathrm{d}}{\mathrm{d}t}\langle \hat{H}_s \rangle &= \frac{\mathrm{d}}{\mathrm{d}t}\langle \hat{H}_A \rangle + \frac{\mathrm{d}}{\mathrm{d}t}\langle \hat{H}_B \rangle + \frac{\mathrm{d}}{\mathrm{d}t}\langle \hat{H}_{\mathrm{int}} \rangle \\ &= \mathrm{Tr}\left\{\hat{H}_A \dot{\hat{\rho}}_A\right\} + \mathrm{Tr}\left\{\hat{H}_B \dot{\hat{\rho}}_B\right\} + \mathrm{Tr}\left\{\hat{H}_{\mathrm{int}}(\dot{\hat{\rho}}_A \otimes \dot{\hat{\rho}}_B)\right\} + \\ &+ \mathrm{Tr}\left\{\hat{H}_{\mathrm{int}} \dot{\hat{C}}_{AB}\right\} + \mathrm{Tr}\left\{\hat{H}_A \dot{\hat{C}}_{AB}\right\} + \mathrm{Tr}\left\{\hat{H}_B \dot{\hat{C}}_{AB}\right\}. \end{aligned} \tag{5.48}$$

The last two terms are equal to zero. For the considered spin system the contributions of the interaction are [3]

$$\begin{aligned}\mathrm{Tr}\left\{\hat{H}_{\mathrm{int}}(\dot{\hat{\rho}}_A \otimes \dot{\hat{\rho}}_B)\right\} &= 4\Delta\lambda^2 \sin(8t\lambda) \\ &= -\mathrm{Tr}\left\{\hat{H}_{\mathrm{int}} \dot{\hat{C}}_{AB}\right\}. \end{aligned} \tag{5.49}$$

As a result of this, one part of the expaction value of $\hat{H}_{\mathrm{int}}$ can be written in

[3] This partition is a result of $\mathrm{Tr}\left\{\hat{H}_{\mathrm{int}} \dot{\hat{\rho}}(t)\right\} = 0$ which is always satisfied and can be traced back to $\left[\hat{H}_s, \hat{H}_{\mathrm{int}}\right] = 0$. The latter is fulfilled for homogeneous spin-chains.

the form

$$\begin{aligned}\mathrm{Tr}\left\{\hat{H}_{\mathrm{int}}(\hat{\rho}_A\otimes\hat{\rho}_B)\right\} &= \frac{1}{2}\mathrm{Tr}_A\left\{\mathrm{Tr}_B\left\{\hat{H}_{\mathrm{int}}(\hat{\rho}_A\otimes\hat{1})(\hat{1}\otimes\hat{\rho}_B)\right\}\right\}+\\ &+\frac{1}{2}\mathrm{Tr}_B\left\{\mathrm{Tr}_A\left\{(\hat{\rho}_A\otimes\hat{1})\hat{H}_{\mathrm{int}}(\hat{1}\otimes\hat{\rho}_B)\right\}\right\}\\ &=\frac{1}{2}\mathrm{Tr}_A\left\{\hat{\rho}_A\underbrace{\mathrm{Tr}_B\left\{\hat{H}_{\mathrm{int}}(\hat{1}\otimes\hat{\rho}_B)\right\}}_{\hat{H}_A^{\mathrm{eff}}}\right\}+\\ &+\frac{1}{2}\mathrm{Tr}_B\left\{\hat{\rho}_B\underbrace{\mathrm{Tr}_A\left\{(\hat{\rho}_A\otimes\hat{1})\hat{H}_{\mathrm{int}}\right\}}_{\hat{H}_B^{\mathrm{eff}}}\right\}. \qquad (5.50)\end{aligned}$$

As indicated, the effective Hamiltonian appears but with a factor 1/2. The derivative of the effective Hamiltonian results in

$$\begin{aligned}\frac{\mathrm{d}}{\mathrm{d}t}\langle\hat{H}_A^{\mathrm{L}}\rangle+\frac{\mathrm{d}}{\mathrm{d}t}\langle\hat{H}_B^{\mathrm{L}}\rangle &= \mathrm{Tr}\left\{\hat{H}_A\dot{\hat{\rho}}_A\right\}+\mathrm{Tr}\left\{\hat{H}_B\dot{\hat{\rho}}_B\right\}+\\ &+\mathrm{Tr}\left\{\dot{\hat{H}}_A^{\mathrm{eff}}\hat{\rho}_A\right\}+\mathrm{Tr}\left\{\dot{\hat{H}}_B^{\mathrm{eff}}\hat{\rho}_B\right\}+\\ &+\mathrm{Tr}\left\{\hat{H}_A^{\mathrm{eff}}\dot{\hat{\rho}}_A\right\}+\mathrm{Tr}\left\{\hat{H}_B^{\mathrm{eff}}\dot{\hat{\rho}}_B\right\} \qquad (5.51)\end{aligned}$$

Comparing this with the derivative of (5.50), it can be seen that by adding twice a correlation current of the form

$$J_{\mathrm{corr}}(t)=\mathrm{Tr}\left\{\hat{H}_{\mathrm{int}}\dot{\hat{C}}_{AB}\right\}=-4\Delta\lambda^2\sin(8t\lambda) \qquad (5.52)$$

would again sum up to zero, because $2J_{\mathrm{corr}}(t)=D$ of (5.47). Next we want to study the influence of this correlation current by means of some numerical data.

The first example are two spins interacting via a Förster type of coupling ($\Delta=0$). Because $\hat{H}^{\mathrm{eff}}=0$ only heat $đQ$ will be exchanged between the spins. Fig. 5.2 shows the heat currents of spin A and spin B as function of time. As can be seen from Fig. 5.2 $đQ_A=-đQ_B$ and thus the energy current is an intensive quantity. The effect of the coupling strength λ on this transport behavior is given in Fig. 5.3. There the amplitudes of $đQ_A$, $đQ_B$ and J_{corr} are depicted as function of λ. With increasing λ also the currents $đQ_\mu$ do increase. J_{corr}, however, is always zero (5.52) and does not affect the transport behavior.

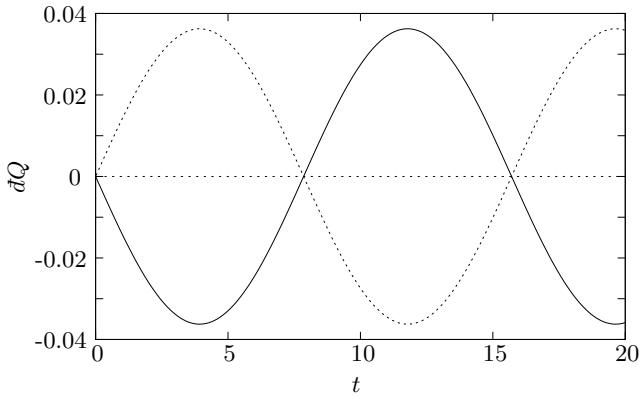

Figure 5.2.: Evolution in time of $đQ$ with the parameter $\delta_A = \delta_B = 1$, $\lambda = 0.01$ and the two states $\hat{\rho}_A = \mathrm{e}^{-\mathrm{i}\hat{H}_A/T_A}$ $(T_A = 5)$ and $\hat{\rho}_B = \mathrm{e}^{-\mathrm{i}\hat{H}_B/T_B}$ $(T_B = 1)$. The solid line represents the current for spin A and the dotted line for spin B

.

A homogeneous Förster coupled system transports energy without inducing correlations.

Now we choose $\Delta = 1$ for the two interacting spins. In contrast to the Förster coupled spin system, in addition to the heat current, a current $đW$ is present induced via $\hat{\sigma}^z \otimes \hat{\sigma}^z$ interaction term [cf. (5.20)]. The evolution in time of $đQ$ (5.16) is shown in Fig. 5.4 and $đW$ (5.15) in Fig. 5.5. Another difference to the Förster coupled spins is given by J_{corr}. In (5.52), J_{corr} is a function of λ and Δ, which is not zero anymore. Therefore correlations will play a crucial role for the energy exchange behavior. In Fig. 5.6, J_{corr} is depicted as function of time. As can be inferred from Fig. 5.5 and Fig. 5.6, for weak coupling (e.g., $\lambda = 0.01$) $đW$ and J_{corr} are of the same order.

The influence of λ on the currents is illustrated in Fig. 5.7. There the amplitudes of the different currents as function of the coupling strength λ are depicted. For very small couplings J_{corr} and $đW$ could be neglected because they do not contribute to the energy current, which is mainly governed by $đQ_\mu$. But with increasing λ, J_{corr} is getting more and more important, and a notable amount of the energy is now included in the interaction.

Finally, the effect of $\hat{H}^{\mathrm{eff}}$ in the Heisenberg system is analyzed by calculating the effective energy splittings δ_μ^{L}. They are depicted as function of time in Fig. 5.8. The local spectrum of each spin is changed by the effective dynamics. This is a kind of additional local potential or binding energy which is given

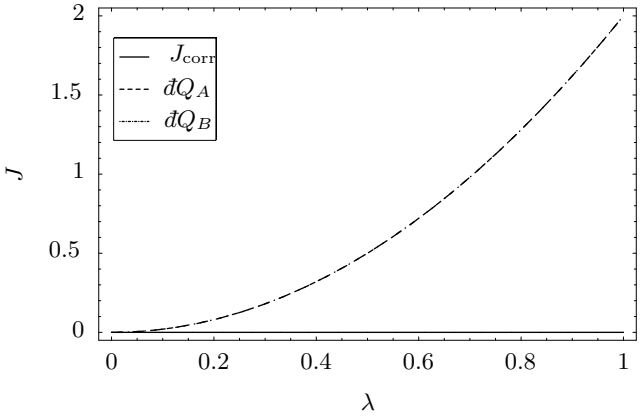

Figure 5.3.: Amplitudes of the currents đQ_A, đQ_B and $J_{\rm corr}$ as function of the coupling strength λ for two Förster coupled spins. We choose $\Delta = 0$, $\delta_A = \delta_B = 1$ and $p_A = 0$, $p_B = 1$.

by

$$\langle E_\mu^{\rm bind}\rangle = {\rm Tr}\left\{\hat{H}_\mu^{\rm eff}\hat{\rho}_\mu(t)\right\} \tag{5.53}$$

From Fig. 5.9, where $\langle E_\mu^{\rm bind}\rangle$ is depicted as function of time, it can be inferred that $\langle E_A^{\rm bind}\rangle = \langle E_B^{\rm bind}\rangle$. This is a property of spin chains and could also be found in larger chains. As a result the effective energy splittings $\delta_\mu^{\rm L}$ and the local states are "aligned" in a manner that $\langle E_A^{\rm bind}\rangle = \langle E_B^{\rm bind}\rangle$ is satisfied.

5.5.2. Inhomogeneous Systems

Like in the foregoing a system of two interacting spins will be discussed. Here the energy splitting of both spins are different, $\delta_A \neq \delta_B$, and we introduce for simplicity a detuning $\omega = \delta_A - \delta_B$. The procedure to calculate the expectation values and the corresponding derivatives are as in the previous sections. Especially we want to demonstrate why the energy current in inhomogeneous spin systems is no longer an intensive quantity, even in the weak coupling limit.

We distinguish, again, the two cases $\Delta = 0$ and $\Delta = 1$. The currents for đQ, đW and $J_{\rm corr}$ are not so simple as for the homogeneous case. They are much more complex due to the crucial role of ω, which contributes to the

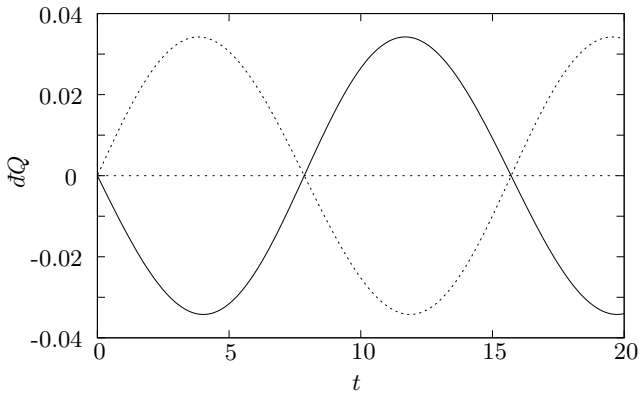

Figure 5.4.: Evolution in time of $đQ$ with the parameters and states as in Fig. 5.2. The solid line represents spin A and the dotted line spin B

currents. The analytical results can be found in App. D. First, we start again with $\Delta = 0$ and study the influence of ω on the behavior of the currents for a Förster coupled system. In Fig. 5.10 the currents are depicted as function of ω (we choose $\delta_B = 1$ and $\delta_A = \delta_B + \omega$). With an increasing detuning ω the heat currents $đQ_\mu$ decrease until $đQ_A \approx J_{\text{corr}}$ and $đQ_B$ gets very small. Instead of the energy flowing out of system A and into system B, it flows into the interaction between both systems and therefore the correlation current is increasing. In contrast to a homogeneous system with $\Delta = 0$, here, J_{corr} plays a crucial role. As a consequence of this result the energy transport cannot be an intensive quantity anymore. This is also true for larger systems with $\mu > 2$. Even in the weak coupling limit the energy current $đQ$ will not be unique throughout the system.

Now the results for a Heisenberg coupled two spin system with $\Delta = 1$ will be discussed. In Fig. 5.11 the amplitudes of the currents are depicted as a function of the detuning ω, as before. In contrast to the Förster scenario, again an additional current $đW$ is present. Nevertheless, the heat currents $đQ_\mu$ do decrease, whereas J_{corr} is increasing until most of the energy flowing out of system A is compensated by J_{corr}. Thus the energy is, again, flowing into the interaction, and the energy current is not an intensive quantity anymore.

To complete this section the amplitudes of both heat currents $đQ_\mu$ in Fig. 5.12 and Fig. 5.13, the correlation current J_{corr} in Fig. 5.14 and the work $đW$ in Fig. 5.15 are depicted as a function of the coupling strength λ and the detuning ω with a fixed local energy splitting $\delta_B = 1$ and the anisotropy $\Delta = 1$. Here, the ferromagnetic case $\lambda < 0$ is included. A difference between

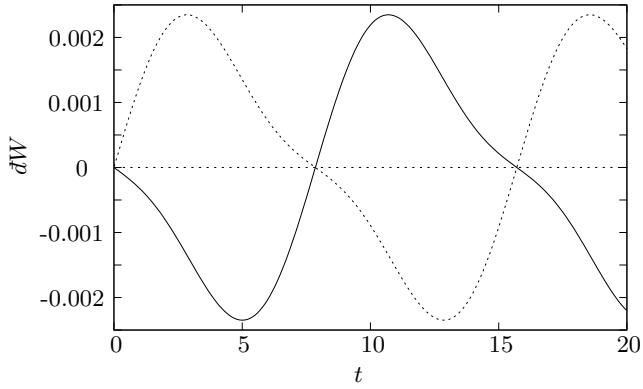

Figure 5.5.: Evolution in time of $đW$ with the parameters and states as in Fig. 5.2. The solid line represents spin A and the dotted line spin B

the ferromagnetic and the antiferromagnetic case can readily be seen: with increasing ω the correlation current J_{corr} increases more rapidly in the ferromagnetic case. On the other side, $đW$ is not influenced by the type of coupling (ferro- or antiferromagnetic coupling).

The ferromagnetic coupling induces an effective Hamiltonian which increases the energy splitting $\delta_\mu^{\mathrm{L}} > \delta_\mu$ in contrast to the antiferromagnetic coupling, where $\delta_\mu^{\mathrm{L}} < \delta_\mu$ holds. But this effect has nothing to do with the different behavior of J_{corr} for both coupling types. In App. D, (D.9), the analytical solution of J_{corr} is independent of $\hat{H}_\mu^{\mathrm{L}}$. Rather it is an effect of the chosen state, which is energetically favorable for the antiferromagnetic case due to the affinity to the ground state as it is for the ferromagnetic case.

5.6. Local Temperature

At last we want to address the question about which temperature a system would have or could be estimated to have within the effective description. Therefore the temperature of, e.g., system A is considered. From the fundamental relation it is known that

$$\mathrm{d}S = \frac{1}{T} đQ. \tag{5.54}$$

Using the definition given for the heat $đQ$ in (5.16) this yields

$$\mathrm{d}S_A = \frac{1}{T^*} \mathrm{Tr}\left\{\hat{H}_A^{\mathrm{L}} \hat{\mathcal{L}}_{\mathrm{inc}}(\hat{\rho})\right\} \mathrm{d}t. \tag{5.55}$$

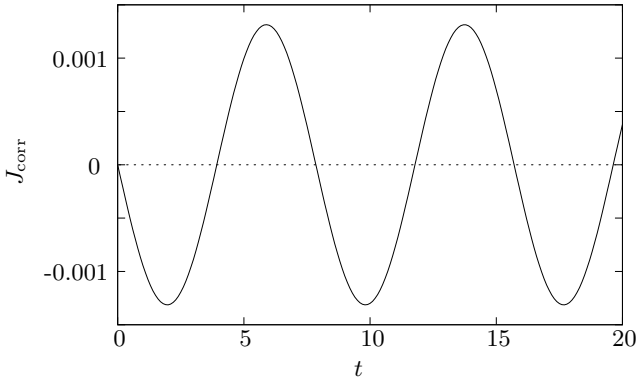

Figure 5.6.: Evolution in time of $J_{\rm corr}$ with the same parameter as in Fig. 5.2.

The temperature T^* should indicate a parameter associated with the local temperature.[4] On the other side, the derivative of the entropy S_A was derived in (5.8). Combining (5.8) with (5.55) yields

$$-\operatorname{Tr}\left\{\hat{\mathcal{L}}_{\rm inc}(\hat{\rho})\log\hat{\rho}_A\right\} = \frac{1}{T_A}\operatorname{Tr}\left\{\hat{H}_A^{\rm L}\hat{\mathcal{L}}_{\rm inc}(\hat{\rho})\right\}$$

$$T^* = \frac{\operatorname{Tr}\left\{\hat{\mathcal{L}}_{\rm inc}(\hat{\rho})\log\hat{\rho}_A\right\}}{\operatorname{Tr}\left\{\hat{H}_A^{\rm L}\hat{\mathcal{L}}_{\rm inc}(\hat{\rho})\right\}}. \tag{5.56}$$

When dealing with canonical states, T^* could explicitly be determined form (5.56) because then $\hat{H}_A^{\rm L}$ commutes with $\hat{\rho}_A$ (see App. A). Thus T^* is given in the energy basis of $\hat{H}_A^{\rm L}$, the local effective measurement basis. Following our notation we get

$$T^{\rm L} = T^* \tag{5.57}$$

the *effective* temperature.

As a consequence, even if the global state of the system is canonical, the effective temperature of a considered subunit is different from the global temperature if an interaction is present. In [40, 42] this was traced back to the difference of the global eigenbasis of the complete system and the product basis. To *measure* locally the global temperature one has to measure a big enough block of many subunits so that the interaction between these blocks can be neglected and one therefore is back in the weak coupling limit.

[4] Until now this must not be equivalent to the thermodynamic temperature. T^* is, for arbitrary states, nothing else but a positive parameter.

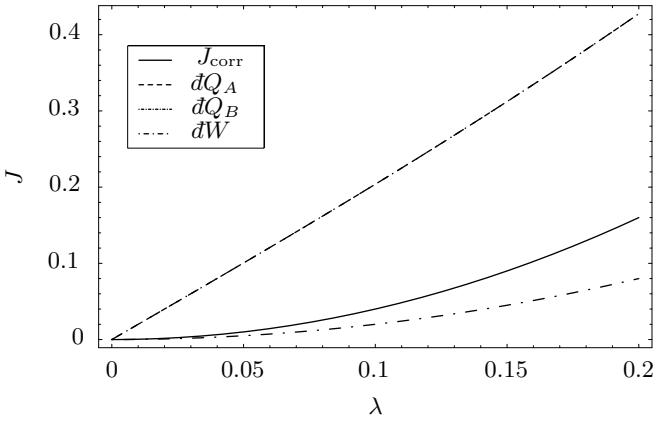

Figure 5.7.: Amplitudes of the currents đQ_A, đQ_B, đW and $J_{\rm corr}$ as a function of the coupling strength λ for two coupled Heisenberg spins. Parameters chosen are $\Delta = 1$, $\delta_A = \delta_B = 1$ and $p_A = 0$, $p_B = 1$.

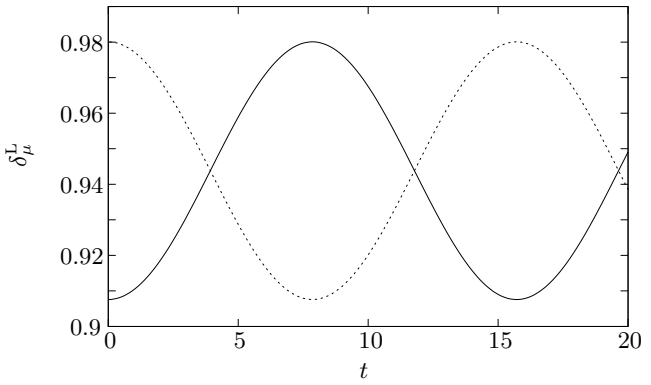

Figure 5.8.: $\delta_A^{\rm L}$ (solid line) and $\delta_B^{\rm L}$ (dashed line) as a function of time with the same parameters and states as in Fig. 5.2.

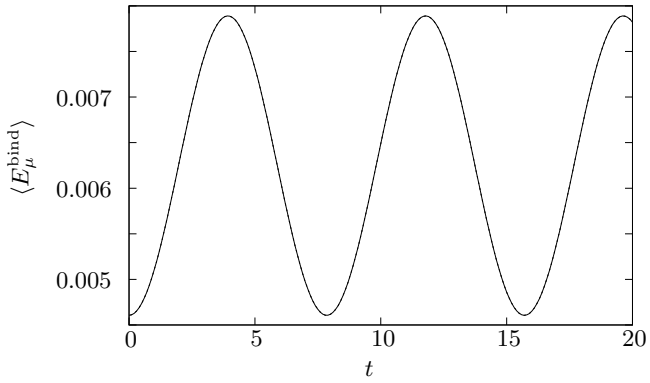

Figure 5.9.: $\langle E_A^{\rm bind}\rangle$ (solid line) and $\langle E_B^{\rm bind}\rangle$ (dashed line) as a function of time with the same parameters and states as in Fig. 5.2. As can be seen, both functions are equal.

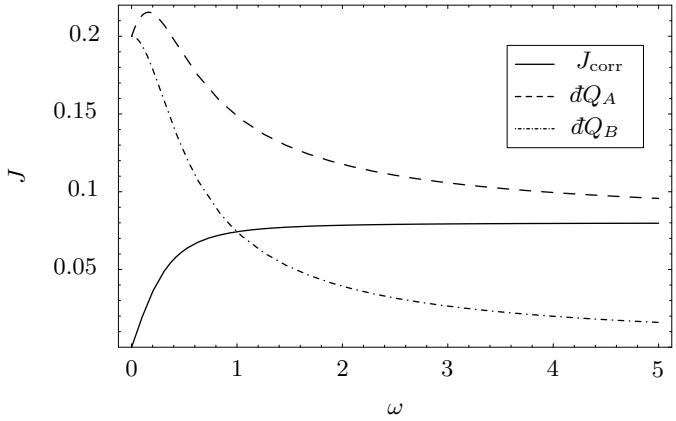

Figure 5.10.: Amplitudes of the currents as a function of the detuning ω for two Förster coupled spins with the parameters $\delta_B = 1$, $\Delta = 0$. The coupling strength $\lambda = 0.1$ (which is not a weak coupling) is chosen for better illustration.

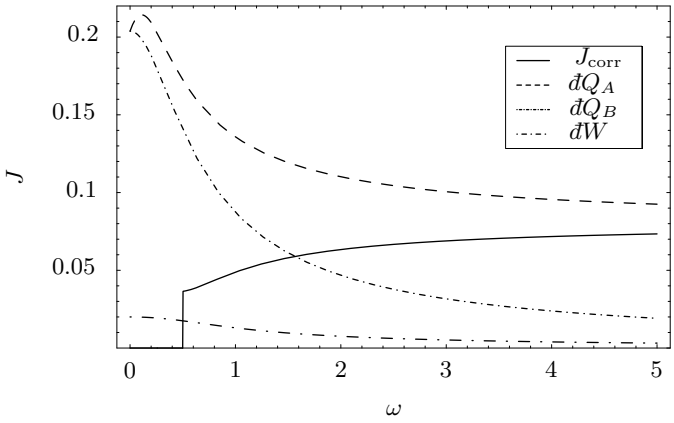

Figure 5.11.: Amplitudes of the currents for Heisenberg coupling with the parameters $\delta_B = 1$, $\Delta = 1$, as a function of the detuning ω. Below $\omega < 0.5$ J_{corr} is corrupted due to numerical errors.

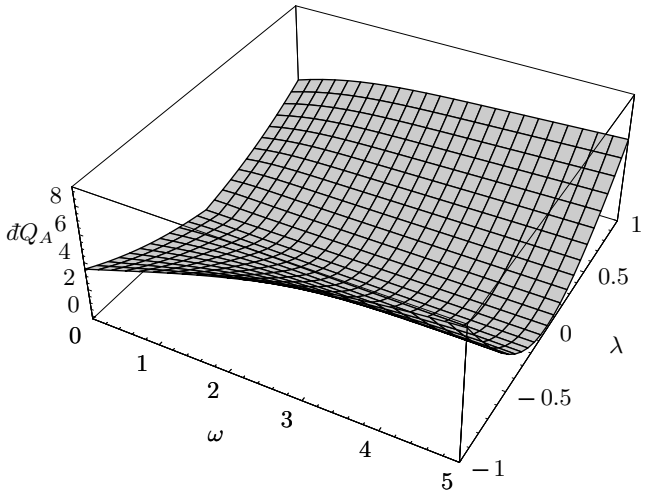

Figure 5.12.: đQ_A as a function of λ and ω with the parameters $\Delta = 1$ and $\delta_B = 1$. With increasing ω an asymmetry between the ferromagnetic case ($\lambda < 0$) and the antiferromagnetic case ($\lambda > 0$) can be seen.

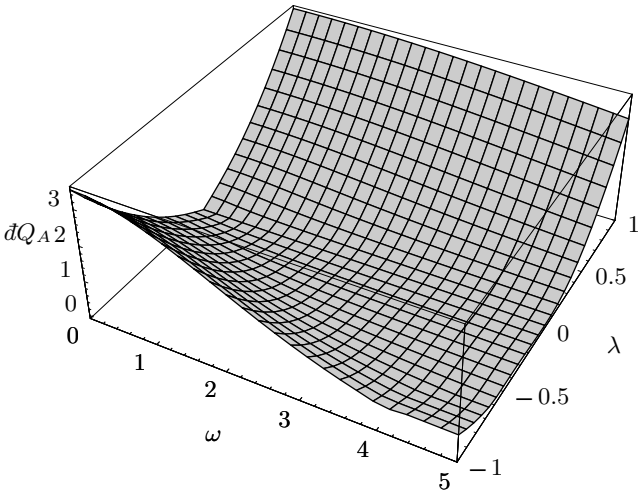

Figure 5.13.: $đQ_B$ as a function of λ and ω with the parameters $\Delta = 1$ and $\delta_B = 1$. The asymmetry between ferro- and antiferromagnetic coupling type can be seen more clearly than in Fig. 5.12.

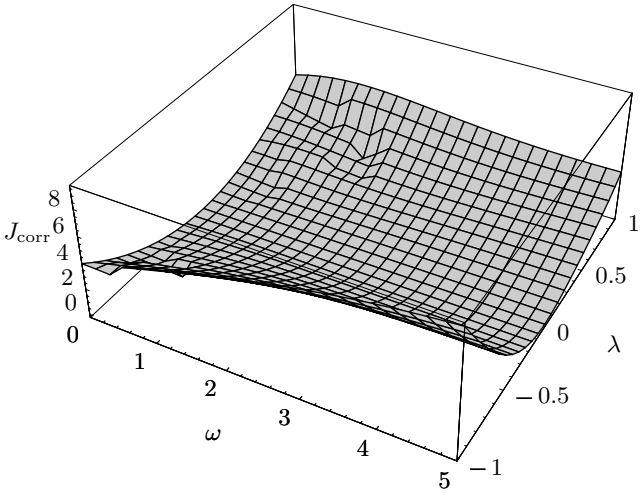

Figure 5.14.: J_{corr} as a function of λ and ω with the parameters $\Delta = 1$ and $\delta_B = 1$. As well as in Fig. 5.13 a asymmetry between ferro- and antiferromagnetic couple can be seen clearly.

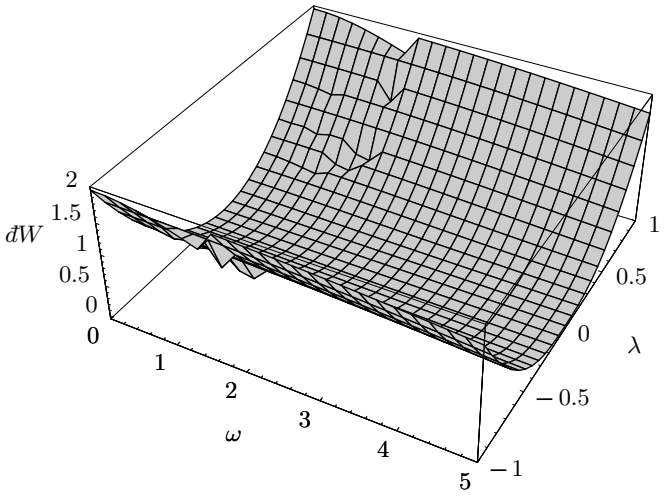

Figure 5.15.: $đW$ as a function of λ and ω with the parameters $\Delta = 1$ and $\delta_B = 1$. In contrast to, e.g., the heat currents the type of coupling (ferro- or antiferromagnetic) does not influence $đW$.

6. Open System Approach to Nonequilibrium

> There is however at present no rigorous mathematical derivation of Fourier's law and ipso facto of Kubo's formula for κ, involving integrals over equilibrium time correlations, for any system (or model) with a deterministic, e.g. Hamiltonian, microscopic evolution.
>
> F. Bonetto et. al. in [7]

This chapter deals with the problem of nonequilibrium steady states and the modelling of nonequilibrium environments. In Chap. 4 an open system approach in form of the QME was derived. Within this approach it is possible to drive a system from an arbitrary initial state to a thermal state. We want to make use of this concept to produce nonequilibrium situations in a very intuitive way by using two heat baths coupled locally to a system. We will give a short remark on a pitfall referring to the Lindblad equation.

The found method paves the way to study the transport behavior of quantum systems. Mainly we are interested in the energy or heat current in chains which will give new aspects on Fourier's law of heat conduction. The application of the LEMBAS principle allows to get some new insight and a possible explanation for the emergence of this law also in integrable systems like the Heisenberg spin-chain. The transport behavior of these chains has been under controversial discussion for quite a long time now. Nevertheless we are still lacking a clear derivation of Fourier's law by a microscopic theory. An overview of transport phenomena can be found in [54] for classical systems and in [101] for quantum systems.

The last part of this chapter deals with peculiar properties of inhomogeneous chains. We have already seen that the energy transport behavior of these systems differ from homogeneous systems. Two effects will be discussed: the resonance effect, which causes a decrease of the heat current through 1-dimensional chains and the diode-effect. The latter describes the occurrence

of a direction-dependent heat flow through quantum chains.

6.1. Open System Approach to Nonequilibrium

To study the thermal transport behavior of, e.g., a rod or wire, the wire is brought between two hot baths with different temperatures. These kinds of experiments are also realized in the mesoscopic scale where the thermal properties of, e.g., a carbon nanotube is investigated [52].

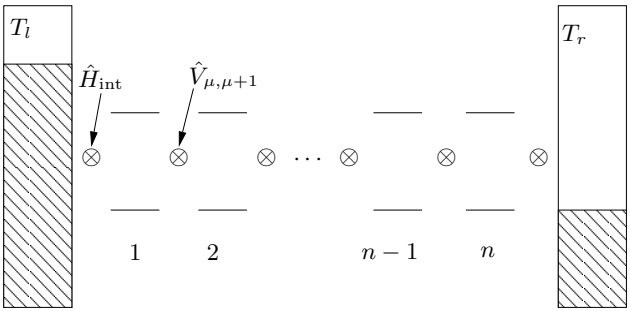

Figure 6.1.: Modular constructed model system between two split baths for studying nonequilibrium states.

Corresponding to these experiments we construct a theoretical model, which enables us to study quantum systems in nonequilibrium. As shown in Fig. 6.1, a modular quantum system is locally coupled at each end to a thermal bath at different temperatures. The Hamiltonian of the chain reads

$$\hat{H} = \sum_{\mu}^{n} \hat{H}_{\mu} + \hat{V}_{\mu,\mu+1}, \tag{6.1}$$

with a local Hamiltonian $\hat{H}_{\mu}$ of the μ'th subsystem, a local energy splitting δ_{μ} and an internal next-neighbor interaction $\hat{V}(\mu, \mu+1)$, in analogy to a spin chain as in Chap. 3.

Each bath is modelled with the open system approach introduced in Chap. 4. The coupling between the system and the respective bath is local, i. e. only the boundary spins exchange energy with the bath. The environment operators take the following form

$$\hat{X}_l = \hat{\sigma}_1^x \otimes \hat{1}_2 \otimes \hat{1}_3 \otimes \cdots \otimes \hat{1}_n \tag{6.2}$$

$$\hat{X}_r = \hat{1}_1 \otimes \hat{1}_2 \otimes \hat{1}_3 \otimes \cdots \otimes \hat{\sigma}_n^x \tag{6.3}$$

where the indices l/r denote the left/right bath. Thus, the summation over the different environment operators vanish and the interaction (4.12) of the Redfield equation between system and bath reads

$$\hat{H}_{\rm int}^{l(r)} = \hat{X}_{l(r)} \otimes \hat{Y}_{l(r)}. \tag{6.4}$$

The QME (4.21) including a second bath is now given in the form

$$\frac{{\rm d}\hat{\rho}_s(t)}{{\rm d}t} = -{\rm i}\left[\hat{H}_s, \hat{\rho}_s(t)\right] + \hat{\mathcal{D}}(\hat{\rho}_s(t))_l + \hat{\mathcal{D}}(\hat{\rho}_s(t))_r. \tag{6.5}$$

A second dissipator (one for each bath l and r) has thus entered (4.21). This equation has first been used in [80] to study thermal transport in quantum systems. Before continuing we want to make some remarks on the Lindblad-form and nonequilibrium scenarios as the one depicted in Fig. 6.1.

6.1.1. Secular Approximation and Nonequilibrium

As discussed in Chap. 4.3, by applying the secular approximation, (6.5) can be brought into the Lindblad-form. It is well known (see [2, 10, 39]) that for a QME in Lindblad-form the dynamics of the diagonal elements (the level population) decouples from the off-diagonal elements (coherences) in the eigenbasis of the considered Hamiltonian $\hat{H}_s$, if the spectrum is nondegenerate. This is also true for the situation with two baths present [89].

This decoupling, which results from the mathematical structure of the two autonomous sets of linear homogeneous differential equations for the diagonal and off-diagonal elements, can be illustrated by the following picture. The coupling operator given in (6.2) and (6.3) will be decomposed referring to (4.23) into transition operators, allowing only transitions where the quantum number m changes by one, independent of side l or r, as depicted in Fig. 6.2 for two coupled spins. For a translational invariant system both decompositions (for $\hat{X}_l$ and $\hat{X}_r$) lead to the same transition operators. The secular approximation weighs the possible transitions by a rate. In contrast, the Redfield equation additionally couples different transitions with different rates and opens therefore more damping channels [see also the additional sandwich-terms in (4.39)].

As a result the stationary state $\hat{\rho}_s^{\rm stat}$ of the QME based on the secular approximation is diagonal in the energy eigenbasis of $\hat{H}_s$. However, a stationary state without any off-diagonal elements does not show typical characteristics like currents. E.g., the expectation value of the energy current introduced in (5.34) with a diagonal state is zero. This result is very unphysical compared to the nonequilibrium situation of the system between two split baths at different temperatures as depicted in Fig. 6.1.

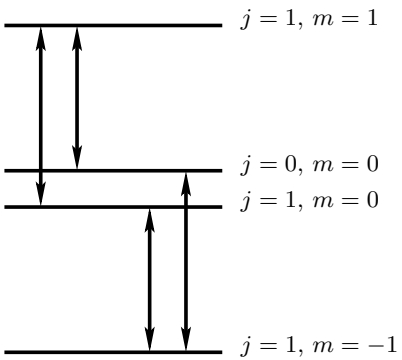

Figure 6.2.: Level structure of a two spin-system. The arrows sketch the possible transitions enabled by $\hat{X}(\omega)$ and $\hat{X}^\dagger(\omega)$.

A Lindblad QME for nonequilibrium situations can only be obtained in the weak coupling limit as shown and used in [99, 100]. There, the environment operator in the interaction picture [see (4.13)],

$$\hat{X}(t) = \mathrm{e}^{\mathrm{i}\hat{H}_s t}\hat{X}\mathrm{e}^{-\mathrm{i}\hat{H}_s t} \simeq \mathrm{e}^{\mathrm{i}\hat{H}_{\mathrm{loc}} t}\hat{X}\mathrm{e}^{-\mathrm{i}\hat{H}_{\mathrm{loc}} t} \tag{6.6}$$

is only be taken in the local interaction picture of $\hat{H}_{\mathrm{loc}}$ of the respective local system coupling to the bath. Thus, (6.2) takes the form

$$\hat{X}_l(t) \simeq \mathrm{e}^{-\mathrm{i}\delta_l/2t}\hat{\sigma}_l^+ + \mathrm{e}^{\mathrm{i}\delta_l/2t}\hat{\sigma}_l^-, \tag{6.7}$$

for the left environment operator and a local energy splitting δ_l. With this approximation a Lindblad QME can be derived as used in [66]. This form is restricted to the weak coupling limit and homogeneous systems, in general. This is a result of the fact that the bath model "only knows" the local damping frequency, which is not sufficient to damp an inhomogeneous system into a stationary canonical state with a temperature equal to the induced bath temperature. As already mentioned, the advantage of a Lindblad QME is the possibility to use the powerful method of stochastic unraveling which enables one to investigate longer spin chains as done in [99].

6.2. Fourier's Law

After a nonequilibrium model has been established, which is able to show nonequilibrium aspects, it is now possible to study the thermal properties of

the stationary nonequilibrium states. Recently, regular or diffusive transport behavior was found in integrable systems like a homogeneous spin-chain with a local field and a next nearest-neighbor Heisenberg interaction within an open system approach [63, 66, 79–81]. Additionally it was found that a Förster coupled chain does show ballistic transport [66].

The appearance of diffusive or ballistic transport was traced back to the current operator (5.34). If the current operator commutes with the system Hamiltonian, as is the case for the Förster coupled chain, the current is a conserved quantity and will therefore never decay ($\rightarrow$ ballistic transport). For the Heisenberg system the current operator does not commute with the system Hamiltonian and is thus no conserved quantity ($\rightarrow$ diffusive transport).

A different method to study thermal transport phenomena in quantum systems is based on the Kubo-formula [53]. As argued in Sect. 2.5, this is a so called linear response theory, where the system reacts to external forces. By diagonalizing the system Hamiltonian, it is possible to calculate the Drude weight, which is related to the transport behavior in the considered system. An overview using this method on low-dimensional transport in quantum systems can be found in [43] and references therein. An overview of the different theoretical methods was given recently in [65].

The transport behavior within the Kubo-formula is studied without any thermal environment. One is interested in the decay of the currents and is using the hypothesis introduced by Einstein [23], that the decay rate of a system is equivalent to the diffusion constant. This is only valid for the linear regime [5]. Only studying the decay behavior can be criticized observing that in an experiment, while measuring the transport behavior, a thermal environment is always present (e.g., [48, 49]).

Here, we want to make use of the LEMBAS principle (cf. Sect. 5.2) and the definitions for the currents made there. Within this approach the emergence of normal transport in a Heisenberg chain is shown in a different light. Beginning with the stationary state of a system as depicted in Fig. 6.1, (6.5) was solved for a Heisenberg chain consisting of five spins. Because of (6.5) being a linear equation constructed to possess only one solution equal to zero, if the spectrum is nondegenerate, the stationary state could be obtained, e.g., by diagonalizing the superoperator and identifying the stationary state with the eigenvector to the corresponding eigenvalue equal to zero.

For the following results a mean temperature $T = 0.5$ was chosen. The temperature gradient can thus be introduced by the variation of the bath temperature of the form $T_h = T + \Delta T$ and $T_c = T - \Delta T$. Fig. 6.3 shows the temperature profile of a Heisenberg chain where the effective temperatures T_μ^{L} are depicted. The local effective temperature includes the effective energy splitting δ'_μ induced by the local field plus a part of the interaction. As a

result of this temperature profile the transport is diffusive.

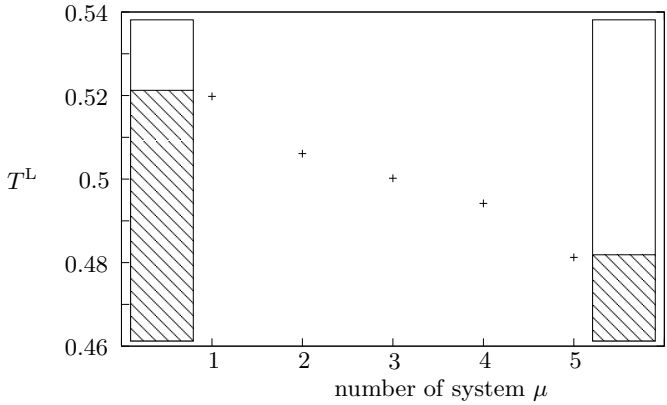

Figure 6.3.: Temperature profile of a Heisenberg coupled spin chain with $\lambda = 0.01$, $\alpha = 0.01$, $T_h = 0.58$ and $T_c = 0.42$.

For a stationary nonequilibrium state the effective energy splittings δ^{L} are arranged as sketched in Fig. 6.4. There, as for the local effective temperatures, the effective splittings decrease from the hot to the cold bath and they arrange like a "funnel". Due to the bath coupling both boundary spins are not as much affected as the rest of the chain. In Fig. 6.5 and Fig. 6.6 the effective energy splittings of the individual spins are depicted as a function of the temperature difference ΔT of both baths. As can be seen from Fig. 6.6, the effective energy splittings $\delta^{\mathrm{L}}_{\mu}$ are not equal and build a funnel with increasing ΔT. The effect is not so dramatic as sketched in Fig. 6.4, but nevertheless, with increasing ΔT, they are arranged in a way that the energy splitting decreases with the decreasing of the effective temperature. The energy splitting of a somewhat "hotter" spin is not so much influenced than that of a "colder" spin, as depicted in Fig. 6.6 by neglecting the spins at the boundaries depicted in Fig. 6.5.

A reason why the funnel-shaped structure is found, can be traced back to the fact that the binding energy given by the expectation value of

$$\langle \hat{H}^{\mathrm{eff}}_{\mu} \rangle = \mathrm{Tr}\left\{ \hat{H}^{\mathrm{eff}}_{\mu} \hat{\rho}_{\mu} \right\} \tag{6.8}$$

is the same for each spin in the chain . This is shown in Fig. 6.7 where all $\langle \hat{H}^{\mathrm{eff}}_{\mu} \rangle$ are depicted as a function of ΔT. From Fig. 6.7 one can infere that each spin has the same binding energy. To keep the $\langle \hat{H}^{\mathrm{eff}}_{\mu} \rangle$ constant for all spins the state or the local energy spectrum must be changed, respectively.

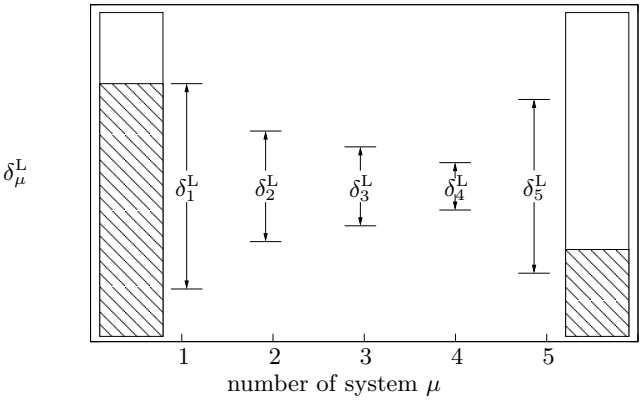

Figure 6.4.: Sketch of the effective energy splittings δ_μ^{L} for a homogeneous spin chain with Heisenberg coupling between two heat baths with different temperatures.

It is thus questionable if one still deals with an integrable system as stated for the homogeneous Heisenberg chain with a local field. The additional effective local field induced via the $\hat{\sigma}^z \otimes \hat{\sigma}^z$ part of the interaction is causing an anisotropy of the spin chain if a temperature gradient is present. By studying infinite spin chains, e.g., by cyclic boundary conditions it could thus not be possible to get diffusive behavior[1].

To confirm Fourier's law, the conductivity κ of the spin chain can be determined from the difference of the local effective temperatures T'_μ and the local heat currents. It can be shown, that the local heat currents are equivalent to the bath currents for a weak internal coupling strength. By neglecting the boundary spins, Fourier's law will be satisfied, if the conductivity obtained between spin 2 and 3, κ_{23}, is equal to the one between spin 3 and 4, κ_{34}. In Fig. 6.8, κ_{23} and κ_{34} are depicted as a function of ΔT. Both values agree with each other quite well and are exactly the same near $\Delta T = 0.08$. With a larger temperature gradient, κ_{23} deviates more and more from κ_{34} and Fourier's law is not fulfilled anymore. This might not be so astonishing because we then leave the linear responce regime [64].

Finally, the influence of the heat baths of the emergence of Fourier's law will be discussed. As said above, the appearance of the funnel in the local effective splittings depends on the temperature gradient. Additional, as shown in Fig. 6.8, there seems to be only a small narrow regime or temperature gradient

[1] E.g., in [94] the decay in the one particle excitation subspace of a Heisenberg chain was studied which have shown ballistic transport

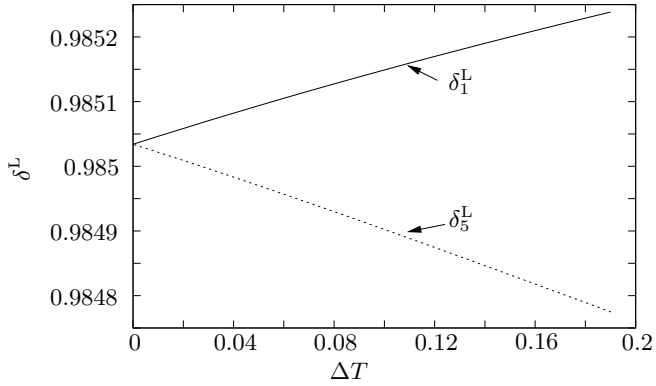

Figure 6.5.: Effective energy splitting δ^{L} of spin 1 and 5 as a function of ΔT. Parameters chosen are $\lambda = 0.01$ and $\alpha = 0.001$.

where Fourier's law is exactly satisfied. Also, the coupling strength of the heat bath affects the transport behavior. To illustrate this, in Fig. 6.9 the conductivities κ_{23} and κ_{34} are depicted as a function of the bath coupling strength α.

For a weak system bath coupling, κ_{23} is almost identical with κ_{34} for the chosen $\Delta T = 0.1$. With increasing bath coupling the difference between both conductivities grows and Fourier's Law is not satisfied anymore. Although the system bath coupling is small (the biggest value is around 0.02 in Fig. 6.9 in comparison with $\delta_\mu = 1$) a small deviation of both conductivities can be observed. If $\alpha > \lambda$, the bath coupling will have a larger influence of the dynamics of the the respective coupling spin than the internal coupling strength controlled by λ. At least the boundary spins are then stronger coupled to the bath than to system (spins), which might be problematic.

6.3. Resonance Effect

In this section we want to discuss the so called "resonance effect", which can be found in inhomogeneous spin chains. The heat current flowing into a system reaches its maximum, if all local energy splittings are the same. As in the previous section, a model as depicted in Fig. 6.1 with four spins between a hot and a cold bath is used. By varying the local energy splitting δ_2 of, e.g., spin 2, the conductivity of the chain is changed and the current will decrease

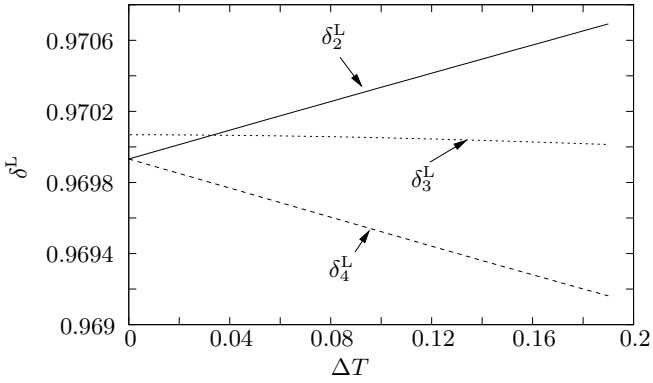

Figure 6.6.: Effective energy splitting δ^{L} of spin 2 - 4 as a function of ΔT. Parameters as in Fig. 6.5.

due to detuning. This is shown in Fig. 6.10, where the bath currents[2] (4.41), J_c and J_h, are depicted as a function of the local splitting δ_2.

If δ_2 is out of tune, the heat current will decrease dramatically about four orders. Thus nearly no heat flows from the hot to the cold bath and both are virtually decoupled from each other. Considering the effective temperatures T', which are shown in Fig. 6.11, underlines this decoupling of both baths from each other. There, the spins take the effective temperatures of the bath next to them. Later on we will use this resonance effect especially for the decoupling of a system from a bath. Why the effective temperatures are distributed as depicted, can be elucidated in the next section.

6.4. Diode-Effect (Rectification)

In the last part of this chapter we want to present another effect within inhomogeneous spin-chains, which will be called the diode-effect. By building a funnel with energy splittings distributed in a way that $\delta_\mu > \delta_{\mu+1}$, as illustrated in Fig. 6.12, and a variation of the bath temperature T_1 from a maximum value $T_1^h > T_2$, to a minimum value $T_1^c < T_2$ it is possible to find an asymmetric heat current through an inhomogeneous spin-chain. This behavior was also studied within the Landauer-Büttiker theory in [87] and is also known from other systems (see e.g. [17] and references therein).

[2]Because of treating an inhomogeneous system, the internal currents could not be used anymore (cf. Sect. 5.5.2).

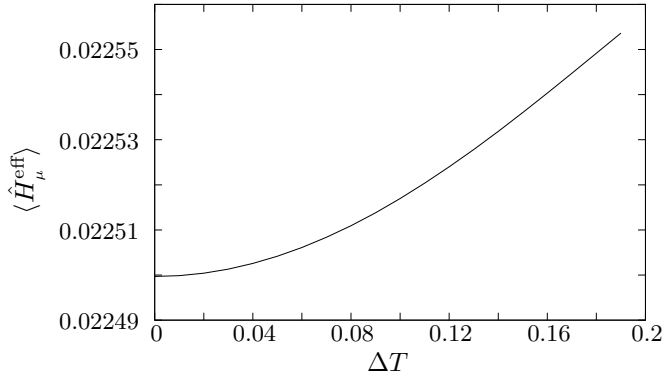

Figure 6.7.: Expaction value $\langle \hat{H}_\mu^{\rm eff} \rangle$ of the binding energy of each spin as a function of ΔT. Parameters as in Fig. 6.5.

As illustration for this asymmetric heat flow in Fig. 6.13 the heat current J_1 as function of the bath temperature T_1 is depicted. We divide the heat current J_1 into two parts: a part J_1^c where $T_1 \leqq T_2$ and take the absolute value of the part J_1^h where $T_1 \geqq T_2$. A considerable difference between both cases can be found. When the temperature gradient "points" in the same direction as the energy gradient the current flowing through the system is smaller as if the temperature gradient is opposite. In contrast to the method described in [17], where the magnetic field strength is able to increase a current over any range, the current in our model is bounded by homogeneity.

An explanation for this behavior can be given by the fact that energy can be released by increasing the energy splitting (cf. Part II). The occupation of the ground state is especially for low temperature much bigger than the excited state. Therefore, it may be easier for the heat current "rolling" down the steps from the right to left (as illustrated in Fig. 6.12), than walking up from left to right. For the "up-walk" the interaction needs more energy to draw the occupation probabilities from the hot to the cold bath than downwards.

The same effect is responsible for the arrangement of the effective temperatures, as depicted in Fig. 6.11 of the previous section. There, the detuned spin takes the effective temperature of the hot bath, because it is energetically favorable for the system.

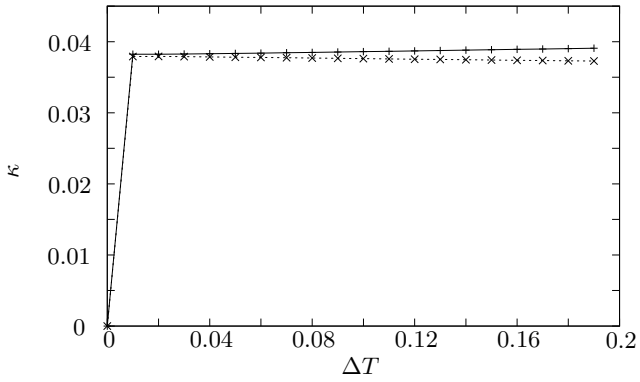

Figure 6.8.: κ_{23} (the solid line) and κ_{34} (the dashed line) as a function of ΔT. Parameters as in Fig. 6.5.

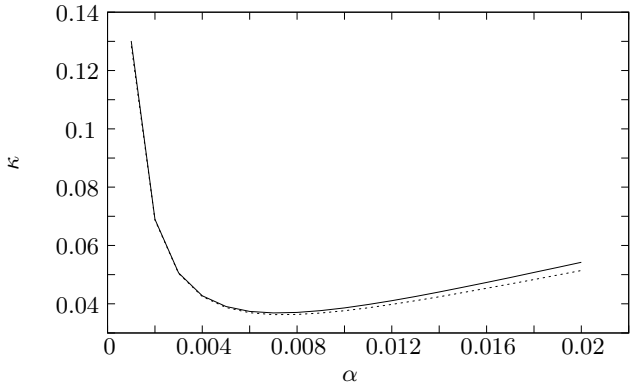

Figure 6.9.: κ_{23} (solid line) and κ_{34} (dashed line) as a function of α, the system bath coupling strength, for $\Delta T = 0.1$ and $\lambda = 0.01$.

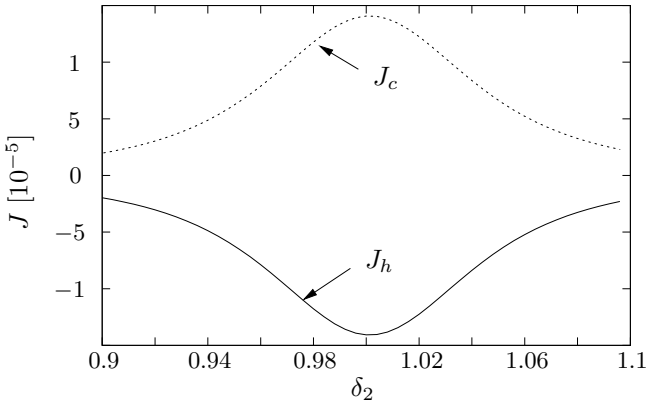

Figure 6.10.: The bath currents j_h and j_c as function of the energy splitting δ_2 with the parameters $\delta_1 = \delta_3 = \delta_4 = 1$, $\Delta T = 0.64$ and $\lambda = \alpha = 0.01$. When $\delta_2 \approx 1$ the current reaches its maximum.

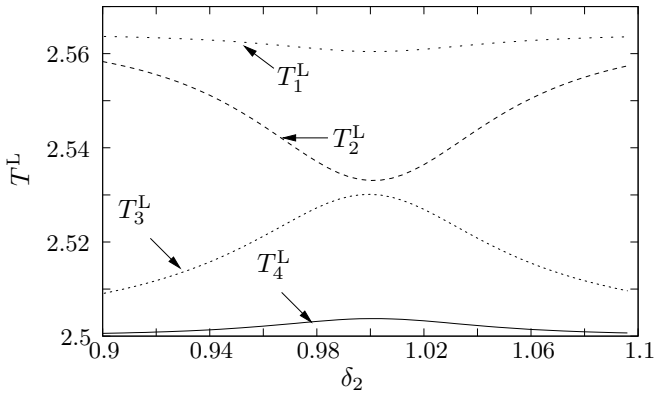

Figure 6.11.: The effective temperatures $T^{\mathrm{L}}\mu$ as function of the energy splitting δ_2 with the parameters as in Fig. 6.10.

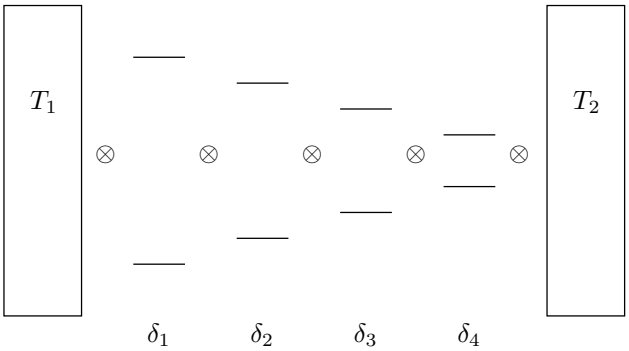

Figure 6.12.: Sketch of the set up for the diode-effect. An inhomogeneous spin-chain with local energy splittings given by $\delta_\mu > \delta_{\mu+1}$. The bath temperature T_1 will be varied between $T_1^h > T_2$ and $T_1^c < T_2$.

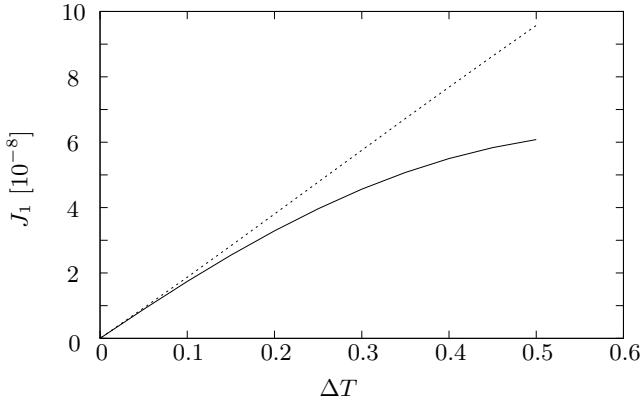

Figure 6.13.: Asymmetric heat flow through an inhomogeneous spin-chain as depicted in Fig. 6.12. The solid line represents the heat current J_1^h ($\Delta T > 0$) and the dashed line J_1^c ($\Delta T < 0$) from bath 1 as a function of ΔT. The parameters chosen are $\delta_1 = 4$, $\delta_2 = 3$, $\delta_3 = 2$, $\delta_4 = 1$, $\lambda = \alpha = 0.01$ and $T_2 = 1$.

7. Temperature Measurement

> Can temperature, which is an equilibrium concept, still be invoked in a nonequilibrium process such as heat flow? [...] The question "What is Temperature?" is really a question about the size of the regions over which a local temperature can be defined.
>
> D. Cahill et. al. in [13]

In this chapter a theoretical model for the measurement of the local temperature will be discussed. M. Hartmann raised the question about the existence of temperature on the nanoscale [40–42]. He used the definition that a local temperature does exist if the considered part of the system is in a canonical state.

It was shown that this can be fulfilled for a modular system in an equilibrium state if the interaction between the considered subunits is so small that, as a result, the product basis is equivalent to the eigenbasis. In other words, the correlations between the considered subunits have to be negligible. Then a local canonical state matches the global canonical state. Even more interesting would be the case when the system is in a nonequilibrium state as discussed in Chap. 6. May a local temperature exist even then and could it be measured?

As in classical thermodynamics, the hypotheses of a contact equilibrium is used to address this question. We mean by contact equilibrium, e.g., the situation where two systems at different temperatures are brought in contact in a way that they can exchange energy and thus the temperatures equalize. Here, we use a measurement device of the same scale as the subunit to be measured to mimic this contact measurement.

Within this model we also want to show which temperature would be detected by a measurement device. Because the global state of the system is a nonequilibrium state, the hope is that only local equilibrium states and thus local temperatures will be measured. The local temperature T^{loc} of a TLS would simply be given as function of the local Hamiltonian $\hat{H}_\mu$. In Chap. 5.6 we have also introduced the effective temperature T_μ^{eff} obtained with the ef-

fective Hamiltonian $\hat{H}_\mu^{\mathrm{L}}$. There we argued that by a measurement one would typically measure $\hat{H}_\mu^{\mathrm{L}}$ and therefore T_μ^{L}. As we will see it is indeed T_μ^{L} and thus $\langle \hat{H}_\mu^{\mathrm{L}} \rangle$ that our auxiliary system will measure.

7.1. A Numerical Experiment

The model we are using to mimic a temperature measurement is depicted in Fig. 7.1. There, as in Chap. 6, a rod or wire is brought in between two split baths at different temperatures and thus is exposed to a temperature gradient. The system is again built up out of spins. The thermometer is also modelled by an additional spin which is only locally coupled to the spin whose temperature should be measured. The possibility of a local measurement of quantities like energy or temperature have been discussed in Chap. 5. There, we have identified as measurement results the quantities obtained with $\hat{H}_\mu^{\mathrm{L}}$. Here, we will now get a justification from our theoretical measurement model for this assumption.

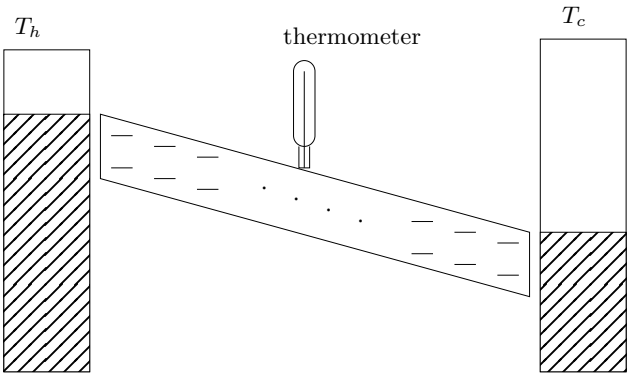

Figure 7.1.: Caricature of a temperature measurement of a nanoscopic system which may be composed out of TLS.

We begin with a "measurement" of the local temperatures T_μ^{loc} as function of the temperature gradient ΔT. In Fig. 7.2 all T_μ^{loc} including the thermometer spin are depicted. On the depicted scale the thermometer never possesses the same temperature as spin 2, the measured spin. With an increasing temperature gradient the thermometer temperature $T_{\mathrm{th}}^{\mathrm{loc}}$ will be equal to T_2^{loc} at one singular ΔT. Thus, it seems that our theoretical experiment is not

appropriate for a local temperature measurement.

The same scenario as above is now repeated, but by analyzing the effective temperatures T_μ^{L} of each subsystem. The result is depicted in Fig. 7.3 with the T_μ^{L} as a function of ΔT. In contrast to the local temperatures T_μ^{loc}, the effective description shows a contact equilibrium scenario where the thermometer spin is able to determine the effective temperature of the system it is in contact with.

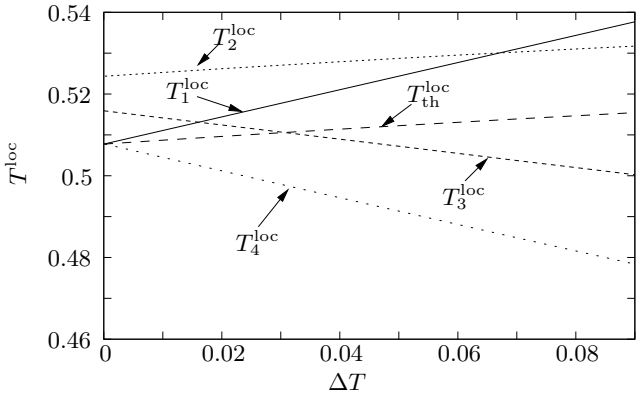

Figure 7.2.: Local temperatures T_μ^{loc} for a homogeneous spin chain as function of λ_{th}. The thermometer spin with temperature $T_{\mathrm{th}}^{\mathrm{loc}}$ couples weakly $\lambda_{\mathrm{th}} = 0.001$ with spin 2. With increasing ΔT the deviation between T_2^{loc} and $T_{\mathrm{th}}^{\mathrm{loc}}$ is also increasing. Following parameters have been chosen: $\delta_\mu = 1$ and $\lambda = 0.01$.

Next the influence of the coupling strength between the measurement device and the system is investigated. In the foregoing we have used a coupling strength between device and system which was one order less than the internal coupling of the system. In Fig. 7.4 the local temperatures T_μ^{loc} and Fig. 7.5 the effective temperatures T_μ^{L} are depicted as a function of the couplings strength λ_{th} between device and system. There, the effective description $T_{\mathrm{th}}^{\mathrm{L}}$ is over some region equal to T_2^{L} until the influence of λ_{th} disturbs the spectrum too much. In contrast, the local temperature $T_{\mathrm{th}}^{\mathrm{loc}}$ never reaches T_2^{loc}.

In conclusion it can be said, that our numerical experiment confirms the effective description as the one, which is able to mirror a contact equilibrium. This dependents on the kind of coupling strength between the system to be measured an the measurement device. Not only the measurement would be wrong also the state of the total system (without measurement device) is changed by the measurement device. This highlights the problem of a

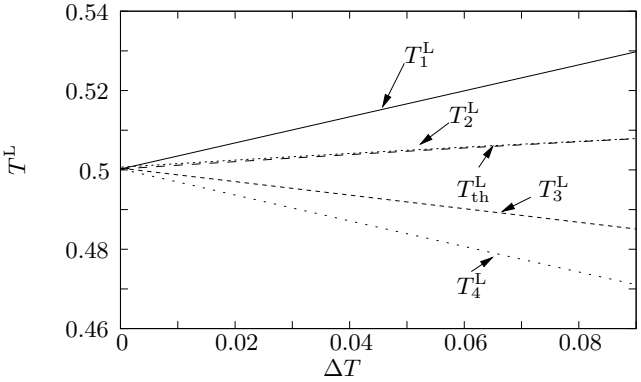

Figure 7.3.: Effective temperatures T_μ^{loc} for a homogeneous spin chain as function of ΔT. The thermometer spin with temperature $T_{\mathrm{th}}^{\mathrm{L}}$ couples weakly $\lambda_{\mathrm{th}} = 0.001$ with spin 2. $T_{\mathrm{th}}^{\mathrm{L}}$ matches T_2^{loc} almost exactly and thus confirms the effective description. We used the same parameters as in Fig. 7.2.

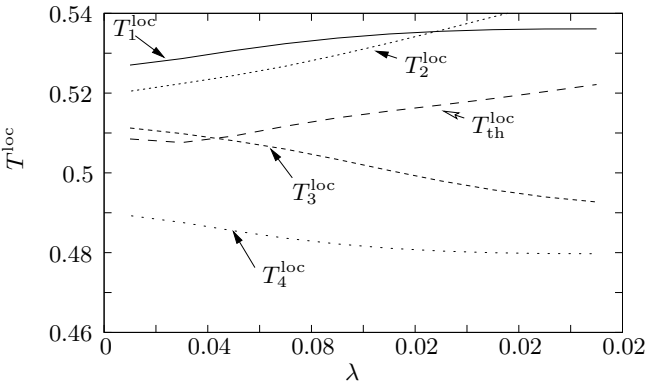

Figure 7.4.: Local temperatures T_μ^{loc} for a homogeneous spin chain as function of λ_{th}. We used the same parameters as in Fig. 7.2 and the temperatures $T_h = \frac{1}{0.504}$ and $T_c = \frac{1}{0.496}$.

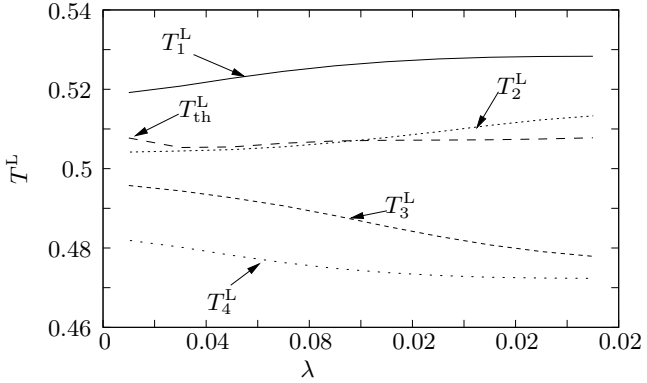

Figure 7.5.: Effective temperatures T_μ^{loc} for a homogeneous spin chain as function of λ_{th}. We used the same parameters as in Fig. 7.4.

nanoscale measurement under the above conditions: To study, e.g., Fourier's law in low dimensional systems on the length scale of a few subunits the emergence of Fourier's law could easily be disturbed or suppressed just by the measuring device.

Part II.

Driven Nonequilibrium States

8. Quantum Thermodynamic Processes

> Heat engines and heat pumps are characterized by three attributes: the working medium, the cycle of operation, and the dynamics that govern the cycle. Heat baths by definition are large enough so that their temperature is constant during the cycle of operation.
>
> T. Feldmann and R. Kosloff in [25]

In the following part externally driven systems in nonequilibrium situations will be studied. As in the first part the focus lies on stationary states which are now, due to the external driving, periodical. The driving we are interested in is a classical driving. By classical we mean that a parameter of the Hamiltonian is now controlled by a time dependent function. E.g., the z-component of the magnetic field inducing an energy gap of a spin is driven periodically. The aim is to characterize thermodynamic processes known from classical thermodynamics. When combined with some bath control cyclic processes like the Carnot or Otto cycle can be obtained.

8.1. Quantum "Working Medium"

Before we analyze the possible thermal processes two different quantum systems which takes the part of the gas in classical systems are introduced: a spin 1/2 and a particle in the box. The latter will also be reduced to a TLS. For very low temperature this simplification is valid. The main difference between these models are their eigenvalues and the eigenfunctions. The eigenvalues for a spin are linear functions in the magnetic field $\epsilon = \pm\delta(B)$ whereas for the particle in the box we get $\epsilon \propto \frac{1}{L^2}$ with the length L for the 1-dim. case. This different scaling will lead to different results for thermodynamic processes.

8.1.1. Two-Level-System: Spin 1/2

We introduce a spin with the Hamiltonian

$$\hat{H}(B) = \frac{\delta(B)}{2}\hat{\sigma}^z, \tag{8.1}$$

with an energy splitting $\delta(B)$ caused by a magnetic field and the Pauli-Matrix $\hat{\sigma}^z$. By considering thermal processes, B could be a simple time dependent function of the form $B(t) = B_0 t$. The conjugate variable to B is given by

$$M = -\left.\frac{\mathrm{d}U(B)}{\mathrm{d}B}\right|_S = \sum_n \frac{\mathrm{d}E_n}{\mathrm{d}B} p_n, \tag{8.2}$$

which is the magnetic moment and we used the definition for the internal energy given in (2.10).

8.1.2. Particle in a box

The next system is the particle in the box where we restrict ourselves to the 1-dimensional case. The obtained results are also valid in the 3-dimensional case. The eigenvalues are given by

$$E_n = \frac{\hbar^2\pi^2 n^2}{2mL^2}, \tag{8.3}$$

with the particle mass m and the length L. The respective eigenfunctions are

$$|\phi_n(x)\rangle = -\sqrt{\frac{2}{L}}\sin\left(\frac{n\pi x}{L}\right). \tag{8.4}$$

A thermodynamic process will be controlled by the parameter L. As in classical thermodynamics one can think of a piston which compresses a gas by changing the volume. In such a process L is a function of t. The conjugate variable to the volume L is given by

$$p = -\left.\frac{\mathrm{d}U(L)}{\mathrm{d}L}\right|_S = \sum_n \frac{\mathrm{d}E_n}{\mathrm{d}L} p_n, \tag{8.5}$$

where p can be identified with the pressure [see (2.6)]. In the following we set $\frac{\hbar^2\pi^2}{m} = 1$.

8.2. Quantum Thermodynamical Processes

As in classical thermodynamics we want to study for the two "working media" different kinds of processes. Typically processes differ by the variables which will be kept fixed. With more and more controlable nano-devices the experimentalist may be able to realize different scenarios.

The processes, which will be analyzed here, are taken to be quasi-static so that we avoid relaxation without bath damping. E.g., the particle in the box possesses eigenfunctions which depend on the parameter L. If the change of L would be to fast transitions would take place and therefore the state would change.

As already mentioned, to obtain analytical results we only take the first two energy levels for the particle in the box. This may seem rather restrictive but nevertheless some qualitative statements can be derived.

8.2.1. Isothermal Process

The system is in contact with a heat bath which keeps the temperature T fixed, whereas all other variables are allowed to vary. Typically the variable X will change and therefore the conjugate variable x. By considering an arbitrary n-level Hamiltonian of the form

$$H(n,n) = E_n(x), \tag{8.6}$$

the work done in such a process can be calculated based on (2.13)

$$W_{\text{iso-T}} = \sum_n \int_{x_i}^{x_f} \frac{\mathrm{d}E_n}{\mathrm{d}x} p_n(T, E_n) \mathrm{d}x \tag{8.7}$$

The exchanged heat reads with (2.14) and the partial integration:

$$\begin{aligned} Q_{\text{iso-T}} &= \sum_n \int_{x_i}^{x_f} E_n(x) \frac{\mathrm{d}p_n(T, E_n)}{\mathrm{d}x} \mathrm{d}x \\ &= \sum_n \left[E_n(x) p_n(x)\right]_{x_i}^{x_f} - \sum_n \int_{x_i}^{x_f} \frac{\mathrm{d}E_n}{\mathrm{d}x} p_n(T, E_n) \mathrm{d}x \\ &= \Delta U - W_{\text{iso-T}}. \end{aligned} \tag{8.8}$$

Example: Spin 1/2

The Hamiltonian of the system is given by (8.1) and the generalized thermodynamic force by (8.2). Putting (8.1) and (8.2) into (8.7) yields

$$\begin{aligned} W_{\text{iso-T}} &= -\int_{\delta_i}^{\delta_f} M \mathrm{d}\delta \\ &= \int_{\delta_i}^{\delta_f} -\frac{1}{2}\tanh\left(\frac{\delta}{2T}\right)\mathrm{d}\delta \\ &= -T\ln\left[\cosh\left(\frac{\delta}{2T}\right)\right]_{\delta_i}^{\delta_f}. \end{aligned} \tag{8.9}$$

Similarly the exchanged heat can be determined with (8.8) to

$$\begin{aligned} Q_{\text{iso-T}} &= \int_{\delta_i}^{\delta_f} \frac{-\delta}{2T + 2T\cosh\left(\frac{\delta}{T}\right)}\mathrm{d}\delta \\ &= \left\{T\ln\left[\cosh\left(\frac{\delta}{2T}\right)\right] - \frac{\delta}{2}\tanh\left(\frac{\delta}{2T}\right)\right\}_{\delta_i}^{\delta_f}. \end{aligned} \tag{8.10}$$

From (8.9) and (8.10) it can be seen that the relation

$$\begin{aligned} \Delta U &= W_{\text{iso-T}} + Q_{\text{iso-T}} = 0 \\ W_{\text{iso-T}} &= -Q_{\text{iso-T}} \end{aligned} \tag{8.11}$$

can only be satisfied for the trivial solution $T \to \infty$. An isothermal process for a spin can therefore never be isoenergetical.

Example: Particle in the box

The Hamiltonian for the particle in the box consisting only of two levels is given by a diagonalmatrix with the eigenvalues of (8.3). Equivalent to the spin example the work for the particle in the box is obtained by (8.9) and reads

$$\begin{aligned} W_{\text{iso-T}} &= -\int_{L_i}^{L_f} p \mathrm{d}L \\ &= \int_{L_i}^{L_f} \frac{1}{\left[1 - \frac{3}{4+\exp(3/2L^2T)}\right]L^3}\mathrm{d}L \\ &= \left\{\frac{2}{L^2} - T\ln\left[1 + \exp\left(\frac{3}{2L^2T}\right)\right]\right\}_{L_i}^{L_f} \end{aligned} \tag{8.12}$$

The exchanged heat (8.8) can be calculated with the help of (8.3) to

$$\begin{aligned} Q_{\text{iso-T}} &= \int_{L_i}^{L_f} E_n(L) \frac{\mathrm{d}p_n(L)}{\mathrm{d}L} \mathrm{d}L \\ &= \left\{ T \ln\left[\cosh\left(\frac{3}{4L^2T}\right)\right] - \frac{3\tanh\left(\frac{3}{4L^2T}\right)}{4L^2} \right\}_{L_i}^{L_f}. \end{aligned} \tag{8.13}$$

As for the spin system we find $W_{\text{iso-T}} + Q_{\text{iso-T}} = \Delta U \neq 0$.

8.2.2. Adiabatic Process

In an adiabatic process the system is typically decoupled from a heat bath. In the ideal case no heat will be exchanged and no transitions take place. The occupation probabilities $p_n(T, E_n)$ at the beginning and the end of the process are the same. Only the spectrum of the Hamiltonian changes by varying, e.g., the volume. Therefor the temperature T of the system changes throughout an adiabatic process control. The achieved or released work simply reads

$$W = \sum_n \Delta E_n p_n, \tag{8.14}$$

with the energy difference $\Delta E_n = E_n(x_f) - E_n(x_i)$ after and before the process multiplied by the corresponded occupation probability p_n. The x indicate as in Sect. 2.1 the conjugate variables like the volume. For a TLS, (8.14) is the difference of the energy expectation value at the end and the beginning of the process.

Example: Spin 1/2

With the same canonical state at the beginning and at the end the Hamiltonian (8.1) the work done for a spin 1/2 system with (8.14) reads

$$W_{\text{ad}} = \frac{\delta_f - \delta_i}{2} \tanh\left(\frac{\delta_i}{2T_i}\right) \tag{8.15}$$

The exchanged heat is $Q_{\text{ad}} = 0$ per definition. Before we continue we want to draw attention to a peculiarity of the adiabatic step performed by a TLS. Because the state during an adiabatic step does not change it is possible to determine the temperature of the TLS after an adiabatic step.

To make this point more clear take a look at Fig. 8.1. We assume that the state of the TLS is a canonical one

$$\hat{\rho} = \frac{1}{Z} \begin{pmatrix} \mathrm{e}^{\delta_i/(2T_i)} & 0 \\ 0 & \mathrm{e}^{-\delta_i/(2T_i)} \end{pmatrix}. \tag{8.16}$$

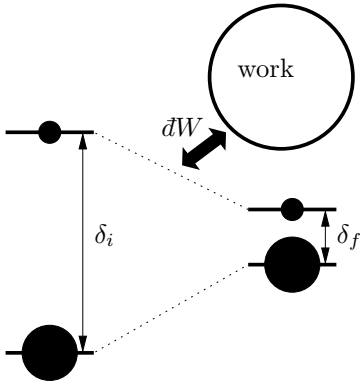

Figure 8.1.: Illustration of an adiabatic step performed by a TLS.

The initial state i could be the result of, e.g., an isothermal process. Then the adiabatic step as depicted in Fig. 8.1 takes place and therefore the temperature of the TLS is decreasing to

$$\frac{\mathrm{e}^{-\delta_i/(2T_i)}}{\mathrm{e}^{\delta_i/(2T_i)}} = \frac{\mathrm{e}^{-\delta_f/(2T_f)}}{\mathrm{e}^{\delta_f/(2T_f)}}$$
$$T_f = T_i \frac{\delta_f}{\delta_i}. \tag{8.17}$$

This relation is valid for all TLS and do not dependent on a spin. Eq. (8.17) will be very useful to make theoretical predictions for the energy balance of cyclic processes.

Example: Particle in the box

Under the same conditions as for the spin 1/2 system the work is obtained again by (8.14) and reads

$$W_{\mathrm{ad}} = \frac{\left(L_f^3 - L_i^3\right)\left(3\tanh\left(\frac{3}{4L_i^2 T_i}\right) - 5\right)}{2L_f^3 L_i^3} \tag{8.18}$$

The exchanged heat for a particle in the box is also $Q_{\mathrm{ad}} = 0$.

8.2.3. Isochoric Process

The volume of the considered system is constant V =const. Only the temperature T (the occupation numbers) can vary and therefore in an isochoric

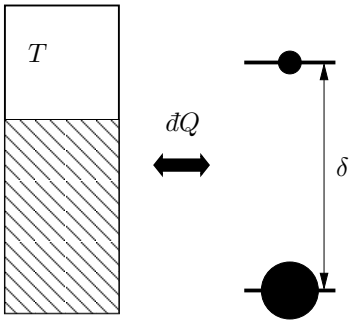

Figure 8.2.: Illustration of an isochoric step performed by a TLS.

process only heat will be exchanged. In Fig. 8.2 an isochoric process for a TLS is sketched. The energy splitting is constant whereas the probabilities could change. As for the adiabatic process the exchanged heat can be calculated for a TLS by the difference of the energy expectation value at the end and the beginning of the process.

Spin 1/2

The amount of heat received or released of a spin 1/2 during an isochoric process is given by

$$Q_{\text{isoc}} = \frac{\delta_f}{2}\left[\tanh\left(\frac{\delta_i}{2T_i}\right) - \tanh\left(\frac{\delta_f}{2T_f}\right)\right] \tag{8.19}$$

The magnetic field is constant during the whole process leading to $\delta_f = \delta_i$. Only the respective occupation numbers given by $\tanh(...)$ are different at the beginning (where $T = T_i$) and the end (where $T = T_f$).

Particle in the box

The exchanged heat during an isochoric process for a particle in the box takes the form

$$Q_{\text{isoc}} = \frac{3}{4L_f^2}\left\{\frac{\sinh\left[\frac{3}{4}\left(\frac{1}{L_i^2 T_i} - \frac{1}{L_f^2 T_f}\right)\right]}{\cosh\left(\frac{3}{4L_i^2 T_i}\right)\cosh\left(\frac{3}{4L_f^2 T_f}\right)}\right\} \tag{8.20}$$

During the process the volume $L = L_i = L_f$ stays constant whereas the occupation numbers changes from the state with $T = T_i$ to $T = T_f$.

9. Quantum Thermodynamic Cycles

> Presently it is not well understood, which (if not all) of the Hamilton parameters of a quantum system may, indeed, be made to operate as such a work variable.
>
> J. Gemmer, M. Michel and G. Mahler in [33]

With the definition of different thermodynamic processes, as done in the previous chapter, we consider now the combination of them to cyclic processes. This is analog to classical thermodynamics where, since the famous work of S. Carnot [16] about the maximum efficiency of a thermodynamic machine, different kinds of cycles are known (e.g., Otto-cycle, Diesel-cycle, Escher-Wyss-cycle, etc.). First investigations on the existence of thermodynamic cycles within quantum mechanical systems have been made by Scovil et. al. [1, 36, 85].

Since this pioneering work considerable progress has been made in the last decades. Different kinds of models like machines built of harmonic oscillators, of uncoupled spins, particles in a potential or different three level systems have been studied (see, e.g., [3, 4, 26, 72, 87]). Even autonomous quantum engines are known and discussed in [92, 93]. Most of these heat engines studied are of the Otto-type consisting of two adiabatic and two isochoric steps [26, 27, 45, 46, 50, 51, 72, 76, 86]. The analysis of other types of heat engines are, as far as known to the author, not so numerous. Studies of Carnot like cycles can be found in [4, 88], of a Brayton engine in [56], and a Stirling engine in [57].

It is sometimes not easy to find out which kind of engine is studied because of some confusion about the different kind of steps involved. E.g., to calculate the efficiency of a heat engine it is mandatory to use the right kind of process control. Otherwise the obtained results would differ compared to the obtained efficiency with its classical counterpart, if it exists.

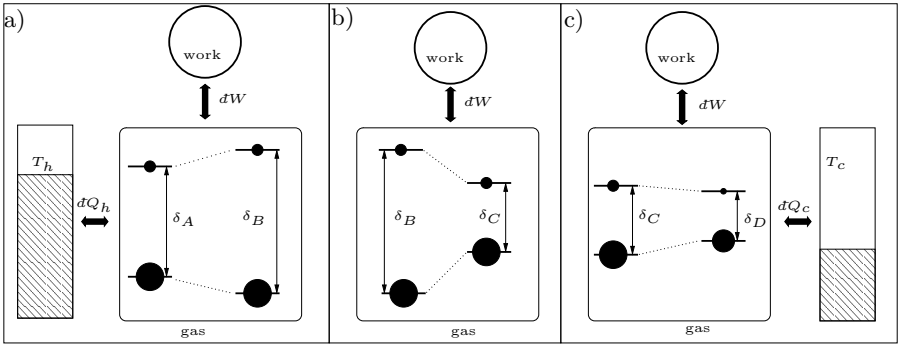

Figure 9.1.: Illustration of the Carnot-cycle for a single TLS

9.1. Carnot-Cycle

According to the 2nd law of thermodynamics the Carnot-cycle is the cycle with best efficiency which could be reached by a machine working between two heat baths. The cycle consists of two isothermal and two adiabatic branches. From classical thermodynamics the efficiency can be derived (e.g., [14]) as

$$\eta = \frac{-W}{Q_h} = 1 - \frac{T_c}{T_h}, \tag{9.1}$$

with the work W, the heat Q_h exchanged with the hot bath, T_c the temperature of the cold bath and T_h of the hot bath. This upper bound holds, irrespectively of the type of working medium used. An illustration of the four steps a TLS will pass through is given in Fig. 9.1.

9.1.1. Spin 1/2

We analyze the four steps for a single spin 1/2 (see Fig. 9.1, Fig. 9.2 and Fig. 9.3):

1. isothermal-step at T_h ($A \to B$): As depicted in Fig. 9.1 a), the system is in contact with the hot bath at temperature T_h the energy splitting and thus the magnetic field changes δ_A from A to δ_B at point B. The exchanged work W_1 is given by (8.9) and the exchanged heat Q_h is given by (8.10).

2. adiabatic step ($B \to C$): The system is decoupled at point B (energy splitting δ_B) from the hot bath and is driven adiabatically until the

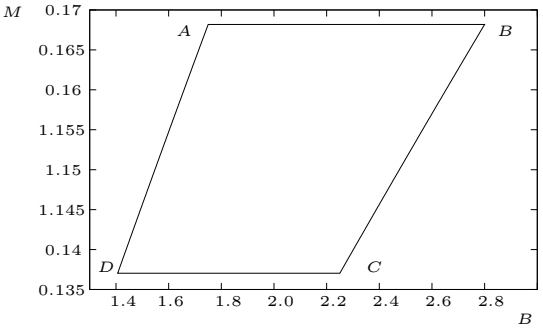

Figure 9.2.: MB-diagram for a spin 1/2 performing a Carnot-cycle [M= magnetic moment, B= magnetic field, see (8.1) and (8.2)]. Following parameters have been chosen: $\delta_B = 2.25$, $\delta_D = 1.75$, $T_h = 4$ and $T_c = 2.5$

energy splitting reaches δ_C at point C. The work W_2 done is given by (8.15). This is illustrated in Fig. 9.1 b).

3. isothermal step at T_c ($C \to D$): The system is in contact with the cold bath at the point C with the energy splitting $\delta = \delta_C$ which will be changed to $\delta = \delta_D$ reached at point D [cf. Fig. 9.1 c)]. The work W_3 can be determined with (8.9) and the exchanged heat Q_c with (8.10).

4. adiabatic step ($D \to A$): The energy splitting δ_D at point D is driven until δ reaches δ_A at point A; work W_4 is given by (8.15).

As an illustration that a spin can perform Carnot-cycles, Fig. 9.2 shows the MB-diagram and Fig. 9.3 the respective TS-diagram.

To calculate the efficiency we make use of the fact that for a TLS with adiabatic steps one can infere δ_A and δ_C from T_h, T_c, δ_B and δ_D (see Sect. 8.2.2). The following parameters can be identified $\delta_A = \frac{T_h}{T_c}\delta_D$, $\delta_C = \frac{T_c}{T_h}\delta_B$. With the help of these relations we get

$$\eta = \frac{-W}{Q_h} = \frac{-(W_1 + W_2 + W_3 + W_4)}{Q_h} = 1 - \frac{T_c}{T_h}, \tag{9.2}$$

i.e. the well known result from classical thermodynamics.

9.1.2. Particle in the Box

As in sec. 9.1.1 for the spin system we calculate the work and heat on the four different steps for the particle in the box (see Fig. 9.1, Fig. 9.4 and Fig. 9.5).

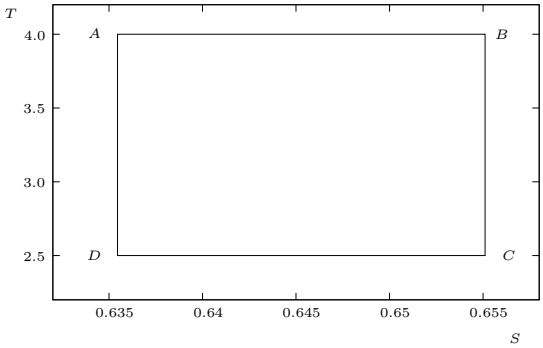

Figure 9.3.: TS-diagram for a spin 1/2 performing a Carnot-cycle. Same parameters as in Fig. Fig. 9.2

1. isothermal-step at T_h ($A \to B$): the system is in contact with the hot bath at temperature T_h. The volume at point A is changed from $L = L_A$ to point B where $L = L_B$. The exchanged work is given by (8.12) and will be called W_1. The exchanged heat from (8.13) is called Q_h.

2. adiabatic step ($B \to C$): the system is decoupled at point B (where $L = L_B$) from the hot bath and is driven adiabatically until $L = L_C$ at point C. The work done is given by (8.18) and will be called W_2.

3. isothermal step at T_c ($C \to D$): the system is in contact with the cold bath from point C with $L = L_C$ until point D with $L = L_D$. The work done is called W_3 and the exchanged heat Q_c.

4. adiabatic step ($D \to A$): From point D with $L = L_D$ the system will be driven until $L = L_A$ at point A. The work is called W_4.

Fig. 9.4 shows the pV-diagram and Fig. 9.5 the TS-diagram of the two-level particle in the box performing Carnot-cycles. L_A and L_C can also be determined by T_h, T_c, L_B and L_D (cf. Sect. 8.2.2) and thus $L_A = \sqrt{\frac{T_c}{T_h}} L_D$, $L_C = \sqrt{\frac{T_h}{T_c}} L_B$. With these relations the efficiency for the particle in the box is also given by the Carnot-efficiency:

$$\eta = \frac{-W}{Q_h} = \frac{-(W_1 + W_2 + W_3 + W_4)}{Q_h} = 1 - \frac{T_c}{T_h}. \tag{9.3}$$

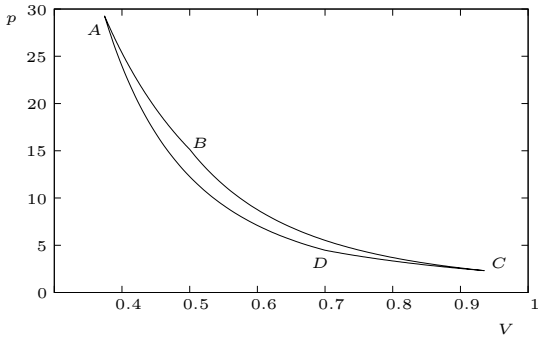

Figure 9.4.: pV-diagram for the particle in the box performing a Carnot-cycle. The following parameters have been chosen: $L_B = 0.5$, $L_D = 0.7$, $T_h = 7$ and $T_c = 2$

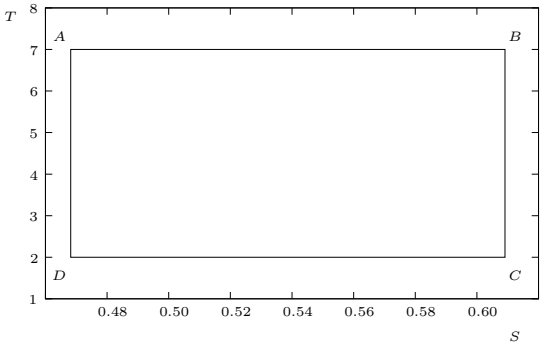

Figure 9.5.: TS-diagram for the particle in the box performing a Carnot-cycle. Same parameters as in Fig. 9.4

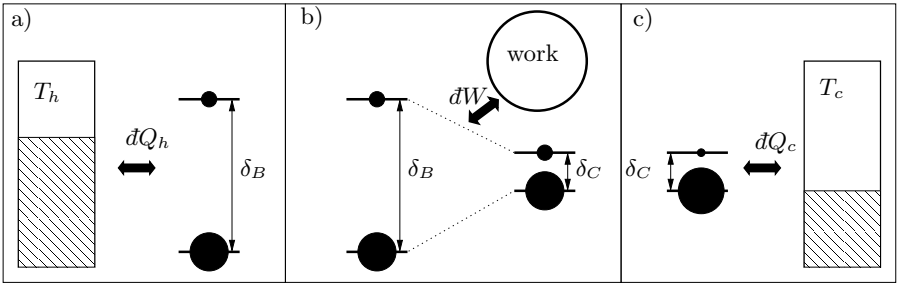

Figure 9.6.: Illustration of the Otto-cycle for a TLS

9.2. Otto-Cycle

The Otto-cycle consists of one isochoric step with bath contact at T_h followed by an adiabatic step, again an isochoric step with bath contact at T_c and at last an adiabatic step. The Otto-cycle is very attractive for treating quantum thermodynamic machines, because it is easy (at least from a theoretical point of view) to change the occupation probabilities during bath contact and to change the spectrum by driving the system without bath contact. A sketch of the Otto-cycle for a TLS is given in Fig. 9.6.

An interesting fact is the simularity of the Otto-cycle with quantum algorithmic cooling [9]. The tool to cool a spin in this approach is a SWAP-gate as used in quantum computing [68]. The implementation of this SWAP-gate consists of a sequence of pulses which exchanges occupation probabilities. The efficiency of this operation is equivalent to the Otto efficiency [47]. Also a cyclic algorithmic cooling protocol was suggested [78].

The efficiency derived from classical thermodynamics for a Otto-cycle only depends on the "compression":

$$\eta_{\mathrm{Otto}} = \frac{-W}{Q_h} = 1 - \frac{V_1}{V_2}^{n-1}, \tag{9.4}$$

where V_i are the two volumes, between which the gas system is driven, and $n-1$ is the polytropic exponent.

9.2.1. Spin 1/2

The four different steps for a spin 1/2 performing an Otto-cycle are (see Fig. 9.6, Fig. 9.7 and Fig. 9.8):

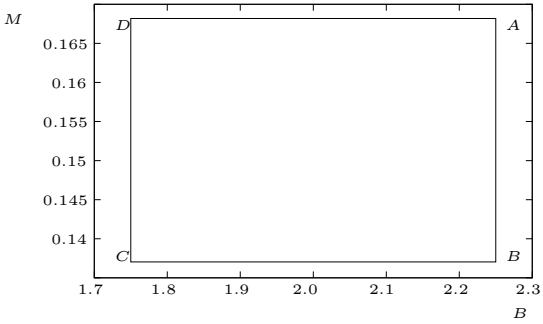

Figure 9.7.: MB-diagram for a spin 1/2 performing an Otto-cycle. Following parameters have been chosen: $\delta_B = 2.25$, $\delta_C = 1.75$, $T_h = 4$ and $T_c = 2.5$.

1. isochoric step ($A \to B$): The occupation probabilities change until $T = T_h$. During the whole step $\delta = \delta_A = \delta_B$. The exchanged heat Q_h is defined by (8.19).

2. adiabatic step ($B \to C$): The system is driven from point B with δ_B to point C with δ_C. The work W_1 released on this step is given by (8.15).

3. isochoric step ($C \to D$): The temperature of the spin at point C is $T_c = T_h \frac{\delta_B}{\delta_D}$. The heat Q_c [cf.(8.19)] will be exchanged until the temperature of the spin equals T_c. During the step $\delta = \delta_C = \delta_D$.

4. adiabatic step ($C \to D$): The system is driven back from δ_D to δ_A as in step 2. The work done on this step is W_2 given by (8.15).

The respective MB-diagram and TS-diagram of a spin performing an Otto-cycle is depicted in Fig. 9.7 and Fig. 9.8. The efficiency can then be evaluated by

$$\eta_{\text{Otto}} = \frac{-(W_1 + W_2)}{Q_h} = 1 - \frac{\delta_B}{\delta_D} \tag{9.5}$$

which is equivalent to (9.4).

An intersting situation occurs in cycles with adiabatic steps in combination with a TLS. If, e.g., $T_C = T_c$ at the end of the adiabatic step (at point C), no heat with the bath will be exchanged. It is thus possible to define a critical temperature difference

$$\Delta T_{\text{crit}} = T_h - T_c = T_h \left(1 - \frac{\Delta\delta_C}{\Delta\delta_B}\right) \tag{9.6}$$

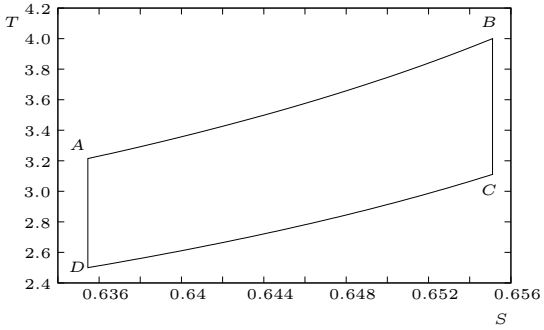

Figure 9.8.: TS-diagram for a spin 1/2 performing an Otto-cycle. Parameters as in Fig. 9.7.

with the help of (8.17). At this critical temperature difference (9.5) reaches the Carnot efficiency. Below this ΔT_{crit} the function of the considered machine will switch from a heat pump to a heat engine (see [45]). This is always valid for a TLS performing cycles including adiabatic steps and could also be found in a heat engine performing Carnot-cycles.

9.2.2. Particle in the Box

As in the previous subsection for the spin we calculate the work and heat on the four different steps for the particle in the box.

1. isochoric step ($A \to B$): The volume $L = L_A = L_B$ stays constant. The temperature of the system changes from $T = T_A$ until it is equal to T_h. The heat Q_h received from the bath is given by (8.20).

2. adiabatic step ($B \to C$): the system is decoupled at $L = L_B$ from the hot bath and is driven adiabatically until it reaches $L = L_C$. The work W_1 done is given by (8.18).

3. isothermal step at T_c ($C \to D$): tThe volume stays constant ($L = L_C = L_D$) and the temperature changes until T_c is reached. The heat Q_c exchanged with the cold bath is defined by (8.20).

4. adiabatic step ($C \to D$): $L = L_D$ at the beginning and is driven until $L = L_A$. The work is called W_4 given by (8.18).

In Fig. 9.9 the pV-diagram and in Fig. 9.10 the TS-diagram of the two-level particle in the box performing Otto-cycles is depicted. L_A and L_C can

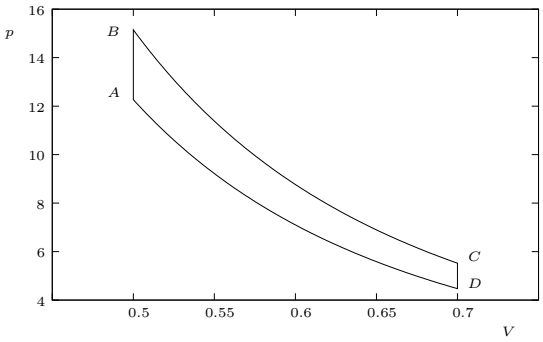

Figure 9.9.: pV-diagram for the particle in the box performing a Otto-cycle. Following parameters have been chosen: $L_B = 0.5$, $L_D = 0.7$, $T_h = 7$ and $T_c = 2$.

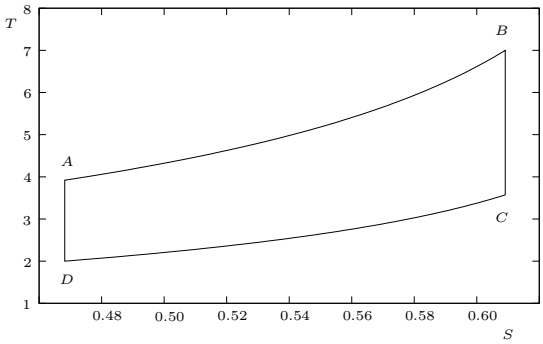

Figure 9.10.: TS-diagram for the particle in the box performing an Otto-cycle. Parameters as in Fig. 9.9.

again be determined by T_h, T_c, L_B and L_D to $L_A = \sqrt{\frac{T_c}{T_h}} L_D$, $L_C = \sqrt{\frac{T_h}{T_c}} L_B$. With this the efficiency for the particle in the box also results in the expected Otto-efficiency (9.4):

$$\eta_{\text{Otto}} = \frac{-W}{Q_h} = \frac{-(W_1 + W_2)}{Q_h} = 1 - \left(\frac{L_B}{L_D}\right)^2. \tag{9.7}$$

In difference to the efficiency for a single spin given by (9.5) the polytropic exponent for the particle in the box is equal to 2.

9.3. Stirling-Cycle

The last cycle we discuss is the Stirling cycle. All other cycles could not be solved analytically for a TLS. Without an adiabatic step it is not so easy to estimate the state at the end of the process. The Stirling-cycle consists of one isothermal step with bath contact at T_h followed by an isochoric step, again an isothermal step with bath contact at T_c and at last an isochoric step.

The efficiency derived for a classical Stirling-cycle is

$$\eta_{\text{Stirling}} = \frac{-W}{Q_h} = 1 - \frac{T_c}{T_h}, \tag{9.8}$$

if the working gas is an ideal one. Only then the heat exchanged on both isochoric steps cancel each other. In general it is not entirely clear which parts of the heat have to be taken for the calculation of the efficiency [90].

9.3.1. Spin 1/2

A spin 1/2 preforming a Stirling-cycle undergoes four different steps (see Fig. 9.11 and Fig. 9.12):

1. isothermal step ($A \to B$): The system is in contact with the hot bath at T_h where the heat Q_h is exchanged and work W_1 is done. The energy splitting δ changes from δ_A to δ_B.

2. isochoric step ($B \to C$): The system releases heat Q_1 given by (8.19) and the energy splitting $\delta = \delta_B = \delta_C$ stays the same, until the temperature of the cold bath T_c is reached.

3. isothermal step ($C \to D$): The system is in contact with the cold bath at T_c. While keeping the temperature of the system constant, δ changes from δ_C to δ_D. Thus heat Q_c and work W_2 is released.

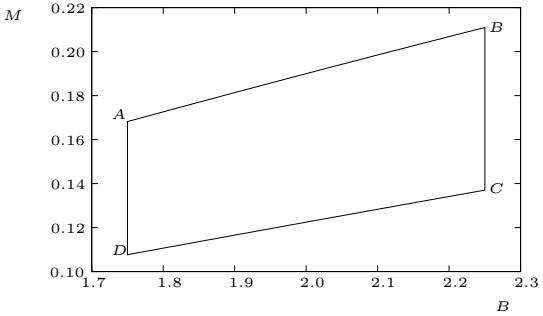

Figure 9.11.: MB-diagram for a spin 1/2 performing a Stirling-cycle. The parameters are: $\delta_B = 2.25$, $\delta_C = 1.75$, $T_h = 4$ and $T_c = 2.5$.

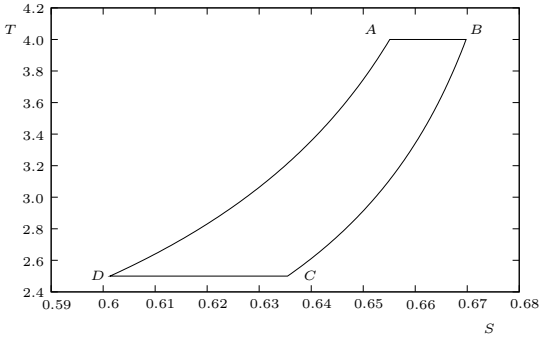

Figure 9.12.: TS-diagram for a spin 1/2 performing a Stirling-cycle. Parameters as in Fig. 9.11.

4. isochoric step ($D \to A$): The energy splitting $\delta = \delta_D = \delta_A$ stays constant and the heat Q_2 will flow between the system and the bath until point A is reached.

The respective MB-diagram and TS-diagram of a spin performing an Stirling-cycle is depicted in Fig. 9.9 and Fig. 9.11.

Due to the fact that the considered system is not an ideal gas, it is not possible to obtain a result for the efficiency as intuitive as for the Carnot- or Otto-cylce.

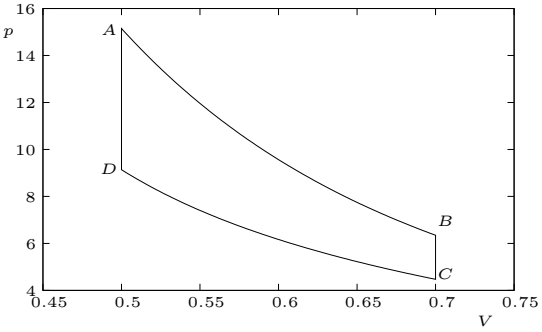

Figure 9.13.: pV-diagram for the particle in the box performing a Stirling-cycle. Following parameters have been chosen: $L_2 = 0.5$, $L_4 = 0.7$, $T_h = 7$ and $T_c = 2$

9.3.2. Particle in the Box

For the particle in the box we calculate the work and heat on the four different steps as for the spin.

1. isothermal step ($A \to B$): The system is in contact with the hot bath at T_h where the heat Q_h is exchanged and work W_1 is done. The volume L changes from L_A to L_B.

2. isochoric step ($B \to C$): The system releases heat Q_1 given by (8.20) and the volume $L = L_B = L_C$ stays the same until the temperature of the cold bath T_c is reached.

3. isothermal step ($C \to D$): The system is in contact with the cold bath at T_c. While keeping the temperature of the system constant, $L = L_C$ changes to $L = L_D$. Thus heat Q_c and work W_2 is released.

4. isochoric step ($D \to A$): The volume $L = L_D = L_A$ stays constant and the heat Q_2 will be exchanged between the system and the bath until point A is reached.

As an illustration, Fig. 9.13 shows the pV-diagram and Fig. 9.14 the corresponding TS-diagram of the particle in the box performing a Stirling-cycle.

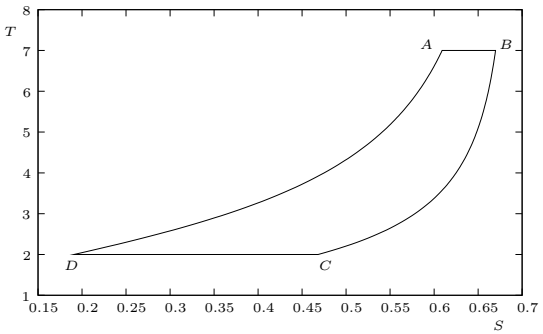

Figure 9.14.: TS-diagram for the particle in the box performing a Stirling-cycle. Parameters as in Fig. 9.13

10. Spin-chain Approach to the Otto-Cycle

> Looking back again to history, we see that thermodynamics was born to describe engines. It is thus natural to ask whether there is a "thermodynamics" of quantum machines, and whether the modern standpoint of quantum information can cast some new light on the foundations of thermodynamics.
>
> V. Scarani et. al. in [82]

The possibilities to control small structures built up of, e.g., a few atoms or a few TLS have been developed over the last decades. Especially for TLS like spins or qubits, which are the essential ingredients for quantum computation [59], much effort has been directed toward control of small clusters and chains of qubits in quantum optical systems [18], nuclear magnetic resonance [35] and solid state systems [61]. A serious problem in any such realization is the unavoidable interaction of the respective quantum network with its environment.

Despite the growing theoretical knowledge about quantum thermodynamic machines as described in Chap. 9 (and references therein), feasible experiments are still far away, as it seems. A good candidate for experimental realization, though, seems to be a machine constructed of TLS. Here, we study a model consisting of three TLS arranged in a chain in contact with two baths of different temperatures as studied for transport scenarios in Chap. 6. An energy gradient on the system and an incoherent driving of the TLS in the middle should make this system act as a thermodynamic machine. For actual experiments the set up may require more TLS.

Under special conditions the Carnot efficiency may be reached by a TLS heat engine but can never go beyond: If the Carnot efficiency is reached the machine flips its function, e.g., from a heat pump to a heat engine as noted in Sect. 9.2. Our numerical results will confirm the occurrence of this critical temperature difference ΔT_{crit}.

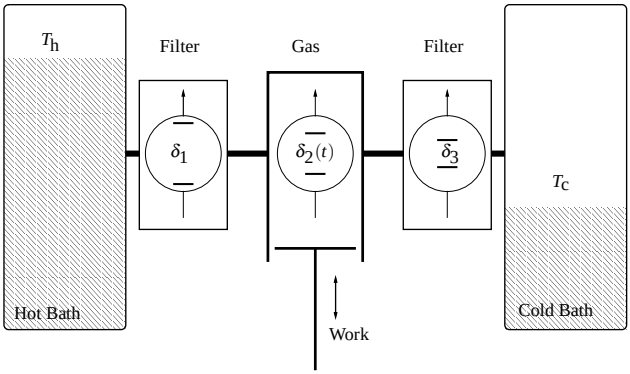

Figure 10.1.: Schematic representation of the system under investigation: An inhomogeneous 3-spin-chain is interfaced between two heat baths. Spin 1 (with energy splitting δ_1) and spin 3 (δ_3) act as filters whereas spin 2 [$\delta_2(t)$] is the working gas by deformation of its spectrum.

10.1. Model

The model under investigation here is an inhomogeneous spin chain with nearest neighbor coupling of Heisenberg type described by the Hamiltonian

$$\hat{H} = \sum_{\mu=1}^{3} \left\{ \frac{\delta_\mu}{2} \hat{\sigma}_\mu^z + \lambda \sum_{i=x,y,z} \hat{\sigma}_\mu^i \otimes \hat{\sigma}_{\mu+1}^i \right\}. \tag{10.1}$$

λ is the coupling strength which is chosen to be small compared to the local Zeeman splitting δ_μ, $\lambda \ll \delta_\mu$. Because $\delta_\mu \neq \delta_{\mu+1}$ we call the spin chain inhomogeneous. We will need at least three spins in order to have this system work as a heat pump or heat engine. The spin chain is brought in contact locally with two baths at different temperatures as depicted in Fig. 10.1. The detuning between spin 1 and spin 3 is $\delta_{13} = (\delta_1 - \delta_3)/2 > 0$.

In Sect. 5.5.2 we have already discussed the transport properties of inhomogeneous spin-chains and the problem to define a local energy current. Therefore the bath current (eq2.30) (introduced in Sect. 4.5) is used to calculate the amount of energy transported through the system. As a first approximation we neglect the coupling between each spin and make no use of the LEMBAS principle.

10.2. Time Dependent Behavior: Spin System as Heat Pump or Heat Engine

In Sect. 2.3 we give the definition of heat (2.14) and work (2.13). For cyclic processes the exchanged amount of work ΔW and heat ΔQ can also be calculated with the help of the ST-diagram. For a closed path in the ST-plane the total energy change $\Delta U = 0$ and thus

$$\Delta W = -\Delta Q = -\oint T \mathrm{d}S. \tag{10.2}$$

While connected with bath α, ΔQ_α can alternatively be calculated from the respective heat current J_α over one cycle of duration τ

$$\Delta Q_\alpha = \int_0^\tau J_\alpha \mathrm{d}t. \tag{10.3}$$

Typically there are two baths $\alpha = h, c$ and thus two contributions (see Fig. 10.1)

$$\Delta Q = \Delta Q_h + \Delta Q_c. \tag{10.4}$$

The efficiency of a heat pump, p, and engine, e, respectively, is given by

$$\eta^p = \frac{-\Delta Q_h}{\Delta W} \quad \text{and} \quad \eta^e = \frac{-\Delta W}{\Delta Q_h} \tag{10.5}$$

Equipped with these relations we want to study the transport properties of the model depicted in Fig. 10.1.

10.2.1. The Heat Current

The resonance effetc was discussed in Sect. 6.3. A detuning of a local energy splitting compared to the homogeneous energy splittings of the rest of the system dramatically reduces the heat conductivity through 1-dim. spin-chains. E.g., in Fig. 10.1 the detuning is able to nearly decouple the two heat baths from each other.

The situation further changes when the energy splitting of spin 2 is chosen to be time-dependent, i.e.,

$$\delta_2(t) = \sin(\omega t) b + b_0. \tag{10.6}$$

Different energy splittings of the boundary spins, e.g., $\delta_1 = 2.25$ and $\delta_3 = 1.75$, are used to install left/right-selective resonance effects. The parameters of

(10.6) are chosen as $b_0 = (\delta_1 + \delta_3)/2$ and b is the detuning δ_{13}. To enable the bath to damp the system, $\omega \ll \delta_2$ must be fulfilled.

To study the time dependent behavior of the system we use the QME (6.5) introduced in Sect. 6.1. Now the dissipators are time dependent because of $\hat{H}_s(t)$. For solving a time dependent QME like in (6.5) we have used a four step Runge-Kutta-algorithm. At each time step the bath correlation function is calculated explicitly. We choose the following parameters for our numerical study: $\lambda = 0.01$, $\alpha = 0.001$, $\delta_1 = 2.25$, $\delta_3 = 1.75$, $\omega = 1/128$, $T_c = 2.5$ and T_h is varied, unless stated otherwise. Both coupling parameters λ and α are chosen to stay in the weak coupling limit.

That the model under investigation is indeed also an Otto-type machine as described in Sect. 9.2, can now be seen, when spin 2 is driven periodically, as in (10.2). We can distinguish four different steps:

1. Spin 2 (the "working gas") is in resonance with spin 3 [$\delta_2(t) \approx \delta_3$] and thus couples with bath c at temperature T_c. Because of this energy resonance, the current J_c via spin 3 will be large, whereas the current J_h via spin 2 will be negligible. The occupation probabilities of spin 2 and 3 approach each other and so do the respective local temperatures.

2. Quasi-adiabatic step: Spin 2 gets out of resonance with spin 3 [$\delta_1 > \delta_2(t) > \delta_3$], now J_c is suppressed while J_h nearly stays unchanged. The occupation probability of spin 2 does not change significantly and there is almost no change in the entropy S_2.

3. Spin 2 is in resonance with spin 1 [$\delta_2(t) \approx \delta_1$] and by that in contact with bath h at temperature T_h. J_h is large whereas J_c is very small. The local temperatures of spin 1 and 2 nearly equal each other.

4. Quasi-adiabatic step, as in step 2.

Fig. 10.2 shows the heat currents J_α of both baths over one period with the bath temperatures $T_h = 2.63$ and $T_c = 2.5$. As can be seen, the resonance effect decouples spin 2 from the bath, if its energy splitting is different from the boundary or filter spins. This decoupling is never perfect, though. As a consequence there is a leakage current J_L which will be discussed in more detail later on.

10.2.2. Heat, Work and Efficiencies

That the studied system, indeed, works as a heat pump, can be seen from the S_2T_2-diagram of spin 2 in Fig. 10.3. The local von Neumann entropy S_2

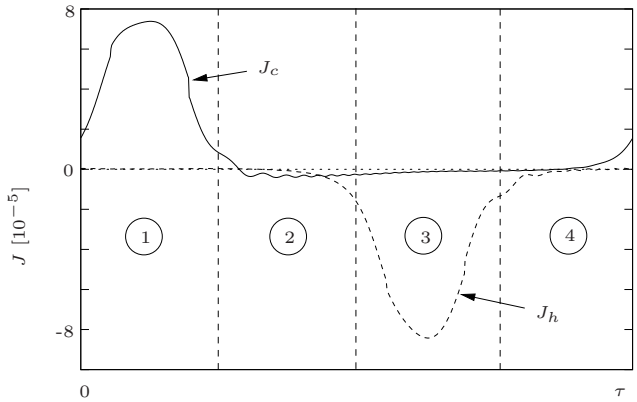

Figure 10.2.: Heat currents $J_\alpha(t)$ for the heat pump over one cycle with duration $\tau = 2\pi/\omega = 804.25$ for $T_h = 2.63$ and $T_c = 2.5$. The peaks are a result of the resonance-effect.

of spin 2 is given by (2.1) and the local temperature T_2 by (2.2). The four different, steps as explained in Sec. 10.2.1, are shown as well as the direction of circulation.

To determine the efficiency of this heat pump, one needs to know the quantity of heat ΔQ_h pumped to the hot bath, and the used work ΔW. ΔQ_h can be calculated by integrating the heat current J_h over one period [cf. (10.3)].

The exchanged work ΔW is given by the area enclosed in the S_2T_2-plane according to (10.2). We find that indeed $\Delta W + \Delta Q_c + \Delta Q_h = 0$ in all cases and by that confirm the use of T_2 and S_2 as effective thermodynamic variables.

In contrast to the Otto model our machine works in finite time: If driven too fast, the bath is not able to damp the system, and if driven too slow (quasi-stationary), the system would have reached its momentary steady state transport configuration (i.e. $\omega \ll \alpha$). The S_2T_2-area then vanishes as depicted in Fig. 10.4. This is caused by the leakage current.

Figure 10.5 shows the Carnot efficiency for the heat pump η^p_{Car}, for the machine η^e_{Car} and the respective efficiencies for our quantum heat pump η^p_{qm} and machine η^e_{qm} [according to (10.5)] as a function of the temperature difference $\Delta T = T_h - T_c$. We point out the following interesting findings:

- The efficiency curve of the quantum heat pump or machine is always below the respective Carnot efficiency. As expected, the 2nd law is never violated.

- For $\Delta T = 0$, η^p_{qm} does neither diverge nor go to zero. In addition, the

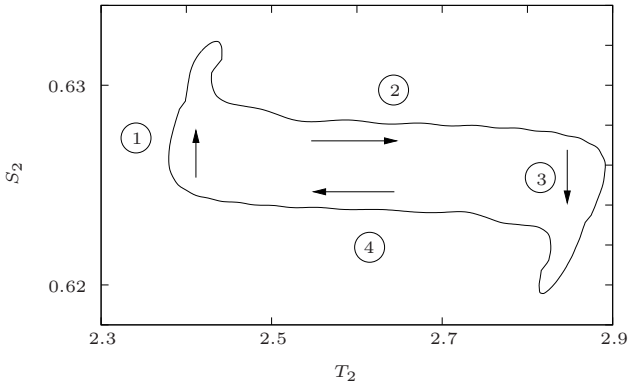

Figure 10.3.: S_2T_2-Diagram for the quantum heat pump for $T_h = 2.63, T_c = 2.5$ ($\Delta T = 0.13$) and $\tau = 2\pi/\omega = 804.25$. The arrows indicate the direction of circulation.

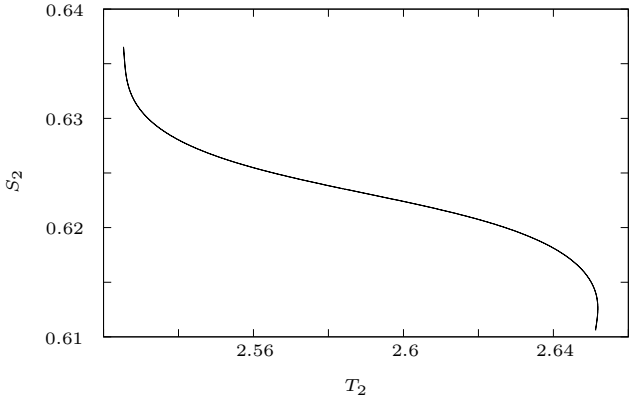

Figure 10.4.: S_2T_2-diagram for the quasi-statically driven quantum heat pump (with parameters as in Fig. 10.3). Because of the leakage current the enclosed S_2T_2-area vanishes and no work is exchanged.

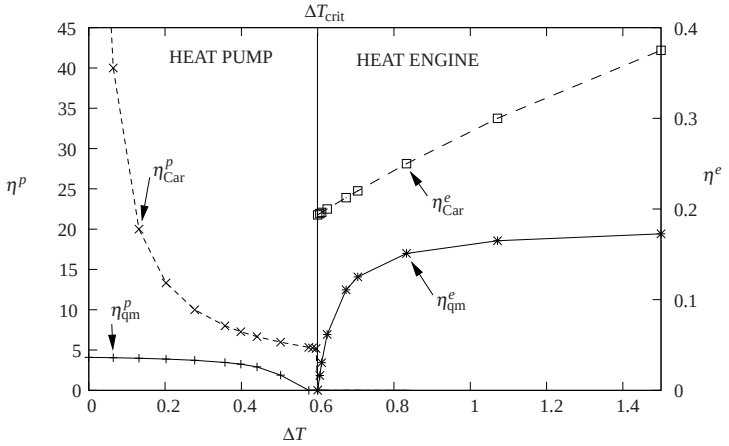

Figure 10.5.: The Carnot-efficiency η^p_{Car} and the efficiency η^p_{qm} of the quantum heat pump ($\Delta T < \Delta T_{\text{crit}}$) and η^e_{Car} and η^e_{qm} of the heat engine ($\Delta T > \Delta T_{\text{crit}}$) as function of the temperature difference ΔT. Following parameters are chosen: $T_c = 2.5, \delta_1 = 2.25, \delta_3 = 1.75$ and $\tau = 2\pi/\omega = 804.25$.

machine can start out of equilibrium and begin to cool a reservoir.

- Above a specific temperature difference ΔT, here $\Delta T_{\text{crit}} \approx 0.6$, the heat pump switches to operate as a heat engine. To illustrate this fact, Fig. 10.6 shows the area in the S_2T_2-plane for $\Delta T = 3.33 > \Delta T_{\text{crit}}$. As depicted, the direction of circulation has reversed.

To make the last point more plausible, Fig. 10.7 shows the work ΔW, the heat ΔQ_h and ΔQ_c as function of ΔT. While ΔT increases, $|\Delta Q_h|$, $|\Delta Q_c|$ and $|\Delta W|$ decrease until first ΔQ_c changes sign, then Q_h and last ΔW. At the point where $\Delta W = 0$ (for $\Delta T = \Delta T_{\text{crit}}$) only the leakage current J_L flows from the hot bath to the cold one. Beyond this ΔT_{crit} the system starts to work as an engine. This is the theoretically predicted behavior of Sect. 9.2 for a TLS performing cycles including adiabatic steps.

10.3. Analytical Results

Here we want to compare the efficiency of the ideal Otto heat pump η^p_{Otto} and engine η^e_{Otto} (given in Sect. 9.2) with the respective Carnot efficiencies for the parameters used for our numerical results.

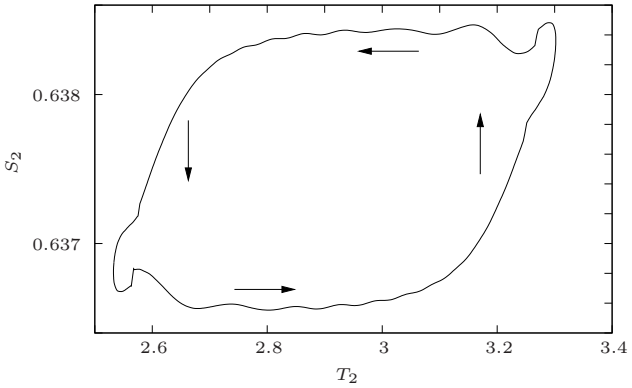

Figure 10.6.: S_2T_2-Diagram for the quantum heat engine ($\Delta T = 0.83 > \Delta T_{\text{crit}}$ with $T_h = 3.33, T_c = 2.5$ and $\tau = 2\pi/\omega = 804.25$. The arrows indicate the direction of circulation.

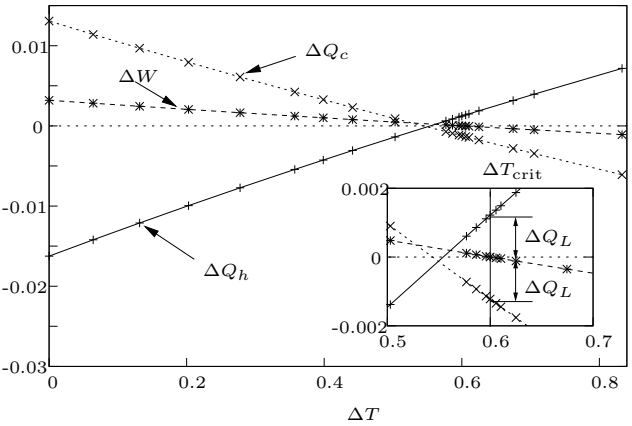

Figure 10.7.: Heat ΔQ_c and ΔQ_h and work ΔW performed over one cycle as function of the temperature difference ΔT (same parameters as in Fig. 10.6. The inset shows these functions around the point $\Delta T = \Delta T_{\text{crit}}$ in more detail. ΔQ_L is the leakage heat per cycle.

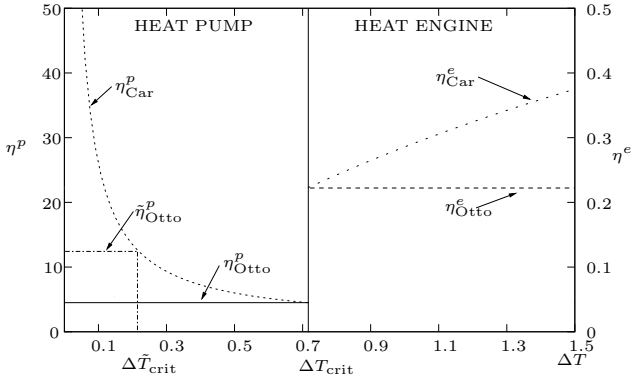

Figure 10.8.: Carnot-efficiency η^p_{Car} for the heat pump and engine η^e_{Car} as function of temperature difference ΔT while $T_c = 2.5, \delta_1 = 2.25$ and $\delta_3 = 1.75$ as in Fig. 10.5. η^p_{Otto} and η^e_{Otto} are the efficiencies of the ideal Otto pump/engine [see (9.7)]. $\tilde{\eta}^p_{\mathrm{Otto}} = 12.36$ and $\Delta\tilde{T}_{\mathrm{crit}} = 0.22$ can be realized for $\delta_1 = 1.904$, $\delta_3 = 1.75$ and $T_c = 2.5$.

Figure 10.8 shows the Carnot efficiencies as well as the one from (9.7). $\eta^{p/e}_{\mathrm{Otto}}$ is always below $\eta^{p/e}_{\mathrm{Car}}$ until it reaches a maximal temperature difference ΔT_{crit} (with $T_c = 2.5, \delta_1 = 2.25$ and $\delta_3 = 1.75$ we get $\Delta T_{\mathrm{crit}} = 0.714$). At this temperature the heat pump works losslessly and no heat can be pumped. Just like the quasi-stationary Carnot heat pump this pump has zero power. Only in this particular case $\eta^p_{\mathrm{Otto}} = \eta^p_{\mathrm{Car}}$. By further increasing the temperature T_h the heat pump starts working as a heat engine.

Figure 10.9 illustrates this behavior where $\Delta W^{\mathrm{Otto}}, \Delta Q_h^{\mathrm{Otto}}$ and $\Delta Q_c^{\mathrm{Otto}}$ are depicted as function of ΔT. At ΔT_{crit} no heat $\Delta Q_h^{\mathrm{Otto}}$ is pumped and therefore no work is used or no heat exhausted to do work.

This is qualitatively the same behavior as our model shows in Fig. 10.5 and Fig. 10.6. Two differences can be seen. First the critical temperature in our numerical result deviates from the theoretically expected one. From the numerics we get $\Delta T_{\mathrm{crit}} \approx 0.6$. Second the inset in Fig. 10.6 shows that ΔQ_c changes its sign before ΔQ_h does. The reason for both effects is due to the leakage current as will be explained below.

For a given bath temperature (like in our example $T_c = 2.5$) it is possible by changing the energy splittings of δ_1 and/or δ_3 to influence ΔT_{crit}. In Fig. 10.8 also a different efficiency $\tilde{\eta}^p_{\mathrm{Otto}}$ is depicted. $\tilde{\eta}^p_{\mathrm{Otto}}$ can be realized by increasing δ_1 so that ΔT_{crit} will be decreased to $\Delta\tilde{T}_{\mathrm{crit}}$.

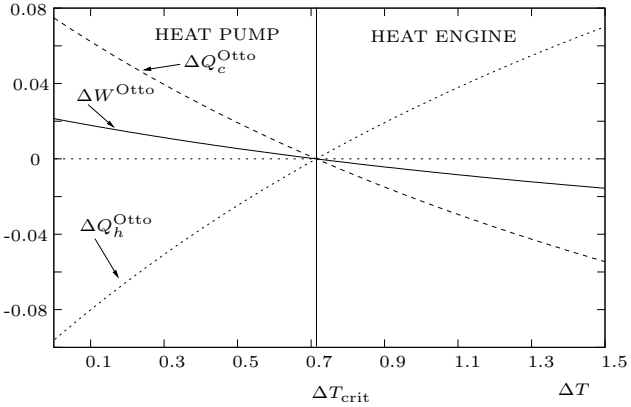

Figure 10.9.: Work $\Delta W^{\rm Otto}$, heat $\Delta Q_h^{\rm Otto}$ from/to the hot bath and heat $\Delta Q_c^{\rm Otto}$ from/to the cold bath for the ideal machine as function of temperature difference ΔT while $T_c = 2.5, \delta_1 = 2.25$ and $\delta_3 = 1.75$ as in Fig. 10.5. At $\Delta T = \Delta T_{\rm crit}$ $\eta^p_{\rm Otto} = \eta^{p/e}_{\rm Car}$ and therefore $\Delta W^{\rm Otto} = 0$, $\Delta Q_h^{\rm Otto} = 0$ and $\Delta Q_c^{\rm Otto} = 0$.

10.3.1. Quantum Machine with Leakage Current

The efficiency of an ideal Otto two level quantum machine is independent of ΔT except at $\Delta T = \Delta T_{\rm crit}$, where it jumps between its heat pump and its heat engine value. The efficiency obtained from the numerical simulation deviates somewhat from this expected behavior. The efficiency of our model is even larger than the "ideal" one for the heat pump (see Fig. 10.10). To understand this effect we analyze the leakage current from a phenomenological point of view.

First we assume that the leakage current causes the gas spin 2 to approach a thermal state, which is not in accordance with the bath temperature. In this case ΔQ_h and ΔQ_c will be decreased. This effect is responsible for the vanishing of $\eta^{p/m}_{\rm qm}$ before reaching $\Delta T_{\rm crit}$. But it cannot explain, why the efficiency of $\eta^p_{\rm qm}$ can become larger than $\eta^p_{\rm Otto}$.

Taking into account that also less work is performed due to the leakage current it is possible to find a larger efficiency. This can be interpreted in that the gas spin 2 does not "see" the full energy splitting δ_1. As shown in Fig. 10.10 our phenomenological model fits the numerical data quite well.

For the efficiency of the heat engine $\eta^e_{\rm qm}$ it can be seen from Fig. 10.10 that it is always worse than the ideal engine $\eta^p_{\rm Otto} < \eta^e_{\rm qm}$.

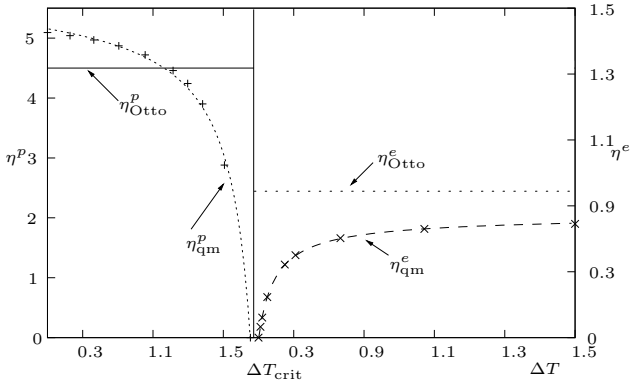

Figure 10.10.: Fitted efficiency $\eta^p_{\rm qm}$ for the quantum heat pump and quantum engine $\eta^e_{\rm qm}$ as function of temperature difference ΔT while $T_c = 2.5, \delta_1 = 2.25$ and $\delta_3 = 1.75$ as in Fig. 10.5. $\eta^p_{\rm Otto}$ and $\eta^e_{\rm Otto}$ are the efficiencies of the ideal pump/engine [see (9.7).

10.3.2. Quantum Machine and LEMBAS Principle

The LEMBAS principle of Chap. 5 has not been applied here due to the fact, that the tools to treat inhomogeneous systems have not yet been developed. To exactly treat the heat current flowing in and out of spin 2 we need to know the local correlation current $J_{\rm corr}$ flowing between system 1 and 2 as well as between 2 and 3. This could be down with the help of an adequate projection operator technique. We think that with the help of this projection operators it will be possible to understand the leakage current discussed phenomenologically in the previous subsection.

We remark that it is not sufficient to include the effective temperatures and Hamiltonians to explain the upshift of the efficiencies and the drifted critical temperature difference. Rather, the driving of spin 2 influences the interaction between spin 1 and 2 as well as between 2 and 3 in a way that energy will be stored in this interaction. As can be seen from Fig. 10.2, the so called leakage current does not flow from the hot to the cold bath because during the adiabatic steps almost no heat current flows at all. Also if spin 2 is in resonance with one of the boundary spins, heat flows into the respective bath only. In fact, it is an effect of the internal dynamics of the spin chain. This has to be proven, but from our point of view there seems to be no other place left where the energy could diffuse as a kind of internal friction.

11. Conclusion and Outlook

> Probleme kann man niemals mit derselben Denkweise lösen, durch die sie entstanden sind.
>
> Albert Einstein

In this thesis we have mainly pursued two aims: First, the existence and characterization of stationary nonequilibrium states in quantum systems and second, the investigation of small quantum system acting as thermodynamic machines. Both have in common the question about the existence of thermodynamic concepts and variables, like temperature, work and heat, etc., in nonequilibrium scenarios on the nanoscale. The way how a system reaches such nonequilibrium states was discussed within the open system approach. Therefore a quantum master equation of the Redfield form was used. In addition, it was argued that the so called secular approximation, widely used in quantum optics, may lead to unphysical solutions for the preparation of nonequilibrium stationary states.

The variables heat and work, cornerstones in the understanding of driven thermodynamic processes, have been given a new foundation in combination with quantum systems. The use of the LEMBAS (Local Effective Measurement Basis) has paved the way to a different look on the definition of heat and work. As a suprise, and in contrast to classical physics, it turns out that heat and work are basis dependent in quantum physics. This is interwoven with the energy measurement of a quantum system, which will be different in different frameworks. In this context interactions between the considered quantum systems play a crucial role. We have shown that even a small coupling between quantum systems can have an effect and change the energy balance. Nevertheless, the local energy measurements of each single subunit are complementary to each other. Thus, the sum of all these local energy measurements will be larger as the energy of the total system.

A particular role within LEMBAS is played by the effective dynamics induced by the rest of the considered system. The effective dynamics makes it possible to study the energy flow into or out of a subunit. It helps to distinguish clearly between coherent energy flow identified with “work” and the incoherent energy flow which could be identified with entropy production and

thus with heat. A continuity equation for the probability flux was derived, especially for the incoherent dynamics. The existence of this continuity equation for quantum systems leads, on the other side, to a nonintensive energy current in inhomogeneous systems. Even in the weak coupling limit the interaction absorbs a considerable amount of energy compared to the local energy expectation value.

The usefullness of the LEMBAS principle was shown also in the application on transport scenarios in 1-dimensional spin-chains. The transport behavior within this systems may be quite different depending on the type of interaction. For homogeneous Heisenberg chains the occurrence of diffusive behavior and therefore Fourier's law can be traced back to an anisotropy effect of the local (effective) energy splittings of each spin induced by the temperature gradient. Thus, a specific effect has been located, which is responsible for the transport behavior.

In a numerical experiment the possible outcome of an energy or temperature measurement has been studied. As in classical physics the experiment was based on the contact equilibrium between the system and the measurement device. Within the effective description motivated by the LEMBAS principle it has been shown that the effective temperatures will be equal. This is only valid for a small enough coupling between the device and the system. Otherwise, the measurement device would disturb not only the local contact subunit but also the complete system. This could have implications for real experiments which might be feasible in near future.

Some peculiarities of inhomogeneous 1-dimensional spin-chains has been discussed. The so called resonance effect enables the decoupling of two baths connected via a spin-chain. This opens the door to realize a heat pump or engine within spin-chains. By modulating the energy splitting of a spin in the chain it is possible to change the transport behavior of the chain dramatically. The modulation has to be in between the energy splittings of the boundary spins which are in contact with either heat bath. Although, driven in finite time, the spin describes Otto-cycles in the TS-diagram. The efficiency of the numerical study was compared to the theoretical expected one. In first approximation our quantum model shows the same properties as the theoretical model. A switching in the operation mode can be observed from the pump function to the engine function. This is typical for TLS working as a thermodynamic machine.

Intersting problems and open questions would be a proof of the transport behavior of 1-dim Heisenberg chains. This controversial discussed issue could be attacked with the LEMBAS principle in a more detailed analysis. By studying the decay of the current in chains without additional environment it might be possible to find a coarse grained description showing diffusive behav-

ior. Also the construction of the stationary state out of the local equilibrium states seems to be feasible. Or at least, a class of typical states could result which could be a good candidate to reproduce Fourier's law.

LEMBAS could also be used to clarify the relation between quantum information and quantum thermodynamics. Identifying the entanglement included in the correlation current this could also give new insights into the transport of entanglement. On the other side, entanglement is the basic ingredient for quantum thermodynamics. Also the relation of magnetic properties of as system with the new definition of heat and work might be interesting.

For quantum thermodynamic machines the influence of coherence and typical quantum effects are an open issue. As mentioned in Sect. 10.3.2, the coupling between the spins seems to play an important role. Although the driving seems classical and the coupling is weak, it influences the internal dynamics in a nonlinear way. The question is interlinked with the transport behavior of inhomogeneous systems in general.

In conclusion, we hope to have contributed, to establish thermodynamic properties and concepts of small quantum systems even in nonequilibrium situations. Maybe, the presented results help to push the border for the far reaching ideas of thermodynamics further.

Part III.

Appendices

A. Evolution of the von Neumann Entropy

The time derivative of the von Neumann entropy S is calculated. Special care is taken for the permutation relation. The derivative of the von Neumann entropy reads

$$\frac{\mathrm{d}}{\mathrm{d}t}S = \underbrace{-\mathrm{Tr}\left\{\dot{\hat{\rho}}\log\hat{\rho}\right\}}_{(I)} - \underbrace{\mathrm{Tr}\left\{\hat{\rho}\frac{\mathrm{d}\log\hat{\rho}}{\mathrm{d}t}\right\}}_{(II)}. \tag{A.1}$$

Using the Liouville-von Neumann equation supplemented by an additional incoherent part $\hat{\mathcal{L}}_{\mathrm{inc}}$, part (I) of (A.1) can be calculated to be

$$\begin{aligned}(I) &= \mathrm{Tr}\left\{\left(-\mathrm{i}\left[\hat{H},\hat{\rho}\right] + \hat{\mathcal{L}}_{\mathrm{inc}}(\hat{\rho})\right)\log\hat{\rho}\right\} \\ &= -\mathrm{i}\mathrm{Tr}\left\{\hat{H}\hat{\rho}\log\hat{\rho} - \hat{\rho}\hat{H}\log\hat{\rho}\right\} + \mathrm{Tr}\left\{\hat{\mathcal{L}}_{\mathrm{inc}}(\hat{\rho})\log\hat{\rho}\right\} \\ &= -\mathrm{i}\mathrm{Tr}\left\{\hat{H}\hat{\rho}\log\hat{\rho} - \hat{H}\hat{\rho}\log\hat{\rho}\right\} + \mathrm{Tr}\left\{\hat{\mathcal{L}}_{\mathrm{inc}}(\hat{\rho})\log\hat{\rho}\right\} \\ &= \mathrm{Tr}\left\{\hat{\mathcal{L}}_{\mathrm{inc}}(\hat{\rho})\log\hat{\rho}\right\},\end{aligned} \tag{A.2}$$

where we used the cyclic permutation under the trace operation. Part (II) of (A.1) needs more care, because in general

$$\frac{\mathrm{d}\log\hat{\rho}}{\mathrm{d}t} \neq \frac{1}{\hat{\rho}}\dot{\hat{\rho}}, \tag{A.3}$$

due to the fact that $\left[\hat{\rho},\dot{\hat{\rho}}\right] \neq 0$. To solve (II), $\hat{\rho}$ should be transformed into the eigenbasis $|k\rangle$. Because $\hat{H}$ could be time dependent, $|k\rangle$ may change. The expansion in $|k\rangle$ leads to

$$\frac{\mathrm{d}\log\hat{\rho}}{\mathrm{d}t} = \sum_k \left(\frac{1}{p_k}\dot{p}_k|k\rangle\langle k| + \log p_k|\dot{k}\rangle\langle k| + \log p_k|k\rangle\langle\dot{k}|\right). \tag{A.4}$$

Multiplying (A.4) with $\hat{\rho}$ yields

$$\begin{aligned}\hat{\rho}\frac{\mathrm{d}\log\hat{\rho}}{\mathrm{d}t} &= \sum_{k,l}\left(\frac{p_l}{p_k}\dot{p}_k|l\rangle\langle l||k\rangle\langle k| + p_l\log p_k|l\rangle\langle l||\dot{k}\rangle\langle k|\right.\\ &\quad \left.+p_l\log p_k|l\rangle\langle l||\dot{k}\rangle\langle k|\right)\\ &= \sum_k \dot{p}_k|k\rangle\langle k| + \sum_{k,l} p_l\log p_l\left(|l\rangle\langle l||\dot{k}\rangle\langle k| + |l\rangle\langle l||k\rangle\langle\dot{k}|\right) \quad \text{(A.5)}\end{aligned}$$

Now we take the trace over (A.5) to get

$$\begin{aligned}\mathrm{Tr}\left\{\hat{\rho}\frac{\mathrm{d}\log\hat{\rho}}{\mathrm{d}t}\right\} &= \mathrm{Tr}\left\{\dot{\hat{\rho}}\right\} + \sum_{k,l,m} p_l\log p_k\left(\langle m|l\rangle\langle l|\dot{k}\rangle\langle k|m\rangle + \right.\\ &\quad \left.+\langle m|l\rangle\langle l|k\rangle\langle\dot{k}|m\rangle\right)\\ &= \underbrace{\mathrm{Tr}\left\{-\mathrm{i}\left[\hat{H},\hat{\rho}\right]\right\}}_{=0} +\\ &\quad + \sum_k p_k\log p_k\underbrace{\left(\langle k|\dot{k}\rangle + \langle\dot{k}|k\rangle\right)}_{\frac{\mathrm{d}}{\mathrm{d}t}\langle k|k\rangle=0}. \quad \text{(A.6)}\end{aligned}$$

Therefore only (I) contributes to the derivative of S and we finally get, as expected

$$\frac{\mathrm{d}S}{\mathrm{d}t} = -\mathrm{Tr}\left\{\hat{\mathcal{L}}_{\mathrm{inc}}(\hat{\rho})\log\hat{\rho}\right\}. \quad \text{(A.7)}$$

B. Bath Correlation Function

For the QME used throughout this thesis a bath was assumed to consist of many uncoupled harmonic oscillators [10, 96, 98]. The Hamiltonian of the bath reads

$$\hat{H}_{\text{env}} = \sum_{j}^{\infty} \omega_j \left(\hat{b}_j^\dagger \hat{b}_j + \frac{1}{2} \right), \tag{B.1}$$

with the bosonic creation and annihilation operators $\hat{b}$. The interaction operators $\hat{Y}$[1] of (4.12) take the form

$$\hat{Y} = \sum_{j}^{\infty} g_j^* \hat{b}^\dagger \mathrm{e}^{\mathrm{i}\omega_j t} + g_j \hat{b} \hat{\mathrm{e}}^{-\mathrm{i}\omega_j t} \tag{B.2}$$

The bath correlation functions (4.17) together with (B.2) yield

$$\begin{aligned} \Gamma(t) &= \sum_{ij}^{\infty} \mathrm{Tr}_{env} \left\{ \left(g_i^* \hat{b}^\dagger \mathrm{e}^{\mathrm{i}\omega_i t} + g_i \hat{b} \hat{\mathrm{e}}^{-\mathrm{i}\omega_i t} \right) \left(g_j^* \hat{b}^\dagger \mathrm{e}^{\mathrm{i}\omega_j t} + g_j \hat{b} \hat{\mathrm{e}}^{-\mathrm{i}\omega_j t} \right) \right\} \\ &= \sum_{i} g_i g_i^* \left(N(\omega_i) \mathrm{e}^{\mathrm{i}\omega_i t} - N(-\omega) \mathrm{e}^{-\mathrm{i}\omega_i t} \right) \end{aligned} \tag{B.3}$$

where we used the Planck-distribution for a bath in a thermal state,

$$N(\omega) = \frac{1}{\mathrm{e}^{\beta\omega} - 1}. \tag{B.4}$$

β is the inverse bath temperature. Also the condition

$$N(\omega) + 1 = -N(-\omega) \tag{B.5}$$

was used. To further simplify (B.3), the delta function $\delta(\omega)$ is introduced by

$$\Gamma(t) = \sum_{i} g_i g_i^* \int_{-\infty}^{\infty} \mathrm{d}\omega \mathrm{e}^{\mathrm{i}\omega t} \left(N(\omega_i) \delta(\omega_i - \omega) - N(-\omega) \delta(\omega - \omega_i) \right) \tag{B.6}$$

[1] We omitted the summation over the index k because we are interested only in a local coupling to the bath.

Performing the Fourier transform of B.6

$$\begin{aligned}\Gamma(\omega) &= (N(\omega_i)\delta(\omega_i-\omega) - N(-\omega)) \\ &= N(\omega)\left(D(\omega) - D(-\omega)\right), \end{aligned} \tag{B.7}$$

with the density of states of the bath $D(\omega)$. Taking into account that the spectrum is dense, a spectral density of the form

$$J(\omega) = \omega^{\gamma}\theta(\omega) \tag{B.8}$$

can be defined. $\theta(\omega)$ is the step-function and γ is a parameter which distinguishes the following cases: For $\gamma = 1$ the bath is called ohmic, the sub-ohmic case results for $\gamma < 1$ and the super-ohmic case for $\gamma > 1$. In the present work we used $\gamma = 1$.

The Redfield equation (4.21)

$$\frac{\mathrm{d}}{\mathrm{d}t}\hat{\rho}_{\mathrm{s}}(t) = -\mathrm{i}[\hat{H}_{\mathrm{s}}, \hat{\rho}_{\mathrm{s}}(t)] + \alpha^2 \int_0^{\infty} \mathrm{d}s\Gamma(\tau)\left[\hat{X}(-\tau)\hat{\rho}_{\mathrm{s}}(t), \hat{X}(0)\right] + \text{H. c.} \tag{B.9}$$

can be brought into a compact form, which is useful for the numerical solution of the QME. By defining the following operator

$$\hat{R} := \int_0^{\infty} \mathrm{d}\tau\Gamma(\tau)\hat{X}(-\tau) \tag{B.10}$$

(B.9) takes the form

$$\frac{\mathrm{d}}{\mathrm{d}t}\hat{\rho}_{\mathrm{s}}(t) = -\mathrm{i}[\hat{H}_{\mathrm{s}}, \hat{\rho}_{\mathrm{s}}(t)] + \alpha^2 \left\{\left[\hat{R}\hat{\rho}_{\mathrm{s}}(t), \hat{X}\right] + \left[\hat{X}, \hat{\rho}_{\mathrm{s}}(t)\hat{R}^{\dagger}\right]\right\} \tag{B.11}$$

The matrix components of $\hat{R}$ in the energy eigenbasis of $\hat{H}_{\mathrm{s}}$ read (see [81])

$$\begin{aligned}\langle n|\hat{\mathcal{D}}|m\rangle &= \int_0^{\infty} \mathrm{d}\tau\Gamma(\tau)\langle n|\hat{X}(-\tau)|m\rangle \\ &= \int_0^{\infty} \mathrm{d}\tau\Gamma(\tau)\langle n|\mathrm{e}^{-\mathrm{i}\hat{H}_{\mathrm{s}}\tau}\hat{X}\mathrm{e}^{\mathrm{i}\hat{H}_{\mathrm{s}}\tau}|m\rangle \\ &= \int_{-\infty}^{\infty} \mathrm{d}\omega \int_0^{\infty} \mathrm{d}\tau\mathrm{e}^{\mathrm{i}\omega\tau}\Gamma(\omega)\mathrm{e}^{\mathrm{i}\omega'\tau}\langle n|\hat{X}|m\rangle. \end{aligned} \tag{B.12}$$

In the last step we have used (B.6) and (B.7). Eq (B.13) can be integrated with the help of the Cauchy principle value

$$\int_0^{\infty} \mathrm{d}\tau\mathrm{e}^{i\omega\tau} = \pi\delta(\omega) - \mathrm{i}\frac{\mathrm{P}}{\omega} \tag{B.13}$$

to

$$\langle n|\hat{R}_l|m\rangle = \pi\Gamma(\omega)\langle n|\hat{X}_l|m\rangle \tag{B.14}$$

by neglecting the Cauchy principle value P, which can be added to the system Hamiltonian [30] (e.g. as the Lamb-shift).

It can be shown that the canonical density operator of the form

$$\hat{\rho} = \frac{1}{Z}\mathrm{e}^{-\beta\hat{H}_s}, \tag{B.15}$$

where Z denotes the partion function and β the bath temperature, is the stationary solution of (B.9). The Redfield equation (B.9) is, at least, appropriate to describe the right stationary state for locally coupled spin chains in equilibrium situation, as was studied in [44].

C. Effective Dynamics for TLS

Here we elaborate on the assignment of the effective dynamics [see (5.10) and (5.10)] for the Heisenberg interaction. Especially, we show why the X and Y contributions vanish in (5.19). Remembering (5.19)

$$\hat{H}^{\text{eff}} = \text{Tr}_B \left\{ (\hat{\sigma}^x \otimes \hat{\sigma}^x + \hat{\sigma}^y \otimes \hat{\sigma}^y + \hat{\sigma}^z \otimes \hat{\sigma}^z)(\hat{1}_A \otimes \hat{\rho}_B) \right\} \tag{C.1}$$

which can be written in the form

$$\begin{aligned} \hat{H}^{\text{eff}} &= \text{Tr}_B \left\{ (\hat{\sigma}^x \otimes \hat{\sigma}^x)(\hat{1}_A \otimes \hat{\rho}_B) + (\hat{\sigma}^y \otimes \hat{\sigma}^y)(\hat{1}_A \otimes \hat{\rho}_B) + \right. \\ &\quad \left. + (\hat{\sigma}^z \otimes \hat{\sigma}^z)(\hat{1}_A \otimes \hat{\rho}_B) \right\}. \end{aligned} \tag{C.2}$$

We omit the last term, because it was explicitly calculated in (5.20). The first term of (C.2) reads

$$(\hat{\sigma}^x \otimes \hat{\sigma}^x)(\hat{1}_A \otimes \hat{\rho}_B) = \begin{pmatrix} 0 & 0 & 0 & 1 \\ 0 & 0 & 1 & 0 \\ 0 & 1 & 0 & 0 \\ 1 & 0 & 0 & 0 \end{pmatrix} \begin{pmatrix} b_{11} & b_{12} & 0 & 0 \\ b_{21} & b_{22} & 0 & 0 \\ 0 & 0 & b_{11} & b_{12} \\ 0 & 0 & b_{21} & b_{22} \end{pmatrix} \tag{C.3}$$

and the second

$$(\hat{\sigma}^x \otimes \hat{\sigma}^x)(\hat{1}_A \otimes \hat{\rho}_B) = \begin{pmatrix} 0 & 0 & 0 & -1 \\ 0 & 0 & 1 & 0 \\ 0 & 1 & 0 & 0 \\ -1 & 0 & 0 & 0 \end{pmatrix} \begin{pmatrix} b_{11} & b_{12} & 0 & 0 \\ b_{21} & b_{22} & 0 & 0 \\ 0 & 0 & b_{11} & b_{12} \\ 0 & 0 & b_{21} & b_{22} \end{pmatrix}. \tag{C.4}$$

As can be seen both terms are equal to zero and thus do not contribute to the effective dynamics.

D. Analytical Expressions of the Energy Currents

The analytical solution for the reduced density operators $\hat{\rho}_A(t)$ and $\hat{\rho}_B(t)$ for to Heisenberg interacting spins is given here. The intial state of the total system is given by

$$\hat{\rho}(0) = \hat{\rho}_A(0) \otimes \hat{\rho}_B(0) \tag{D.1}$$

with the

$$\hat{\rho}_\mu = \begin{pmatrix} p_\mu & 0 \\ 0 & 1 - p_\mu \end{pmatrix}, \tag{D.2}$$

with $\mu = A, B$. The solution of the von Neumann equation for the reduced density operators for system A for the diagonal elements are given by

$$\begin{aligned} \rho_A^{11}(t) &= \frac{8\alpha\lambda^2 + p_A\omega^2 + 8\gamma\lambda^2 \cos\left(t\sqrt{\phi}\right)}{\phi} \\ \rho_A^{22}(t) &= \frac{-8(\alpha-2)\lambda^2 - (p_A-1)\omega^2 - 8\gamma\lambda^2 \cos\left(t\sqrt{\phi}\right)}{\phi} \end{aligned} \tag{D.3}$$

and for system B

$$\begin{aligned} \rho_B^{11}(t) &= \frac{8\alpha\lambda^2 + p_B\omega^2 - 8\gamma\lambda^2 \cos\left(t\sqrt{\phi}\right)}{\phi} \\ \rho_B^{22}(t) &= \frac{-8\alpha - 2\lambda^2 - (p_B-1)\omega^2 + 8\gamma\lambda^2 \cos\left(t\sqrt{\phi}\right)}{\phi}. \end{aligned} \tag{D.4}$$

with following abbriviations: $\alpha = p_A + p_B$, $\gamma = p_A - p_B$ and $\phi = 16\lambda^2 + \omega^2$. $\omega = \delta_A - \delta_B$ is the detuning between the systems. In the following we use $\delta_A = \delta_B - \omega$.

The analytical solution of the energy expectation value for the effective

Hamiltonians with the states (D.3) and (D.4) yields

$$\begin{aligned}\langle H'_A\rangle &= -\frac{16(\alpha-1)\lambda^2+(2p_A-1)\omega^2+16\gamma\lambda^2\cos\left(t\sqrt{\phi}\right)}{2\phi^2}\\ &\frac{1}{2\phi^2}\left\{16\lambda^2\left[\delta_B-2(\alpha-1)\Delta\lambda\right]+16\lambda^2\omega+\right.\\ &+\left[\delta_B+2(1-2p_B)\Delta\lambda\right]\omega^2+\omega^3+\\ &\left.+32\gamma\Delta\lambda^3\cos\left(t\sqrt{\phi}\right)\right\} \qquad \text{(D.5)}\end{aligned}$$

and

$$\begin{aligned}\langle H'_B\rangle &= -\frac{16(\alpha-1)\lambda^2+(2p_B-1)\omega^2-16\gamma\lambda^2\cos\left(t\sqrt{\phi}\right)}{2\phi^2}\\ &\frac{1}{2\phi^2}\left\{16\lambda^2\left[\delta_B-2(\alpha-1)\Delta\lambda\right]+\right.\\ &+\left[\delta_B+2(1-2p_A)\Delta\lambda\right]\omega^2-\\ &\left.-32\gamma\Delta\lambda^3\cos\left(t\sqrt{\phi}\right)\right\} \qquad \text{(D.6)}\end{aligned}$$

The results for the heat currents $đQ_\mu$ can then be calculated from $\hat{\mathcal{L}}_{\text{inc}}$ and reads

$$\begin{aligned}đQ_A &= \frac{8\gamma\lambda^2}{\phi^{3/2}}\left\{\sin\left(t\sqrt{\phi}\right)\left[16\lambda^2(\delta_B-2(\alpha-1)\Delta\lambda)+\right.\right.\\ &+16\lambda^2\omega+(\delta_B+2(1-2p_B)\Delta\lambda)\omega^2+\omega^3\left.\right]+\\ &\left.+16\gamma\Delta\lambda^3\sin\left(2t\sqrt{\phi}\right)\right\} \qquad \text{(D.7)}\end{aligned}$$

and

$$\begin{aligned}đQ_B &= \frac{8\gamma\lambda^2}{\phi^{3/2}}\sin\left(t\sqrt{\phi}\right)\left\{16\lambda^2\left[2(\alpha-1)\Delta\lambda-\delta_B\right]-\right.\\ &-\left[\delta_B+2(1-2p_A)\Delta\lambda\right]\omega^2+\\ &\left.+32\gamma\Delta\lambda^3\cos\left(2t\sqrt{\phi}\right)\right\} \qquad \text{(D.8)}\end{aligned}$$

In (D.7) and (D.8) there is one term which is linear in the coupling strength λ if we neglect the detuning in ϕ and remember the λ^2 term in ϕ. If a detuning is present and is larger than λ, $đQ_A$ will grow in the order of ω because of the ω^3 term (because ϕ depends quadratic of ω what result in a linear dependence). In contrast $đQ_B$ depends only on ω^2.

The correlation current takes the form

$$J_{\text{corr}} = -\frac{8\gamma\lambda^2 \sin\left(t\sqrt{\phi}\right)}{\phi^{3/2}} \left\{\omega\left(16\lambda^2 + 4\gamma\Delta\lambda\omega + \omega^2\right) + 64\gamma\Delta\lambda^3 \cos\left(t\sqrt{\phi}\right)\right\}. \quad \text{(D.9)}$$

At last the results for $đW_\mu$ is given by

$$đW_A = \frac{\gamma\Delta\lambda^3 \sin\left(t\sqrt{\phi}\right)}{(16\phi)^{3/2}} \left\{16(\alpha-1)\lambda^2 + (2p_A - 1)\omega^2 + 16\gamma\lambda^2 \cos\left(t\sqrt{\phi}\right)\right\} \quad \text{(D.10)}$$

and

$$đW_B = \frac{\gamma\Delta\lambda^3 \sin\left(t\sqrt{\phi}\right)}{(16\phi)^{3/2}} \left\{16(1-\alpha)\lambda^2 + (1 - 2p_B)\omega^2 + 16\gamma\lambda^2 \cos\left(t\sqrt{\phi}\right)\right\} \quad \text{(D.11)}$$

The energy change given by $đW_\mu$ depends in third order of λ and can thus with decreasing λ be omitted.

E. Pauli Operators and Trace Relations

E.1. Pauli Operators

The following form of the Pauli operators are used:

$$\hat{\sigma}^x = \begin{pmatrix} 0 & 1 \\ 1 & 0 \end{pmatrix}, \tag{E.1}$$

$$\hat{\sigma}^y = \begin{pmatrix} 0 & \mathrm{i} \\ -\mathrm{i} & 0 \end{pmatrix} \tag{E.2}$$

and

$$\hat{\sigma}^z = \begin{pmatrix} -1 & 0 \\ 0 & 1 \end{pmatrix}, \tag{E.3}$$

E.2. Trace Relations

Some useful relations for the calculation of the partial trace are summarized here. Especially they are used in Chap. 5 for the calculation of the effective dynamics (see [84]).

For the tensor product the following relation for the trace holds

$$\mathrm{Tr}\left\{A \otimes B\right\} = \mathrm{Tr}\left\{A\right\} \mathrm{Tr}\left\{B\right\}. \tag{E.4}$$

The partial traces over different subsystems for a product state yields

$$\mathrm{Tr}_1\left\{[A \otimes 1, B]\right\} = 0 \quad \text{and} \tag{E.5}$$

$$\mathrm{Tr}_2\left\{[1 \otimes A, B]\right\} = 0, \tag{E.6}$$

and for the adjoint operator

$$\mathrm{Tr}_i\left\{A^\dagger\right\} = \left(\mathrm{Tr}_i\left\{A\right\}\right)^\dagger. \tag{E.7}$$

Additionally, the following can be verified using the partial trace over, e.g., subsystem 2.

$$\mathrm{Tr}_2\left\{\left(A\otimes\hat{1}\right)B\right\} = A(\mathrm{Tr}_2\left\{B\right\}) \quad \text{and} \tag{E.8}$$

$$\mathrm{Tr}_2\left\{B\left(A\otimes\hat{1}\right)\right\} = (\mathrm{Tr}_2\left\{B\right\})A. \tag{E.9}$$

F. German Summary – Deutsche Zusammenfassung

> Das Höchste, wozu der Mensch gelangen kann, ist das Staunen.
>
> J. W. von Goethe

Die Thermodynamik und statistische Physik hat sich als eines der fruchtbarsten physikalischen Konzepte entwickelt. Vom wissenschaftlichen Standpunkt aus gesehen erstreckt sich ihr Anwendungsbereich über weite Gebiete, nicht nur der Physik. Ihre wissenschaftliche Geburtsstunde feierte die Thermodynamik mit den Untersuchungen S. Carnots über die maximale Effizienz thermodynamischer Maschinen in [16]. Ein wichtiger Schritt zur Weiterentwicklung der Theorie war die Erkenntnis, dass Wärme eine Form von Energie ist. R. Clausius war es schließlich, der den Begriff Entropie einführte und damit den berühmten zweiten Hauptsatz der Thermodynamik formulierte [19].

Der Begriff, oder vielmehr die Natur der Entropie blieb aber lange Zeit unklar. Durch die Arbeiten von L. Boltzmann wurde das Anwachsen der Entropie zurückgeführt auf molekulares Chaos der einzelnen Atome, welche zu dem berühmten H-Theorem führte [6]. W. Gibbs arbeitete den statistischen Aspekt der Thermodynamik weiter aus durch seine Ensemble-Theorie [37]. Es blieb aber weiter im Verborgenen, wie aus reversiblen mikroskopischen Bewegungsgleichungen irreversible Prozesse entstehen können ohne der Zuhilfenahme zusätzlicher Annahmen, wie z. B. der Ergodenhypothese.

Äußerst schwierig gestaltete sich auch die Einbeziehung der Quantenmechanik als grundlegende mikroskopische Beschreibung, da die statistischen Konzepte im klassischen Phasenraum arbeiteten. Kürzlich ist es schließlich J. Gemmer et. al. gelungen, auf Basis der Quantenmechanik irreversibles Verhalten zur erklären [33]. Die so genannte *Quantenthermodynamik* regte zu weiteren Forschungen speziell im Bereich der Nichtgleichgewichtsthermodynamik an. Von großem Interesse sind dabei Transporteigenschaften und die Entstehung stationärer Zustände [63].

Ein wichtiger Punkt bei den Untersuchungen von Nichtgleichgewichtsphänomenen, und im Besonderen in Verbindung mit der Quantenthermodynamik,

ist die Anwendbarkeit der bereits bekannten Konzepte aus der klassischen Thermodynamik. Fragen nach der Extensivität der Energie und Entropie, sowie nach der Existenz einer Temperatur sind dabei genauso wichtig wie die Untersuchung thermodynamischer Kreisprozesse für Quantensysteme.

F.1. Erzeugung von Nichtgleichgewichtsmodellen

Das theoretische Modell zur Erzeugung von Nichtgleichgewichtszuständen, welches in der Arbeit verwendet wurde, basiert auf der Quanten-Mastergleichung (QME). Hierbei wurde eine Redfield-Gleichung [77] verwendet. Diese wurde mit Hilfe der Nakajima-Zwangzig-Projektionstechnik abgeleitet (z. B. [10]). Die hier zum Tragen kommenden Nichtgleichgewichtsmodelle koppeln lokal, d. h. nur an einer Untereinheit des gesamten Quantensystems mit dem Bad (siehe Abb. F.1).

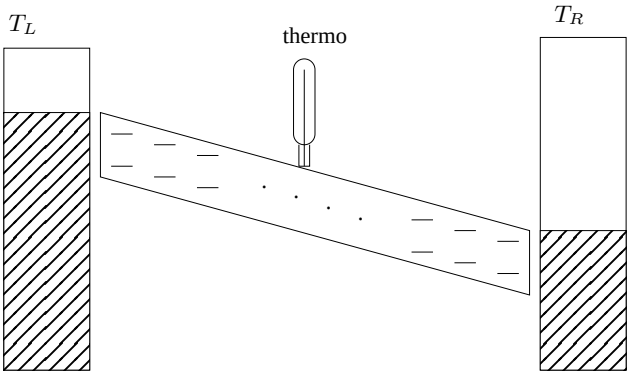

Abbildung F.1.: Modular aufgebautes Modellsystem zwischen zwei Bädern zur Untersuchung von Nichtgleichgewichtsphänomenen.

Die Verwendung einer Lindbladform [58], welche typischerweise im Bereich der Quantenoptik angewendet wird, ist im allgemeinen für Nichtgleichgewichtsphänomene jedoch unzureichend. Die Standardableitung der Lindbladform (siehe [10]) verwendet eine zusätzliche, so genannte "secular approximation" (SA). Diese ermöglicht ein Entkoppeln der Dämpfung der Diagonalelemente und der Nichtdiagonalelemente und liefert als stationären Zustand einen Zustand, der diagonal in der Eigenbasis des Systems ist. Dieser stationäre Zustand weist somit keinerlei Ströme auf und entspricht damit nicht der physikalisch vorgegebenen Nichtgleichgewichtssituation.

Der phänomenologische Grund für das Scheitern der Lindbladform ist begründet in der Struktur des Spektrums der zu untersuchenden Systeme. Spin-Ketten mit schwacher Nächster-Nachbar-Wechselwirkung besitzen ein Spektrum mit kleinen Frequenzen, welches durch die Aufhebung der Entartung entsteht. Diese kleine Frequenzen werden nun von der SA vernachlässigt. Eine Möglichkeit, eine Lindbladform für Nichtgleichgewichtsszenarien abzuleiten, besteht nun darin, die Raten nicht nach der Systemeigenbasis zu entwickeln, sondern in der Eigenbasis des Untersystems, welches mit dem Bad direkt wechselwirkt.

F.2. Lokale Thermodynamische Eigenschaften

Betrachtet man ein quantenmechanisches Vielteilchensystem, beeinflussen die Kopplungen zwischen den einzelnen Teilchen die Teilchen selbst. Ist man nun aber an lokalen Größen der einzelnen Teilchen interessiert, stellt sich die Frage, in wie weit die Wechselwirkung die Messung beeinflusst. Es ist möglich für, z. B. ein Zwei-Teilchensystem, eine effektive Bewegungsgleichung der Form

$$\frac{\mathrm{d}\hat{\rho}_A}{\mathrm{d}t} = -\mathrm{i}\left[\hat{H}_A + \hat{H}^{\mathrm{eff}}, \hat{\rho}_A(t)\right] + \hat{\mathcal{L}}_{\mathrm{inc}}(\hat{\rho}). \tag{F.1}$$

für Teil A aufzustellen. $\hat{H}^{\mathrm{eff}}$ generiert dabei ein lokale effektive Dynamik, welche mittels der Wechselwirkung von System B induziert wird. Neben diesem kohärenten Anteil existiert noch ein inkohärenter Anteil $\hat{\mathcal{L}}_{\mathrm{inc}}(\hat{\rho})$, weshalb keine geschlossene Differentialgleichung für System A vorliegt. $\hat{H}^{\mathrm{eff}}$ kann nun zerlegt werden in zwei Anteile

$$\hat{H}^{\mathrm{eff}} = \hat{H}_1^{\mathrm{eff}} + \hat{H}_2^{\mathrm{eff}}, \tag{F.2}$$

wobei folgende Relationen erfüllt sein müssen:

$$\left[\hat{H}_1^{\mathrm{eff}}, \hat{H}_A\right] = 0 \quad \text{and} \quad \left[\hat{H}_2^{\mathrm{eff}}, \hat{H}_A\right] \neq 0. \tag{F.3}$$

Diese Aufteilung zerlegt quasi die effektive Dynamik, und damit den Einfluss der Wechselwirkung, in einen Teil, der das lokale Spektrum ändert und damit messbar ist. Somit kann man einen *effektiven* Hamiltonian definieren

$$\hat{H}_A^{\mathrm{L}} = \hat{H}_A + \hat{H}_1^{\mathrm{eff}}, \tag{F.4}$$

welcher die Grundlage für alle lokalen Größen bildet. Dies ist das so genannte LEMBAS (Lokale Effektive Measurement Basis) Prinzip. Mit Hilfe der zeitlichen Ableitung von (F.4) können dann Größen wie Arbeit und Wärme neu

definiert werden in der Form

$$đW = \mathrm{Tr}\left\{(\dot{\hat{H}}_A + \dot{\hat{H}}_1^{\mathrm{eff}})\hat{\rho}_A - \mathrm{i}\left[\hat{H}_A + \hat{H}^{\mathrm{eff}}, \hat{\rho}_A\right]\right\}\mathrm{d}t \quad \text{und} \tag{F.5}$$

$$đQ = \mathrm{Tr}\left\{\hat{H}_A^{\mathrm{L}}\hat{\mathcal{L}}_{\mathrm{inc}}(\hat{\rho})\right\}\mathrm{d}t. \tag{F.6}$$

Es kann gezeigt werden, dass der inkohärente Anteil $\hat{\mathcal{L}}_{\mathrm{inc}}(\hat{\rho})$ in (F.1) für die Entropieänderung des Systems verantwortlich ist. Unter Berücksichtigung dieses Aspekts kann gezeigt werden, dass der Wahrscheinlichkeitsstrom eine Erhaltungsgröße ist. Diese Eigenschaft führt nun dazu, dass bei z. B. inhomogenen 1-dimensionale Spinketten der Energiestrom keine intensive Größe mehr sein kann. Die Energie wird vielmehr von der Wechselwirkung absorbiert, auch im so genannten Schwachkopplungslimes.

F.3. Transport und lokale Eigenschaften im Nichtgleichgewicht

Von großem wissenschaftlichem Interesse ist das Transportverhalten niederdimensionaler Systeme. Angeregt durch Experimente an Isolatoren mit magnetischen Eigenschaften (z. B. [48, 49]) und Carbon-Nanotubes (z. B. [13, 52] wurden verschieden theoretische Modelle und Ansätze zur Klärung der Transporteigenschaften entwickelt. Die Ergebnisse sind zum Teil stark voneinander abweichend, auch wenn vermeintlich das gleiche Modell (sprich Hamiltonian) zur Ableitung verwendet wurde, die Methoden jedoch unterschiedlich sind.

Die verbreitetesten Methoden zur Beschreibung von Transporteigenschaften ist zum einen die Peierls-Boltzmann-Gleichung [74]. Der Transport wird mit Hilfe von Phononen und den so genannten Umklapp-Prozessen beschrieben. Es konnte jedoch nachgewiesen werden, dass speziell magnetische Systeme auch einen magnetischen Transportanteil haben [48], die nicht von Phononen herrühren können. Die nächste Stoßrichtung basiert auf der Kubo-Formel [53] und ist eine lineare Antworttheorie. Dabei wird der Zerfall der Strom-Strom-Korrelationen beobachtet. Ein Überblick findet sich in [43]. Die Anwendung der Kubo-Formel auf Wärmetransport ist allerdings strittig, da im Gegensatz zum elektronischen Transport nicht zwangsläufig Teilchen für den Transport verantwortlich sein müssen. Die Kubo-Formel wurde aber unter dieser Annahme abgeleitet.

Eine neue, "teilchenfreie"Methode wurde kürzlich in [66, 79] verwendet. Dort wurde gezeigt, dass integrable Systeme wie die homogene Heisenberg-Kette normalen (diffusiven) Transport zeigen können. Fouriers Gesetz der

Wärmeleitung wurde in diesen Ketten gefunden. Das Auftreten dieses Transportverhaltens wurde darauf zurückgeführt, dass der Strom (bzw. der Stromoperator) keine Erhaltungsgröße ist. Eine Förster-gekoppelte Spinkette hingegen zeigt ballistischen Transport, da der Strom nun eine Erhaltungsgröße ist.

Die Emergenz des Fourier-Gesetzes beruht sehr stark auf lokalen Eigenschaften wie der Temperatur. Durch die Verwendung des LEMBAS Prinzips kann gezeigt werden, dass die Heisenberg-Kette einen Anteil in der Wechselwirkung besitzt, welcher das lokale Spektrum deformiert (siehe Abb. F.2). Durch die beiden Bäder, welche an den Rand der Kette koppeln, wird die Isotropie des Systems nachhaltig gestört. Diese Störung hebt somit die Integrabilitätsbedingung auf, warum es somit nicht mehr verwunderlich ist, weshalb diese Ketten diffusive Transporteigenschaften zeigen. Eine Förster-gekoppelte Kette hingegen hat keinen Anteil in der Wechselwirkung welcher in der Lage ist, das lokale Spektrum zu deformieren. Das System bleibt auch durch den Randeffekt der Bäder isotrop und somit integrabel.

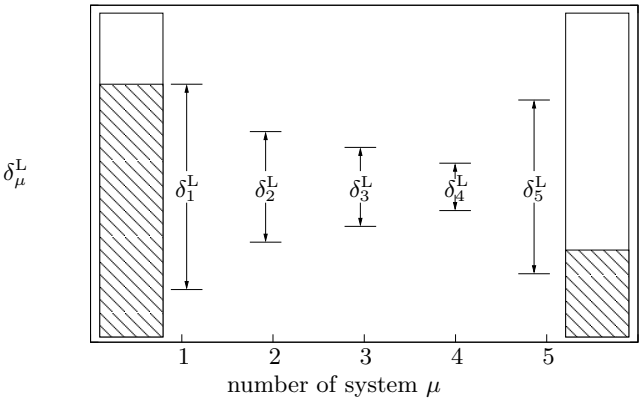

Abbildung F.2.: Skizze der effektiven Aufspaltungen δ'_μ für eine homogene Spinkette mit Nächster-Nachbar-Heisenberg-Wechselwirkung zwischen zwei Bädern unterschiedlicher Temperatur.

Ein weiterer interessanter Aspekt 1-dimensionaler Spinketten ist das Transportverhalten in Abhängigkeit der lokalen Energieaufspaltungen. In inhomogenen Systemen ist ein Resonanzeffekt feststellbar. Wird die Aufspaltung, z. B. eines Spins, in einer ansonsten homogen aufgespaltenen Kette variiert, fällt der Strom durch das System schnell ab, wenn das System "off-resonant" ist. Es ist somit möglich, Systeme von Bädern zu entkoppeln. Desweiteren kann ein von außen aufgeprägter Energiegradient (in Form eines B-Feldes) einen

asymmetrischen Wärmefluss in den Ketten induzieren. Es entsteht somit ein Dioden-Effekt, wonach 1-dimensionale Spinketten den Strom entgegen dem Energiegradienten besser leiten als mit. Dies lässt sich darauf zurückführen, dass die Wechselwirkung zwischen den Systemen unterschiedlich viel Energie aufwendet, um die Besetzungszahlen zu transportieren.

F.4. Temperaturmessmodell

Möchte man die Temperatur eines modular aufgebauten Systems im Nichtgleichgewicht lokal messen, so stellt sich im Nanobereich die Frage, welche Temperatur gemessen wird. Kürzlich wurde gezeigt, dass die Temperatur abhängig von der zu messenden Systemgröße und der Wechselwirkung zwischen den einzelnen Systemen ist [40]. Für Nichtgleichgewichtsszenarien ist mit großer Wahrscheinlichkeit auch noch der Temperaturgradient ausschlaggebend.

Unter Zuhilfenahme der oben beschriebenen Modelle (vgl. Abb. F.1) ist es möglich ein numerisches Experiment durchzuführen, welches mittels des Kontaktgleichgewichts eine lokale Temperatur messen soll. Die verwendete Hypothese dabei ist, dass ein System eine messbare Temperatur besitzt, wenn es sich in einem kanonischen Zustand befindet. Es kann gezeigt werden, dass mittels eines Kontaktgleichgewichts nicht die Temperatur gemessen wird, die über den lokalen Hamiltonian bestimmt wird, sondern vielmehr diejenige gemessen wird, welche mit dem effektiven Hamiltonian (F.4) berechnet werden kann. Dies ist eine numerische Bestätigung des LEMBAS Prinzips, welches sich noch in real durchgeführten Experimenten beweisen muss.

F.5. Kreisprozesse und quantenthermodynamische Maschinen

Die fortschreitende Nanotechnologie macht es erforderlich, dass auch die klassischen thermodynamischen Kreisprozesse auf ihre Existenz auf der Quantenebene überprüft werden müssen. Die Manipulation einzelner Atome eröffnet möglicherweise in naher Zukunft die Konstruktion von Nanomaschinen. Erste richtungweisende Untersuchungen wurden in [1, 36, 85] gemacht. In den letzten Jahrzehnten kamen immer neue Modelle hinzu (vgl. z. B. [4, 26, 26, 27, 46, 50, 51, 72, 72, 76, 86, 87, 93]).

Die verwendeten "Gassysteme“ unterscheiden sich beträchtlich. Als aussichtsreichster Kandidat entpuppt sich ein Zwei-Niveau-System (TLS) oder

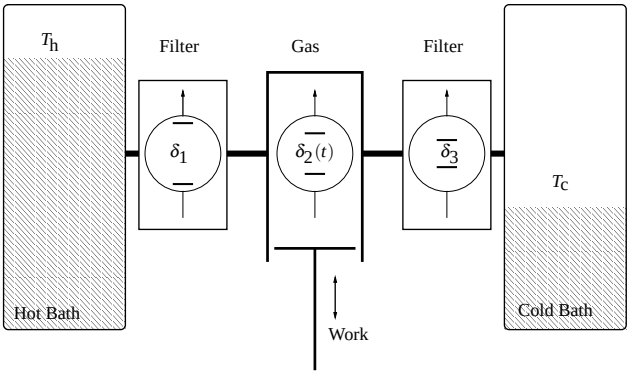

Abbildung F.3.: Schematischer Aufbau einer thermodynamischen Maschine bestehend aus drei Spins: Eine inhomogene 3-Spinkette ist in Kontakt mit zwei Bädern unterschiedlicher Temperatur. Spin 1 (mit der Energieaufspaltung δ_1) und Spin 3 (δ_3) agieren als Filter, wohingegen Spin 2 [$\delta_2(t)$] als Arbeitsgas durch Spektrumsdeformation arbeitet.

auch Qubit, bzw. Spin. Diese Systeme wurden bereits intensiv im Zusammenhang mit der Quanteninformation studiert [59]. Großer Auffand wurde betrieben um kleine Cluster und Ketten, bestehend aus mehreren Spins, zu kontrollieren, z. B. in optischen Systemen [18], mit Hilfe der NMR [35] und in Festkörpersystemen [61].

Unter Ausnutzung des Resonanzeffekts ist es möglich, dass eine Spinkette, bestehend aus mindestens drei Spins, als Wärmepumpe oder Wärmekraftmaschine arbeitet. Das Modell ist in Abb. F.3 dargestellt. Der zu analysierende Kreisprozeß ist ein Otto-Prozess. Aufgrund seiner einfachen Realisierbarkeit für Quantensysteme, findet der Otto-Zyklus sogar seine Anwendung beim Algorithmischen Kühlen [78]. Dass das oben skizzierte System in der Lage ist als Wärmepumpe zu arbeiten, illustriert Abb. F.4, wo das S_2T_2-Diagramm von Spin 2 dargestellt ist.

Eine Eigenheit von TLS als Maschinen ist die Tatsache, dass es einen Umschlagspunkt der Arbeitsfunktion von der Pumpe zur Maschine gibt, sobald adiabatische Prozessschritte eingebunden sind. Dies passiert dann, wenn die Besetzungszahlen und somit die Temperatur von Spin 2 nach den adiabatischen Schritten gleich der des jeweiligen Badspins 1 oder 3 ist. In diesem Fall wird keine Wärme mehr transportiert oder genutzt um Arbeit zu verrichten. Als Folge erreicht der Wirkungsgrad der Quanten-Otto-Maschine den Carnot-Wirkungsgrad. Da aber "nichts mehr passiert", ist auch der zweite Hauptsatz

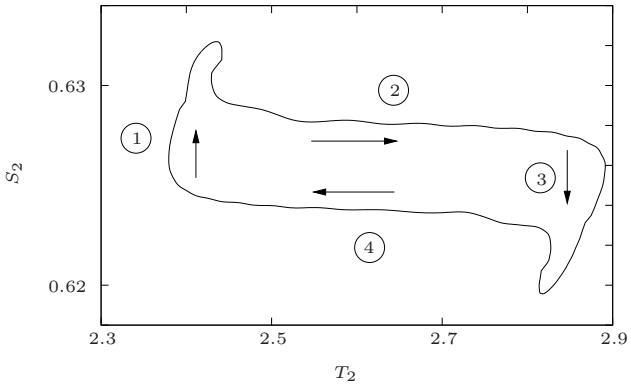

Abbildung F.4.: S_2T_2-Diagramm für eine Quantenwärmepumpe mit $T_h = 2.63, T_c = 2.5$ ($\Delta T = 0.13$) und $\tau = 2\pi/\omega = 804.25$. Die Pfeile symbolisieren die Umlaufrichtung.

nicht in Gefahr. Dies ist für das obige Modell in Abb. F.5 illustriert, wo die Wirkungsgrade als Funktion des Temperaturgradienten ΔT aufgetragen sind.

Der Vergleich zwischen dem numerischen Drei-Spin-Modell und dem theoretisch zu erwartenden Wert der Wirkungsgrade stimmt nur in erster Ordnung überein. Der theoretische Wirkungsgrad einer Quanten-Otto-Wärmekraftmaschine ist gegeben durch

$$\eta_{\text{Otto}} = \frac{-W}{Q_h} = 1 - \frac{\delta_1}{\delta_3}, \tag{F.7}$$

mit den Energieaufspaltungen δ_μ. Der Kehrwert ergibt den Wirkungsgrad für die Wärmepumpe. Der Wirkungsgrad (F.7) ist unabhängig von den jeweiligen Badtemperaturen, wie im klassischen Fall. Der Unterschied kann auf einen Leckstrom zurückgeführt werden, welcher eine Folge der Wechselwirkung von Spin 2 mit seinen Nachbarn ist. Deshalb ist die Schwachkopplungsnäherung nur bedingt anwendbar.

F.6. Fazit

Das Anliegen dieser Arbeit ist, thermodynamische Konzepte auf ihre Anwendbarkeit in der Quantenthermodynamik und in der Nichtgleichgewichtsquantenthermodynamik zu überprüfen. Mit Hilfe der Einführung des LEMBAS Prinzips ist es gelungen, lokale (hier effektiv genannte) Größen einzuführen,

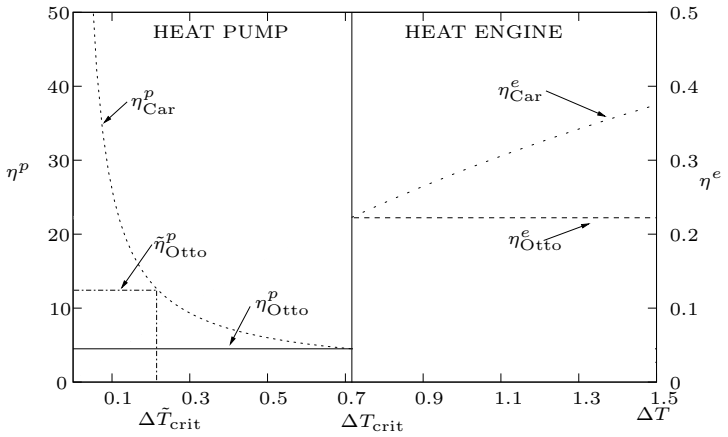

Abbildung F.5.: Der Carnot-Wirkungsgrad η^p_{Car} und die Wirkungsgrade η^p_{Otto} der Quantenwärmepumpe ($\Delta T < \Delta T_{\mathrm{crit}}$) und η^e_{Car} und η^e_{Otto} der Wärmekraftmaschine ($\Delta T > \Delta T_{\mathrm{crit}}$) als Funktion der Temperaturdifferenz ΔT. Folgende Parameter wurden verwendet: $T_c = 2.5, \delta_1 = 2.25$ und $\delta_3 = 1.75$. Die kritische Temperatur, bei der die Maschinenfunktion umschlägt kann durch die Energieaufspaltung beeinflusst werden. $\tilde{\eta}^p_{\mathrm{Otto}}$ und somit $\tilde{\Delta}T_{\mathrm{crit}}$ wurden mit $\delta_1 = 1.904$, $\delta_3 = 1.75$ erreicht.

welche thermische Eigenschaften wiederspiegeln können. Der wesentliche Unterschied zur herkömmlichen Vorgehensweise ist die Berücksichtigung der Wechselwirkungen der Untereinheiten, aus welchen das Gesamtsystem besteht, untereinander. Typisch für die Quantenmechanik kann auch eine schwache Wechselwirkung einen spürbaren Einfluss auf das System ausüben.

Es scheint möglich zu sein, dass das kontrovers diskutierte Transportverhalten 1-dimensionaler Heisenbergketten mit dieser Methode erklärbar ist. Der Einfluss der Bäder und damit eine Störung der Isotropie konnte nachgewiesen werden. Ebenso konnte der teilchenlose Energietransport im stationären Zustand auf einen Entropiestrom zurückgeführt werden und damit eindeutig als Wärme im herkömmlichen Sinn bestimmt werden.

Die aus der klassischen Thermodynamik bekannten Kreisprozesse sind in der Quantenwelt für die einfachsten Quantensysteme, wie z. B. Spins, genauso realisierbar. Dies beruht zum größten Teil auf der Tatsache, dass ein Bad alle Kohärenzen eines Quantensystems löscht und nur ein kanonischer Zustand zurückbleibt. Bemerkenswerterweise können die klassischen Wirkungsgrade, welche für quasi-stationäre Prozessführung realisierbar sind, hier in endlicher Zeit erreicht werden. Eine offene Frage bleibt zunächst die Rolle der Kohärenz für den Wirkungsgrad und die Arbeitsweise einer quantenthermodynamischen Maschine. Es besteht die Hoffnung, dass die vorgelegten Ergebnisse und Konzepte einen Beitrag dazu leisten, die ohnehin schon weiten Grenzen der Thermodynamik ein Stück weiter zu schieben.

List of Symbols

LEMBAS	Local Effective Measurement Basis
QME	Quantum Master Equation
SA	Secular Approximation
TLS	Two-Level System(s)
$\hat{1}$	Identity operator
α	System-bath coupling strength
$\hat{b}$, $\hat{b}^\dagger$	Bosonic annihilation and creation operators
B	Magnetic field
b_0	Up-shift of the local energy splitting
b_{ij}	Matrix-elements of $\hat{\rho}_B$
$\langle\cdot\vert$	Bra
b	Detuning parameter
c_{ij}	Matrix-elements of $\hat{C}$, the correlation operator
$\hat{C}_{AB}$	Correlation operator
Δ	Anisotropy factor
δ	Energy splitting
D	Energy deviation
δ_{13}	Detuning parameter
δ_b	Additional energy splitting
$\hat{\mathcal{D}}$	Dissipator
δ^{L}	Effective energy splitting obtained with LEMBAS
E_n	Energy eigenvalue of level n
$\langle E_\mu^{\mathrm{bind}}\rangle$	Expectation value of the binding energy of system μ
ΔE_n	Energy difference after an adiabatic step
η	Efficiency
η_{Car}	Efficiency of the Carnot-cycle
$\eta^{e/p}$	Efficiency of a heat engine/pump
η_{Otto}	Efficiency of the Otto-cycle
η_{Stirling}	Efficiency of the Stirling-cycle
ϵ	Energy eigenvalue
$\langle\mathcal{O}\rangle$	Expectation value of the observable $\mathcal{O}$
$\hat{\mathcal{F}}$	Affinity
g_j	Complex numbers

Γ	Correlation function
γ	Correlation function
$\hat{H}$	Hamiltonian
$\hat{H}_{A/B}$	Hamiltonian of system A/B
$\hbar$	Planck constant
H. c.	Hermitian conjugate
$\hat{H}_{\mathrm{env}}$	Hamiltonian of the environment
$\hat{H}^{\mathrm{eff}}$	Hamiltonian inducing an effective dynamics
$\hat{H}^{\mathrm{eff}}_{1/2}$	Diagonal/off-diagonal part of $\hat{H}^{\mathrm{eff}}$
$\hat{H}_{\mathrm{int}}$	Interaction Hamiltonian
$\hat{H}^{\mathrm{L}}$	Effective Hamiltonian obtained with LEMBAS
$\hat{H}_{\mathrm{L}}$	Lamb-shift Hamiltonian
$\hat{H}^{\mathrm{loc}}$	Local Hamiltonian
$\hat{H}_s$	Hamiltonian of the system
J	Current
J_{corr}	Correlation current
$J_{c/h}$	Heat current of the cold/hot bath
J_{L}	Leakage current
$\hat{J}_{\mu,\mu+1}$	Internal current operator
κ	Thermal conductivity
k_B	Boltzmann constant
$\lvert\cdot\rangle$	Ket
$[\cdot,\cdot]$, $[\cdot,\cdot]_+$	Commutator and anti-commutator
L_{ij}	Transport coefficients
λ	Internal coupling strength
λ_{th}	Coupling strength of the measurement device
L	Length of the 1-dimensional potential well
$\hat{\mathcal{L}}_{\mathrm{inc}}$	Incoherent part of the system dynamics
$\hat{\mathcal{L}}$	Super- or Liouville operator
B	Magnetization
m	Particle mass
μ	Index of the subunit
N	Particle number
$N(\omega)$	Planck distribution
ω	Angular frequency/detuning factor
p_n	Occupation probability of level n
$\hat{\sigma}^x$, $\hat{\sigma}^y$, $\hat{\sigma}^z$	Pauli operators
$\hat{\sigma}^-$, $\hat{\sigma}^+$	Lowering and raising operators
π	Pi
$\hat{P}_{ii}$	Projection operator on subspace i

$n-1$	Polytropic exponent
p	Pressure
$\hat{\mathcal{P}}$	Projection operator to the relevant part
$\hat{\pi}$	Projection operator to an eigenspace
$\hat{\mathcal{Q}}$	Projection operator to the irrelevant part
ψ	Wave function
$đQ$	Heat
Q_c	Heat exchanged with a cold bath
ΔQ	Exchanged Heat
Q_h	Heat exchanged with a hot bath
$Q_{\text{iso-T}}$	Heat exchanged during an isothermal step
Q_{isoc}	Heat exchanged during an isochoric step
j, m	Quantum numbers
m	Entropy of system A
$\hat{\rho}$	Density operator
$\hat{\hat{\rho}}$	Density operator
$\hat{\rho}_{\text{env}}$	Density operator of the environment
$\hat{\rho}_s$	Density operator of the system
S	von Neumann Entropy
S_A	Entropy of system A
σ	Entropy production rate
T	Temperature
ΔT_{crit}	Critical temperature
$T_{c/h}$	Bath temperature of the cold/hot bath
T^{L}	Effective temperature obtained with LEMBAS
T^{loc}	Local temperature obtained with $\hat{H}_{\text{loc}}$
T_{th}^{L}	Effective temperature of the measurement device obtained with LEMBAS
$T_{\text{th}}^{\text{loc}}$	Local temperature of the measurement device obtained with $\hat{H}_{\text{loc}}$
$\text{Tr}\{\cdot\}$	Trace operation
T^*	Formal temperature
$\hat{U}$	Unitary time-evolution operator
U	Internal energy
u	Energy density
ΔU	Internal energy change
$\hat{V}_{\mu,\mu+1}$	Next nearest-neighbor interaction Hamiltonian
V	Volume
$đW$	Work
W_{ad}	Work exchanged during an adiabatic step

ΔW	Exchanged Work
$W_{\text{iso-T}}$	Work exchanged during an isothermal step
W_{isoc}	Work exchanged during an isochoric step
$\hat{X}$	Environment operator
X	Extensive variable
x	Intensive variable
$\hat{X}(t)$	Interaction picture operator
$\hat{X}_{l/r}$	Environment operator of the left/right boundary
$\hat{Y}$	Operator of the bath
Z	Partition sum

Bibliography

[1] R. Alicki. The quantum open system as model of the heat engine. *J. Phys. A: Math. Gen.*, **12(5)**, L103 – L107, (1979).

[2] R. Alicki and M. Fannes. *Quantum Dynamical Systems*. Oxford University Press, Oxford, (2001).

[3] A. E. Allahverdyan, R. Serral Gracia, and Th. M. Nieuwenhuizen. *Phys. Rev. E*, **71**, 046106, (2005).

[4] C. Bender, D. Brody, and B. Meister. Quantum mechanical carnot engine. *J. of Phys. A: Math. Gen.*, **33**, 4427–4436, (2000).

[5] V. Blickle, T. Speck, C. Lutz, U. Seifert, and C. Bechinger. Einstein Relation Generalized to Nonequilibrium. *Phys. Rev. Lett.*, **98**, 210601, (2007).

[6] L. Boltzmann. *Lectures on Gas Theory*. University of California Press, Los Angeles, (1964).

[7] F. Bonetto, J. L. Lebowitz, and L. Rey-Bellet. Fourier Law: A Challenge to Theorists. *arXiv:math-ph/0002052v1*, (2000).

[8] M Born. Zur Quantenmechanik der Stoßvorgänge. *Z. Phys.*, **37**, 863–867, (1926).

[9] P. Boykin, T. Mor, V. Roychowdhury, and F. Vatan. Algorithmic cooling and scalable NMR quantum computers. *Proc. Natl. Acad. Sci.*, **99(6)**, 3388 – 3393, (2002).

[10] H.-P. Breuer and F. Petruccione. *The Theory of Open Quantum Systems*. Oxford University Press, (2002).

[11] H.P. Breuer, J. Gemmer, and M. Michel. Non-Markovian quantum dynamics: Correlated projection superoperators and Hilbert space averaging. *Phys. Rev. E*, **73**, 016139, (2006).

[12] M. Buchanan. Heated Debated in Different Dimensions. *Nature Physics*, **1**, 71, (2005).

[13] D. G. Cahill, W. K. Ford, K. E. Goodson, G. D. Mahan, A. Majumdar, H. J. Maris, R. Merlin, and S. R. Phillpot. Nanoscale thermal transport. *J. Apll. Phys.*, **93(2)**, 793–818, (2003).

[14] H. B. Callen. *Thermodynamics and an introduction to thermostatistics*. Wiley, New York, 2. edition, (1985).

[15] H. Carmichael. *An Open System Approach to Quantum Optics*. Lecture Notes in Physics, Monographs Series. Springer-Verlag (Berlin Heidelberg), (1993).

[16] S. Carnot. *Refléctions sur la Puissance Motrice du Feu et sur les Mchines Propres à Développer Cette Puissance*. Bachlier, Paris, (1824).

[17] G. Casati, C. Mejia-Monasterio, and T. Prosen. Magnetically induced thermal rectification. *Phys. Rev. Lett.*, **98**, 104302, (2007).

[18] J. I. Cirac and P. Zoller. A scalable quantum computer with ions in an array of microtraps. *Nature*, **404**, 579–581, (2000).

[19] R. Clausius. Über die bewegende kraft der wärme. *Ann. Phys.*, **79**, 368 – 397, (1850).

[20] C. Cohen-Tannoudji, B. Diu, and F. Laloë. *Quantenmechanik 1*. de Gruyter, 2 edition, (1999).

[21] B. Diu, C. Guthmann, D. Lederer, and B. Roulet. *Grundlagen der Statistischen Physik*. Hermann Editeurs des Sciences et des Arts, Paris, (1989).

[22] R. Dümcke and H. Spohn. The Proper Form of the Generator in the Weak Coupling Limit. *Zeit. Physik B*, **34**, 419 – 422, (1979).

[23] A. Einstein. Über die von der molekularkinetischen Theorie der Wärme geforderte Bewegung von in ruhenden Flüssigkeiten suspendierten Teilchen. *Ann. Phys.*, **17**, 549 – 560, (1905).

[24] J. Eisert and M. B. Plenio. Quantum Classical Correlatoins in Quantum Brownian Motion. *Phys. Rev. Lett.*, **89(13)**, 137902, (2002).

[25] T. Feldmann and R. Kosloff. Performance of discrete heat engines and heat pumps in finite time. *Phys. Rev. E*, **61(5)**, 4774 – 4790, (2000).

[26] T. Feldmann and R. Kosloff. Quantum four-stroke heat engine: Thermodynamic observables in model with intrinsic friction. *Phys. Rev. E*, **68(016101)**, 016101, (2003).

[27] T. Feldmann and R. Kosloff. Characteristics of the limit cycle of a reciprocating quantum heat engine. *Phys. Rev. E*, **70**, 046110, (2004).

[28] R. P. Feynman and F. L. Vernon. The theory of a general quantum system interacting with a linear dissipative system. *Ann. Phys.*, **24**, 118–173, (1963).

[29] E. Fick and G. Sauermann. *The Quantum Statistics of Dynamic Processes*. Springer, Berlin, Heidelberg, (1990).

[30] G. W. Ford, J. T. Lewis, and R. F. O'Connell. Quantum lagenvine equation. *Phys. Rev. A*, **37(11)**, 4419 – 4428, (1988).

[31] J. B. J. Fourier. *The analytical theory of heat*. New York Dover Publishers, (1955).

[32] J. Gemmer and G. Mahler. Entanglement and the factorization-approximation. *Euro. Phys. J. D*, **17**, 385–393, (2001).

[33] J. Gemmer, M. Michel, and G. Mahler. *Quantum Thermodynamcis - Emergence of Thermodynamic Behavior within Composite Quantum Systems*. Springer LNP, Berlin, New York, (2004). in press.

[34] J. Gemmer, A. Otte, and G. Mahler. Quantum approach to a derivation of the second law of thermodynamics. *Phys. Rev. Lett.*, **86**, 1927–1930, (2001).

[35] N. A. Gershenfeld and I. L. Chuang. Bulk spin-resonance quantum computation. *Science*, **275**, 350–356, (1997).

[36] E. Geusic, E. Schultz-Duboi, and H. Scovil. Quantum Equivalent of the Carnot Cycle. *Phys. Rev.*, **156**, 262, (1967).

[37] J. W. Gibbs. *Elementary Principles in Statistical Mechanics*. Dover Publications, New York, (1960).

[38] Zachary N. C. Ha. *Quantum Many-Body Systems in One Dimension*, volume 12 of *Series on Advances in Statistical Mechanics*. World Scientific, Singapore, New Jersey, London, Hong Kong, (1998).

[39] Fritz Haake. *Quantum Signatures of Chaos*. Springer Series in Synergetics. Springer, 2nd revised and enlarged edition edition, (2001).

[40] M. Hartmann. *On the Microscopic Limit for the Existence of Local Temperature*. PhD thesis, 1. Institut für Theoretische Physik, Universität Stuttgart, (2005).

[41] M. Hartmann and G. Mahler. Measurable Consequences of the Local Breakdown of the Concept of Temperature. *Europhys. Lett.*, **70**, 579 – 585, (2005).

[42] M. Hartmann, G. Mahler, and O. Hess. Existence of Temperature on the Nanoscale. *Physical Review Letters*, **93(8)**, 4 2004.

[43] F. Heidrich-Meisner. *Transport Properties of Low-Dimensional Quantum Spin Systems*. PhD thesis, Technische Universität Carolo-Wilhelmina zu Braunschweig, (2005).

[44] M. J. Henrich, M. Michel, M. Hartmann, G. Mahler, and J. Gemmer. Global and local relaxation of a spin-chain under exact Schrödinger and master-equation dynamics. *Phys. Rev. E*, **72**, 026104, (2005).

[45] M. J. Henrich, M. Michel, and G. Mahler. Small quantum networks operating as thermodynamic machines. *Europhys. Lett.*, **76**, 1057 – 1063, (2006).

[46] M. J. Henrich, M. Michel, and G. Mahler. Driven Spin Systems as Quantum Thermodynamic Machines: Fundamental Limits. *Phys. Rev. E*, **75**, 051118, (2007).

[47] M. J. Henrich, F. Rempp, and G. Mahler. Quantum Thermodynamic Otto-machines: A Spin-System Approach. *to appear in European Physical Journal Special Topics*, (2007).

[48] C. Hess, C. Baumann, U. Ammerahl, B. Büchner, F. Heidrich-Meisner, W. Brenig, and A. Revcolevschi. Magnon Transport in (Sr,La)$_{14}$Cu$_24$O$_41$. *cond-mat/0105407*, (2001).

[49] C. Hess, H. ElHaes, A. Waske, B. Buechner, C. Sekar, G. Krabbes, F. Heidrich-Meisner, and W. Brenig. Linear temperature dependence of the magnetic heat conductivity in CaCu2O3. *Phys. Rev. Lett.*, **98(2)**, 27201, (2007).

[50] T. D. Kieu. Quantum heat engines, the second law and Maxwell's daemon. *Eur. Phys. J. D*, **39**, 115 – 128, (2006).

[51] Tien D. Kieu. The second law, maxwell's demon, and work derivable from quantum heat engines. *Phys. Rev. Lett.*, **93(14)**, 140403, (2004).

[52] P. Kim, L. Shi, A. Majumdar, and P. L. McEuen. Thermal Transport Measurements of Individual Multiwalled Nanotubes. *Phys. Rev. Lett.*, **87**, 215502, (2001).

[53] R. Kubo, M. Toda, and N. Hashitsume. *Statistical Physics II: Nonequilibrium Statistical Mechanics*. Number 31 in Solid-State Sciences. Springer, Berlin, Heidelberg, New-York, 2. edition, (1991).

[54] S. Lepri, R. Livi, and A. Politi. Thermal conduction in classical low-dimesional lattices. *Phys. Rep.*, **377**, 1 – 80, (2003).

[55] E. H. Lieb, Th. Niemeijer, and G. Vertogen. Models in Statistical Mechanics. In *Statistical Mechanics and Quantum Field Theory*, volume Proceedings of 1970 Ecole d'Eté de Physique Théorique (Les Houches), pages 281–326. Gordon and Breach, (1971).

[56] B. Lin and J. Chen. Otimization on the performance of a harmonic quantum Brayton heat engine. *J. Appl. Phys.*, **94(9)**, 6185 – 6191, (2003).

[57] B. Lin and J. Chen. Performance analysis of irreversible quantum Stirling cryogenic refrigeration cycles and their parametric optimum criteria. *Phys. Scr.*, **74**, 251–258, (2006).

[58] G. Lindblad. On the Generators of Quantum Dynamical Semigroups. *Commun. Math. Phys.*, **48**, 119–130, (1976).

[59] D. Loss and P. DiVincenzo. Quantum computation with quantum dots. *Phys. Rev. A*, **57**, 120, (1998).

[60] G. Mahler and V.A. Weberruß. *Quantum Networks*. Springer, Berlin, Heidelberg, 2. edition, (1998).

[61] Y. Makhlin and G. Schön. Josephson-junction qubits with controlled couplings. *Nature*, **398**, 305–307, (1999).

[62] V. May and O. Kühn. *Charge and Energy Transfer Dynamics in Molecular Systems*. Wiley-VCH, (2000).

[63] M. Michel. *Nonequilibrium Aspects of Quantum Thermodynamics*. PhD thesis, 1. Institut für Theoretische Physik, Universtität Stuttgart, (2006).

[64] M. Michel, J. Gemmer, and G. Mahler. Quantum Heat Transport: Perturbation Theory in Liouville Space. *Physica E*, **29**, 136 – 144, (2005).

[65] M. Michel, J. Gemmer, and G. Mahler. Microscopic Quantum Mechanical Foundation of Fourier's Law. *Int. J. Mod. Phys. B*, **20**, 4855 – 4883, (2006).

[66] M. Michel, M. Hartmann, J. Gemmer, and G. Mahler. Fourier's Law confirmed for a class of small quantum systems. *Euro. Phys. J. B*, **34**, 325–330, (2003).

[67] S. Nakajima. On quantum theory of transport phenomena. *Progr. Theor. Phys.*, **20**, 948 – 959, (1958).

[68] M. A. Nielsen and I. L. Chuang. *Quantum Computation and Quantum Information*. Cambridge University Press, Cambridge, (2000).

[69] L. Onsager. Reciprocal Relations in Irreversible Processes. I. *Phys. Rev.*, **37**, 405, (1931).

[70] L. Onsager. Reciprocal Relations in Irreversible Processes. II. *Phys. Rev.*, **38**, 2265 – 2279, (1931).

[71] A. Otte. *Separabilität in Quantennetzwerken*. PhD thesis, Universität Stuttgart, Stuttgart, (2001).

[72] J. P. Palao, R. Kosloff, and J. M. Gordon. Quantum thermodynamic cooling cycle. *Phys. Rev. E*, **64(056130)**, 056130, (2001).

[73] P. Pechukas. Reduced Dynamics Need Not Be Completely Positive. *Phys. Rev. Lett.*, **73(8)**, 1060 – 1062.

[74] R. E. Peierls. *Quantum Theory of Solids*. Clarendon Press, Oxford, (2001).

[75] M. B. Plenio and P. L. Knight. The quantum-jump approach to dissipative dynamics in quantum optics. *Rev. Mod. Phys.*, **70(1)**, 101 – 144, (1998).

[76] H. T. Quan, P. Zhang, and C. P. Sun. Quantum heat engine with multilevel quantum systems. *Phys. Rev. E*, **72**, 056110, (2005).

[77] A. G. Redfield. On the Theory of Relaxation Processes. *IBM J. Res. Dev.*, **1**, 19 – 31, (1957).

[78] F. Rempp, M. Michel, and G. Mahler. A cyclic cooling algorithm. *arXiv:quant-ph/0702071v1*, (2007).

[79] K. Saito. Strong evidence of normal heat conduction in a one-dimensional quantum system. *Europhys. Lett.*, **61**, 34–40, (2003).

[80] K. Saito, S. Takesue, and S. Miyashita. Thermal conduction in a quantum system. *Phys. Rev. E*, **54**, 2404–2408, (1996).

[81] K. Saito, S. Takesue, and S. Miyashita. Energy transport in the integrable system in contact with various types of phonon reservoirs. *Phys. Rev. E*, **61**, 2397–2409, (2000).

[82] V. Scarani, M. Ziman, P. Štelmachovič, N. Gisin, and V. Bužek. Thermalizing Quantum Machines: Dissipation and Entanglement. *Phys. Rev. Lett.*, **88(9)**, 097905, (2002).

[83] H. Schröder. private communication.

[84] H. Schröder. On the measurability of thermodynamic characteristics of driven nanomechanical systems. Master's thesis, 1. Institut für Theoretische Physik, Universität Stuttgart, (2006).

[85] H. Scovil and E. Schultz-Dubois. Three Level Masers as Heat Engines. *Phys. Rev. Lett.*, **2(6)**, 262, (1959).

[86] M. O. Scully. Quantum Afterburner: Improving the Efficiency of an Ideal Heat Engine. *Phys. Rev. Lett.*, **88(5)**, 050602, (2002).

[87] D. Segal. Heat flow in nonlinear molecular junctions: Master equation analysis. *Phys. Rev. B*, **73**, 205415, (2006).

[88] D. Segal and A. Nitzan. Molecular heat pump. *Phys. Rev. E*, **73**, 026109, (2006).

[89] M Stollsteimer. *Thermodynamische Eigenschaften periodisch kontrollierter Quantensysteme*. PhD thesis, 1. Institut für Theoretische Physik, Universität Stuttgart, (2006).

[90] H. Stumpf and A. Rieckers. *Thermodynamik*. Number Band 1. vieweg, (1976).

[91] M. Takahashi. *Thermodynamics of One-Dimensional Solvable Models*. Cambridge University press, (1999).

[92] F. Tonner. *Autonome quantenmechanische Maschinen*. PhD thesis, 1. Institut für Theoretische Physik, Universität Stuttgart, (2006).

[93] F. Tonner and G. Mahler. Autonomous quantum thermodynamic machines. *Phys. Rev. E*, **72(066118)**, 066118, (2005).

[94] P. A. Vidal Miranda. Nanothermodynamics: Transport in One-Dimensional Spin Chains. Master's thesis, 1. Institut für Theoretische Physik, Universität Stuttgart, (2005).

[95] J. von Neumann. *Mathematischen Grundlagen der Quantenmechanik*. Die Grundlehren der Mathematischen Wissenschaften. Springer, Berlin, Heidelberg, New York, (1968).

[96] D. F. Walls and G. J. Milburn. *Quantum Optics*. Springer, Berlin, Heidelberg, 2. edition, (1995).

[97] H. Weimer, M. J. Henrich, F. Rempp, and H. Schröder. Local effective dynamics of quantum systems: A generalized approach to work and heat. *submitted*, (2007).

[98] U. Weiss. *Quantum Dissipative Systems*. World Scientific, Singapore, second edition, (1999).

[99] H. Wichterich. Projection Operator and Hilbertspache Average Method: A comparison. Master's thesis, Universität Osnabrück, (2007).

[100] H. Wichterich, M. J. Henrich, H. P. Breuer, J. Gemmer, and M. Michel. Modelling heat transport through completely positive maps. *submitted to Phys. Rev. E*, (2007).

[101] X. Zotos and P. Prelovšek. Transport in One Dimensional Quantum Systems. *arXiv:cond-mat/0304630v2*, (2003).

[102] R. Zwanzig. Memory Effects in Irreversible Thermodynamics. *Phys. Rev.*, **124**, 983–992, (1961).

[103] R. Zwanzig. On the Identity of Three Generalized Master Equations. *Physica*, **30**, 1109 – 1123, (1964).

List of Previous Publications

[i] M. J. Henrich, M. Michel, and G. Mahler. Small quantum networks operating as thermodynamic machines. *Europhys. Lett.*, **76**, 1057 – 1063, (2006).

[ii] M. J. Henrich, M. Michel, and G. Mahler. Driven Spin Systems as Quantum Thermodynamic Machines: Fundamental Limits. *Phys. Rev. E*, **75**, 051118, (2007).

[iii] H. Wichterich, M. J. Henrich, H. P. Breuer, J. Gemmer, and M. Michel. Modelling heat transport through completely positive maps. *accepted for publication in Phys. Rev. E*, (2007).

[iv] M. J. Henrich, F. Rempp, and G. Mahler. Quantum Thermodynamic Otto-machines: A Spin-System Approach. *to appear in European Physical Journal Special Topics*, (2007).

[v] H. Weimer, M. J. Henrich, F. Rempp, and H. Schröder. Local effective dynamics of quantum systems: A generalized approach to work and heat. *submitted*, (2007).

Danksagung

Folgenden Personen möchte ich von Herzen danken. Ohne Ihre Unterstützung, Ratschläge und viele andere Dinge wäre es mir nicht möglich gewesen, die vorliegende Arbeit anzufertigen.

Prof. Dr. G. Mahler möchte ich dafür danken, dass er mir die Gelegenheit gab, in seiner Arbeitsgruppe zu forschen. Für seine sehr gute Betreuung und die vielen anregenden Diskussionen. Seine offene Art neuen Ideen gegenüber, hat mich beeindruckt.

Prof. Dr. U. Weiß, danke ich herzlich für die Übernahme des Mitberichts.

Ohne die anregenden Ideen und Diskussionen von und mit Dr. M. Michel wären manche Teile dieser Arbeit nicht denkbar. Ihm gilt mein besonderer Dank.

Ich danke der "LEMBAS-Crew", F. Rempp., H. Schröder und H. Weimer für die gemeinsame Entwicklung von "LEMBAS". Es war, nicht nur wissenschaftlich, eine fruchtbare Zeit.

Den Kollegen am 1. Institut für Theoretische Physik, Dr. M. Hartmann, Th. Jahnke, A. Kettler, G. Reuther, F. Rempp., H. Schmidt, H. Schröder, Dr. M. Stollsteimer, J. Teifel, Dr. F. Tonner, P. Vidal, H. Weimer und M. Youssef für viele Diskussionen nicht nur über Physik. H. Schmidt möchte ich noch für die unzähligen LaTeX-Tipps danken. Dr. M. Stollsteimer und J. Teifel danke ich für das Korrekturlesen verschiedener Kapitel.

Jun. Prof. Dr. J. Gemmer (Universität Osnabrück), Dr. H.-P. Breuer (Universität Freiburg) und H. Wichterich (Universität Osnabrück) möchte ich für die gute Zusammenarbeit sowie Anregungen und Diskussionen danken.

Meinem Bruder O. Henrich danke ich für die Bereitstellung des technischen Equipements, welche die Anfertigung dieser Arbeit beschleunigte und für vieles mehr.

Danken möchte ich auch meinen Eltern, U. und K. Henrich sowie meinen Schwiegereltern, E. und R. Wolf für die Unterstützung in all den Jahren.

Zu guter Letzt, möchte ich meinen Kindern, Anica und Benita danken für die Geduld und die wenigen Stunden in der Endphase dieser Arbeit, in denen ich für sie Zeit hatte. Meiner Frau Gabi danke ich für das Korrekturlesen, sowie für alles und noch vieles mehr, was in Kürze nicht geschrieben werden kann.

Stuttgart, Juli 2007 Markus J. Henrich